


2012

# MDA-7/IL-24; A PROMISING CANCER THERAPEUTIC AGENT

Hossein Hamed

*Virginia Commonwealth University*

Follow this and additional works at: <http://scholarscompass.vcu.edu/etd>

 Part of the [Biochemistry, Biophysics, and Structural Biology Commons](#)

© The Author

---

Downloaded from

<http://scholarscompass.vcu.edu/etd/2847>

This Dissertation is brought to you for free and open access by the Graduate School at VCU Scholars Compass. It has been accepted for inclusion in Theses and Dissertations by an authorized administrator of VCU Scholars Compass. For more information, please contact [libcompass@vcu.edu](mailto:libcompass@vcu.edu).

© Hossein A. Hamed 2012|

All Rights Reserved

MDA-7/IL-24; A PROMISING CANCER THERAPEUTIC AGENT  
A Dissertation submitted in partial fulfillment of the requirements for the degree of  
Doctor of Philosophy at Virginia Commonwealth University.

by

HOSSEIN AKBARI HAMED  
Bachelors of Science, University of Mary Washington, 2003

Director: PAUL DENT, PH.D.  
VICE CHAIR, DEPARTMENT OF NEUROSURGERY

Virginia Commonwealth University  
Richmond, Virginia  
June 2012

This Thesis is dedicated to my Wonderful Parents.

## Table of Contents

	Page
Acknowledgements.....	ii
List of Tables .....	v
List of Figures .....	vi
List of Abbreviations .....	xii
 Chapter	
1 INTRODUCTION: GENERAL.....	1
1.1 Cancer.....	1
1.2 Glioblastoma Multiforme .....	2
1.3 Conventional Treatments .....	3
1.4 Gene Therapy and MDA-7/IL-24.....	4
1.5 Raf/MEK/ERK Mitogen-activated protein kinase (MAP) pathway .....	9
1.6 JNK1/2 MAPK Pathway .....	13
1.7 p38 MAPK Pathway.....	14
1.8 PI3K/Akt Pathway.....	15
1.9 Receptor Tyrosine Kinases – ERBB receptor family proteins.....	19
1.10 Apoptosis: Extrinsic and Intrinsic Pathways.....	20
1.11 Regulation of Apoptosis Signaling.....	25
1.12 Autophagy: Function and Process .....	26
1.13 Autophagy: Regulation.....	29

1.14 Autophagy and Cancer .....	30
1.15 Molecular Chaperones in Protein Folding.....	33
1.16 Hsp90 Structure and Function .....	34
1.17 Hsp90 inhibitors .....	37
1.18 ER Stress: The Unfolded Protein Response .....	38
1.19 Small Molecule Inhibitors/Drugs used in this study .....	41
2 MATERIALS AND METHODS: OSU-03012 AND MDA-7/IL-24.....	44
2.1 Materials .....	44
Methods:	
2.2 Generation of Ad.5- <i>mda-7</i> or Ad.5/3- <i>mda-7</i> .....	45
2.3 Synthesis of GST-MDA-7/IL-24 .....	45
2.4 Cell Culture .....	46
2.5 <i>In vitro</i> Eposure of Cells to GST-MDA-7/IL-24, Recombinant	
Adenoviral Vectors and all other drugs.....	47
2.6 Assessment of Cell Viability .....	47
2.7 Colony Formation Assay for Cell Survival .....	48
2.8 Western Blot Analysis for Protein Expression.....	49
2.9 Plasmid and siRNA Transfections .....	50
2.10 Microscopy for LC3-GFP Expression.....	51
2.11 Intracerebral Inoculation of GBM cells.....	52

2.12	<i>Ex vivo</i> Manipulation of Tumors.....	53
2.13	Immunohistochemistry and Staining of Fixed Tumor Sections .....	54
2.14	Data Analyses.....	55
3	INTRODUCTION: OSU-03012 ENHANCES MDA-7/IL-24 KILLING OF GBM CELLS VIA ER STRESS AND AUTOPHAGY AND BY DECREASING EXPRESSION OF MITOCHONDRIAL PROTECTIVE PROTEINS .....	56
4	RESULTS: OSU-03012 AND MDA-7/IL-24 .....	58
4.1	Ad. <i>mda-7</i> lethality in GBM 6, 12 and 14 is enhanced by OSU-03012.	58
4.2	Ad. <i>mda-7</i> and OSU-03012 synergize to kill GBM 6 cells in colony formation assays .....	59
4.3	Ad. <i>mda-7</i> infected GBM 6 cells treated with OSU-03012 revealed decreased levels of pro-survival proteins: BCL-XL, MCL-1 and the phosphorylation of ERK1/2.....	60
4.4	Overexpression of BCL-X <sub>L</sub> , or inhibition of components of the intrinsic apoptosis pathway in GBM 6 cells, reduced Ad. <i>mda-7</i> or OSU-03012 toxicity as single agents or in combination .....	61
4.5	Activation of MEK protects GBM 6 cells from MDA-7/IL-24 and OSU-03012 toxicity .....	63

4.6	Constitutive expression of MCL-1 protects GBM 6 cells from MDA-7/IL-24 and OSU-03012 toxicity.....	65
4.7	OSU-03012 treatment enhances Ad. <i>mda-7</i> induced toxic autophagy but does not promote additional activation of PERK in primary human GBM cells.....	66
4.8	Expression of dominant negative PERK suppresses the lethal interaction between OSU-03012 and Ad. <i>mda-7</i> in primary human GBM cells....	67
4.9	The additive increase of LC3-GFP vesicularization in GBM cells caused by OSU-03012 and Ad. <i>mda-7</i> is blocked by expression of dominant negative PERK .....	69
4.10	Knockdown of ATG5 or Beclin1 expression profoundly reduced the toxicity of Ad. <i>mda-7</i> , OSU-03012 or the combination in GBM cells ..	71
4.11	MDA-7/IL-24 stimulates enhances the toxicity of ionizing radiation	73
4.12	Transfection of uninfected GBM cells with an siRNA to knock down MDA-7/IL-24 expression prevented conditioned media from Ad. <i>mda-7</i> infected GBM cells from increasing MDA-7/IL-24 expression, as well as enhancing the toxicity of OSU-03012 or ionizing radiation.....	75
5	DISCUSSION: OSU-03012 AND MDA-7/IL-24 .....	77



6	INTRODUCTION: INHIBITORS OF MULTIPLE PROTECTIVE SIGNALING PAHTWAYS AND Ad.5/3 DELIVERY ENHANCES MDA-7/IL-24 KILLING .....	82
7	RESULTS: INHIBITORS AND AD.5/3 MDA-7 .....	84
7.1	Serotype Ad.5- <i>mda-7</i> killing was significantly enhanced with coexpression of dnMEK1 and dnAKT. Ad.5- <i>mda-7</i> lethality was almost abolished with coexpression of activated MEK1 and AKT in primary human GBM cells .....	84
7.2	17AAG, PD184352/PX866 and PD184352/PI-103 treatments all promote Ad.5 <i>mda-7/IL-24</i> toxicity that is abolished by upregulation of pro-survival BCL-2 family proteins found in GBM cells. ....	88
7.3	Knockdown of mTOR expression <i>in vitro</i> enhanced Ad.5- <i>mda-7</i> toxicity to a similar extent as expression of dnMEK1 and a dn-p85 PI3K subunit.....	91
7.4	Combined inhibition of PI3K/MEK/mTOR modestly suppressed tumor growth of orthotopic GBM tumors <i>in vivo</i> and profoundly enhanced Ad.5- <i>mda-7</i> tumoricidal capability.....	93

7.5 Small molecule inhibitors of mTOR, PI3K and MEK1/2 signaling: 17AAG, PX866 and PD184352 respectively, enhanced Ad.5- <i>mda-7</i> toxicity in primary human GBM cells. This correlated closely with enhanced JNK1/2 activation and reduced expression of BCL-XL and MCL-1 .....	95
7.6 Treatment of GBM6 cells with multi-PI3K inhibitor PI-103 in combination with PD184352, had a greater killing effect than PX866; however, without further activation of JNK1-3 .....	98
7.7 Inhibition of JNK1-3 blocks MDA-7/IL-24 toxicity and inhibited the promotion of cell death by small molecule kinase inhibitors.....	103
7.8 17AAG, Rapamycin, PD184352/PX866 and PD184352/PI-103 treatments all promote Ad.5- <i>mda-7</i> toxicity through the intrinsic apoptotic pathway of GBM cells.....	105
7.9 Infection of tumor cells with Ad.5- <i>mda-7</i> was shown to increase PERK phosphorylation and LC3-II processing, without further enhancement when Ad.5- <i>mda-7</i> was combined with the small molecule inhibitors, 17AAG or PD184352/PX866.....	109
7.10 17AAG or PD184352/PX866 treatments enhance Ad.5- <i>mda-7</i> induced autophagy by causing an increase in autophagic flux .....	111

7.11 Knockdown of Beclin1 or ATG5 abolished Ad.5- <i>mda-7</i> toxicity and significantly reduced the abilities of 17AAG and to a lesser extent PD184352/PX866 exposure to cause cell death.....	113
7.12 MDA-7/IL-24 sensitizes GBM cells to radiation therapy and enhances survival <i>in vivo</i> .....	115
7.13 MDA-7/IL-24 and temozolomide interact in at least an additive fashion to kill primary human GBM cells in short term viability assays.....	119
7.14 Radiation, MDA-7/IL-24 and temozolomide interact in a greater than additive fashion to kill primary human GBM cells .....	121
7.15 Radiation, MDA-7/IL-24 and temozolomide interact in a greater than additive fashion to kill primary human GBM cells in colony formation assays.....	123
7.16 A tropism-modified type 5/3 adenovirus infects GBM cells in a CAR independent fashion and to a greater extent than a serotype 5 virus <i>in vivo</i> .....	125
7.17 In a colony-formation assay, infection of GBM6, GBM12 and U87-MG cells with Ad.5/3- <i>mda-7</i> caused a greater reduction in cell survival than cells infected with Ad.5- <i>mda-7</i> .....	129

7.18 A tropism-modified type 5/3 adenovirus infects GBM cells more readily than a type 5 adenovirus, and enhances tumor killing <i>in vivo</i>	131
7.19 Ad.5/3- <i>mda-7</i> is more effective at killing and reducing rodent GL261 glioma viability <i>in vitro and in vivo</i>	134
8 DISCUSSION: INHIBITORS AND AD.5/3 MDA-7	138
9 CONCLUSIONS	145
Literature Cited	146

List of Tables

Page

Table 2.1: Cell Line Information. ....	46
--	----

## List of Figures

	Page
Figure 1.1: Signaling pathways associated with Ad. <i>mda-7</i> and MDA-7/IL-24 activity. ....	7
Figure 1.2: Signaling pathways associated with MDA-7/IL-24.....	8
Figure 1.3: Mammalian MAPK cascades .....	11
Figure 1.4: Activation of the Raf/MEK/ERK Mitogen-activated protein kinase (MAP) pathway .....	12
Figure 1.5: Model of PI3K/Akt Pathway Activation .....	18
Figure 1.6: The Apoptosis Signaling Pathways.....	24
Figure 1.7: The Cellular Aspect of Autophagy.....	31
Figure 1.8: The Molecular Aspect of Mammalian Autophagy.....	32
Figure 1.9: Hsp70 and Hsp90 protein folding and degradation.....	36
Figure 1.10: Structure of 17-AAG (17-allylamino-17-demethoxygeldanamycin).....	37
Figure 1.11: The Unfolded Protein Response.....	40
Figure 1.12: Structure of PD184352 (CI-1040).....	41
Figure 1.13: Structure of PI-103 .....	41
Figure 1.14: Structure of PX-866.....	42
Figure 1.15: Structure of Rapamycin.....	42
Figure 1.16: Structure of OSU-03012 (AR-12) .....	43
Figure 1.17: Structure of Temazolomide (TMZ).....	43
Figure 4.1: Ad. <i>mda-7</i> lethality is enhanced by OSU-03012.....	58

Figure 4.2: Ad. <i>mda-7</i> lethality is enhanced by OSU-03012 .....	59
Figure 4.3: Ad. <i>mda-7</i> inhibition of pro-survival proteins is enhanced by OSU-03012 .....	60
Figure 4.4: Overexpression of BCL-XL or inhibition of components of the intrinsic apoptosis pathway, reduced Ad. <i>mda-7</i> or OSU-03012 toxicity .....	62
Figure 4.5: Activation of MEK and constitutive MCL-1 expression protect GBM cells from MDA-7/IL-24 and OSU-03012 toxicity.....	64
Figure 4.6: Constitutive MCL-1 expression protects GBM cells from MDA-7/IL-24 and OSU-03012 toxicity .....	65
Figure 4.7: OSU-03012 treatment enhances Ad. <i>mda-7</i> -induced toxic autophagy but does not promote additional activation of PERK.....	66
Figure 4.8: Expression of dominant negative PERK suppresses the lethal interaction between OSU-03012 and Ad. <i>mda-7</i> in primary human GBM cells.....	68
Figure 4.9: The additive increase of LC3-GFP vesicularization in GBM cells caused by OSU-03012 and Ad. <i>mda-7</i> is blocked by expression of dominant negative PERK.....	70
Figure 4.10: Knockdown of ATG5 or Beclin1 expression reduced the toxicity of Ad. <i>mda-7</i> , OSU-03012 or the combination in GBM cells.....	72
Figure 4.11: MDA-7/IL-24 sensitizes GBM6 cells to radiation .....	74
Figure 4.12: MDA-7/IL-24 stimulates expression of MDA-7/IL-24 and increases toxicity of GBM6 cells to drug and ionizing radiation .....	76

Figure 7.1.1: Ad.5- <i>mda-7</i> lethality is enhanced by combined inhibition of PI3K/MEK/mTOR pathways in GBM 6 cells .....	86
Figure 7.1.2: Ad.5- <i>mda-7</i> lethality is enhanced by combined inhibition of PI3K/MEK/mTOR pathways in GBM 12 cells .....	87
Figure 7.2.1: BCL-2 overexpression abolishes 17AAG, PD184352/PX866 and PD184352/PI-103 enhancement of Ad.5 <i>mda-7/IL-24</i> toxicity in GBM6 cells .....	89
Figure 7.2.2: MCL-1 overexpression abolishes 17AAG, PD184352/PX866 and PD184352/PI-103 enhancement of Ad.5 <i>mda-7/IL-24</i> toxicity in GBM6 cells .....	90
Figure 7.3: Ad.5- <i>mda-7</i> lethality is enhanced by combined inhibition of PI3K/MEK/mTOR pathways .....	92
Figure 7.4: Ad.5- <i>mda-7</i> lethality is enhanced by combined inhibition of PI3K/MEK/mTOR pathways in vivo .....	94
Figure 7.5: Inhibition of mTOR, PI3K, and MEK1/2 signaling enhances Ad.5- <i>mda-7</i> lethality in GBM cells .....	97
Figure 7.6.1: Inhibition of mTOR, PI3K, and MEK1/2 signaling enhances Ad.5- <i>mda-7</i> -induced inhibition of growth/survival in GBM cells – Trypan Blue Assay .....	100
Figure 7.6.2: Inhibition of mTOR, PI3K, and MEK1/2 signaling enhances Ad.5- <i>mda-7</i> -induced inhibition of growth/survival in GBM cells – Colony Formation Assay .....	101
Figure 7.6.3: Inhibition of mTOR, PI3K, and MEK1/2 signaling enhances Ad.5- <i>mda-7</i> lethality in GBM cells .....	102



Figure 7.7: Inhibition of JNK1-3 blocks MDA-7/IL-24 toxicity and any promotion of toxicity by small molecule kinase inhibitors .....	104
Figure 7.8.1: Activation of the intrinsic pathway plays a key role in the facilitation of Ad.5- <i>mda-7</i> toxicity by kinase inhibitors PD+PX.....	106
Figure 7.8.2: Activation of the intrinsic pathway plays a key role in the facilitation of Ad.5- <i>mda-7</i> toxicity by kinase inhibitor 17AAG .....	107
Figure 7.8.3: Activation of the intrinsic pathway plays a key role in the facilitation of Ad.5- <i>mda-7</i> toxicity by kinase inhibitors Rapamycin and PI-103+PD .....	108
Figure 7.9: Inhibition of signaling pathways enhances Ad.5- <i>mda-7</i> -induced autophagy, but does not promote additional activation of PERK .....	110
Figure 7.10: Inhibition of signaling pathways enhances Ad.5- <i>mda-7</i> -induced autophagy, with out promoting the additional activation of PERK .....	112
Figure 7.11: Knockdown of Beclin1 or ATG5 abolished Ad.5- <i>mda-7</i> toxicity and significantly reduced the abilities of 17AAG and to a lesser extent PD184352/PX866 exposure to cause cell death .....	114
Figure 7.12.1: Ad.5- <i>mda-7</i> /IL-24 sensitizes GBM 14 cells to radiation therapy and enhances survival <i>in vivo</i> .....	117
Figure 7.12.2: Ad.5- <i>mda-7</i> /IL-24 sensitizes GBM 14 cells to radiation therapy and enhances survival <i>in vivo</i> .....	118
Figure 7.13: Temozolomide (TMZ) potentiates Ad.5- <i>mda-7</i> lethality in GBM cells ....	120

Figure 7.14: Temozolomide (TMZ) potentiates Ad.5- <i>mda-7</i> lethality and radiosensitivity .....	122
Figure 7.15: Temozolomide (TMZ) potentiates Ad.5- <i>mda-7</i> lethality and radiosensitization .....	124
Figure 7.16.1: A tropism-modified type 5/type 3 adenovirus infects GBM 6 cells more readily than a type 5 adenovirus .....	127
Figure 7.16.2: A tropism-modified type 5/type 3 adenovirus infects U87 cells more readily than a type 5 adenovirus .....	128
Figure 7.17: A tropism-modified type 5/3 adenovirus infects GBM6, GBM12 and U87-MG cells more readily than a type 5 adenovirus, in a colony formation assay, to generate a greater cytotoxic effect .....	130
Figure 7.18.1: A tropism-modified type 5/3 adenovirus infects GBM6 cells more readily than a type 5 adenovirus, and enhances tumor killing <i>in vivo</i> .....	132
Figure 7.18.2: In isolated GBM6 tumor sections, at 2 and 7 days after infection, Ad.5/3- <i>mda-7</i> caused a greater and more rapid induction of tumor apoptosis than Ad.5- <i>mda-7</i> .....	133
Figure 7.19.1: Ad.5/3- <i>mda-7</i> is more effective at killing and reducing rodent GL261 glioma viability <i>in vitro</i> .....	135
Figure 7.19.2: Ad.5/3- <i>mda-7</i> is more effective at killing and reducing rodent GL261 glioma viability <i>in vivo</i> .....	136

Figure 7.19.3: Ad.5/3- <i>mda-7</i> is more effective at killing and reducing immune competent rodent GL261 glioma viability <i>in vivo</i> .....	137
---	-----

## List of Abbreviations

<b>Full Name</b>	<b>Abbreviation</b>
3-phosphoinositide-dependent Protein Kinase	PDK
Activator Protein 1	AP1
Adenosine Tri-phosphate	ATP
Adenosine Mono-phosphate	AMP
AKT8 Virus Oncogene Cellular Homolog	Akt
Apoptosis-inducing Factor	AIF
Apoptotic Protease-activating Factor 1	Apaf-1
B-cell Lymphoma 2	Bcl-2
B-cell Lymphoma-extra Large	Bcl-xL
BH3 Interacting-Domain death agonist	Bid
Binding Immunoglobulin Protein (Grp78)	BiP
c-Jun NH <sub>2</sub> -terminal kinase	JNK
Coxsackievirus and Adenovirus Receptor	CAR
Cyclic-AMP Response Element-Binding	CREB
Cytomegalovirus	CMV
Cytokine response modifier A	CrmA
Death Domain	DD
Death Effector Domain	DED
Death-inducing Signaling Complex	DISC

Dulbecco's Modified Eagle's Medium	DMEM
Dimethyl Sulfoxide	DMSO
Endoplasmic Reticulum	ER
Epidermal Growth Factor	EGF
Epidermal Growth Factor Receptor	EGFR
Ethylenediaminetetraacetic Acid	EDTA
Eukaryotic translation initiation factor 2 alpha	eif2 $\alpha$
Extracellular Signal-Regulated Kinase	ERK
FADD-like interleukin-1 $\beta$ -converting enzyme-like protease	FLIP
Fas-associated Protein with Death Domain	FADD
Fas Ligand	FasL
Fas Receptor	FasR
G-protein coupled receptors	GPCR
Glioblastoma multiforme	GBM
Glucose-regulated Protein 78	Grp78
Glutathione S-transferase	GST
Growth Arrest and DNA Damage Protein	GADD
Guanosine Diphosphate	GDP
Guanosine Triphosphate	GTP
Heat Shock Protein	Hsp
Horseradish Peroxidase	HRP
Induced Myeloid leukemia cell differentiation protein	Mcl-1

Inhibitor of apoptosis	IAP
Interferon	IFN
Interleukin	IL
Mammalian Target of Rapamycin	mTor
MAPK/ERK Kinase	MEK
MAP Kinase-activationg Death Domain	MADD
Melanoma Differentiation-associated 7	MDA-7
Micro ( $10^{-6}$ )	$\mu$
Microtubule-associated Protein 1 Light Chain 3	LC3
Milli ( $10^{-3}$ )	m
Mitogen Acitvated Protein Kinase	MAPK
Mitogen and Stress-activated Protein Kinase	MSK
Molar	M
3-[4,5-Dimethylthiazol-2-yl]-2,5-diphenyltetrazolium bromide	MTT
N-acetyl Cysteine	NAC
Nano ( $10^{-9}$ )	n
Nitric Oxide Species	NOS
p21-activated Kinase	PAK
Phosphate-buffered Saline	PBS
Phosphatidylinositol 3'-kinase	PI3K
Poly-(ADP-ribose) Polymerase	PARP
Preautophagosome	PAS

Protein Kinase C	PKC
Protein kinase-like ER kinase	PERK
Reactive Oxygen Species	ROS
Receptor Tyrosine Kinase	RTK
Ribosomal S6 Kinase	RSK
Serine/threonine-protein kinase/endoribonuclease	IRE1
Sodium Dodecyl Sulfate	SDS
Sodium Dodecyl Sulfate Polyacrylamide Gel Electrophoresis	SDS-PAGE
Sphingomyelinase	SMase
Sphingosine-1-Phosphapate	S1P
Stress-activated Protein Kinase	SAPK
Suberoylanilide Hydroxamic Acid	SAHA
Truncated Bid	tBid
TNF-receptor Associated Death Domain	TRADD
TNF-related Apoptosis-inducing Ligand	TRAIL
Transforming Growth Factor	TGF
Tris-buffered Saline plus Tween 20	TBST
Tumor Necrosis Factor	TNF
Tumor Necrosis Factor Receptor	TNFR
Unfolded Protein Response	UPR
X-chromosome Linked Inhibitor of Apoptosis	XIAP

## Abstract

### MDA-7/IL-24; A PROMISING CANCER THERAPEUTIC AGENT

By Hossein A. Hamed, BS

A Dissertation submitted in partial fulfillment of the requirements for the degree of Doctor of Philosophy at Virginia Commonwealth University.

Virginia Commonwealth University, 2012

Major Director: Paul Dent, Ph.D.  
Vice Chair, Department of Neurosurgery

Glioblastoma multiforme (GBM) is an aggressive cancer that affects millions of patients per year. Conventional therapies combining chemotherapeutic agents with radiation can only extend survival by a few months; therefore, there is a dire need for an effective means of treating this deadly disease. Melanoma differentiation-associated gene-7/interleukin-24 (*mda-7/IL-24*), currently in the early stages of FDA pre-IND drug trials, has proven to be an effective cancer specific cytokine, able to trigger the onset of mitochondrial dysfunction and/or autophagy. GBM's have mutations that often result in the activation of cytoprotective cell signaling pathways, preventing cancer therapeutics and even MDA-7/IL-24 treatments from being effective. Since the discovery of MDA-7/IL-24 a number of groups have shown toxic effects in a variety of tumor cells. However, the lethality of MDA-7/IL-24 is not enough to eradicate the tumor. We hypothesized two



rationales for this minimalistic effect. First, the MDA-7/IL-24 gene delivery mechanisms are not efficient or second, active pro-survival pathways are playing a role in protection. Here we have shown that the inhibition of cytoprotective cell-signaling pathways using small molecule inhibitors of mitogen-activated extracellular regulated kinase (MEK)1/2 and phosphatidyl inositol 3-kinase (PI3K) or AKT; mammalian target of rapamycin (mTOR) and MEK1/2; HSP90 inhibitor 17AAG; and the autophagy-inducing drug OSU-03012 (AR-12), enhances the toxicity of MDA-7/IL-24. In addition, the use of a modified recombinant adenovirus comprised of the tail and shaft domains of a serotype 5 virus and the knob domain of a serotype 3 virus expressing MDA-7/IL-24, Ad.5/3-*mda-7*, proved to be a more effective, CAR-independent means of infecting and killing GBM cells *in vitro* and *in vivo* when compared to Ad.5-*mda-7*. Collectively, our data demonstrate that the induction of autophagy and mitochondrial dysfunction by a combinatorial treatment approach represents a potentially viable strategy to kill primary human GBM cells.

## **CHAPTER 1 INTRODUCTION: GENERAL**

### **1.1 Cancer:**

Cancer (malignant neoplasm), is a group of diseases that stems from the unrestrained cell division of normal cells originating from almost any organ or tissue in the body. Under normal circumstances, cells are highly regulated by signaling processes necessary for the proper control of growth or death. A loss in this functionality can lead a normal cell to exhibit one of six recognized characteristics of a cancer cell. “The Hallmarks” of a cancer cell include: overactive cell proliferation signaling, loss of contact inhibition, resistance to cell death, resistance to growth suppressors and metastatic potential. On a daily basis, a normal cell is stressed to a certain degree by both internal (inherited mutations, hormones and immune conditions) and external factors (tobacco, infectious organisms, chemicals and radiation) potentially acting together to dysregulate the cells protective signaling machinery, promoting carcinogenesis.<sup>1</sup> This explains the staggering statistics presented this year by the National Cancer Institute; were nearly one-quarter of deaths occurring due to disease in the United States are cancer related, exceeded only by heart disease. Since 2008, cancer has been the leading cause of death worldwide, claiming the lives of over 7 million people.<sup>2</sup>

## **1.2 Glioblastoma multiforme:**

Globally, glioblastoma multiforme (GBM) often found in the posterior cranial fossa in children or the anterior two-thirds of the cerebrum in adults, is the most common and lethal malignant primary brain cancer, diagnosed in over 125,000 patients and claiming the lives of over 95,000 patients per year.<sup>2</sup> Even under optimal conditions, where essentially all of the tumor can be surgically removed and the patients maximally treated with radiation and chemotherapy, the mean survival of this disease is extended from a few months to one year, with a 5 year survival rate of only 5%.<sup>3</sup> The main reason for this poor prognosis is to the ability of GBM to invade brain tissue and to inherently develop drug resistance. Drug resistance has been shown by many groups to be due to, but not limited to, drug efflux, hypoxia, cancer stem cells, DNA damage repair machinery and miRNA's. In addition, much like all other cancers, GBMs have mutations that further enable their survival. For example, GBM6 cells contain a mutant variant III EGFR (Epidermal Growth Factor Receptor). This mutation has been shown to stimulate mTORC2 activity which in turn promotes NF- $\kappa$ B activity promoting cell growth, survival and resistance to chemotherapy. GBM14 cells contain a mutation that prevents the production of PTEN, a protein necessary for the inactivation of the pro-survival and growth signaling cascades involving AKT/mTOR. GBM12 cells possess a mutant active full-length EGFR. In this situation, the receptor, a tyrosine kinase receptor involved in the activation of the Raf/MEK/Erk signaling cascade is in a constant active state, leading to promotion of growth and survival

of these cancer cells.<sup>4,5</sup> Following surgery or drug treatment, the loss of inhibitory control and cross-talk of signaling pathways prevent the efficacy of cancer therapeutics and result in the return of a more invasive and aggressive cancer growth. These realities emphasize the need to further advance therapeutic intervention or create more effective modalities to combat this devastating and consistently fatal disease.

### **1.3 Conventional Treatments:**

Various treatments for cancer exist, each dependent upon the type and/or stage of the cancer. Treatment options for GBM include:

1. Surgery (removal of the tumor) via craniotomy, is not always possible if access to the tumor is impeded or if the cancer has metastasized.
2. Radiation therapy (also called irradiation) in which ionizing radiation is used to kill cancer cells and shrink the tumor. The effects of radiation therapy are not localized and/or confined to only the tumor. Ionizing radiation damages the genetic material of a cell by way of dislodging electrons from atoms impacted by it; generating damaging ions within the cells. Unfortunately, it will also damage the DNA of healthy cells; this is the reason why radiation is given in small fractions to allow for damaged non-tumor cells time to recover proper functionality.
3. Chemotherapy, treatment with drugs that can destroy cancer cells. This term refers to cytotoxic drugs which affect rapidly dividing cells but are not specific for cancer cells, also harming healthy tissue. More recently, specific targeting

chemotherapeutic agents are being sought after to reduce the unwanted side-effects to this effective mode of tumor cell killing, such as Temazolomide (TMZ).<sup>6</sup>

4. Combination Therapy; combining drugs that have different modes of action and different toxicities. One advantage of combination therapy is that it may delay or prevent drug resistance.<sup>1</sup> Another advantage lies in obtaining synergistic killing of tumor cells, with minimal exposure to treatments such as radiation and/or chemotherapeutic agents; ultimately, reducing the presently observed side effects of conventional therapies.

#### **1.4 Gene Therapy and MDA-7/IL-24**

The advent of gene therapy has proven partially successful for the treatment of tumor cells. Recombinant viruses containing specific gene modulating properties, such as tumor suppressor genes or genes involved in production of toxic cytokines, have shown to be partially effective in reducing tumor cell growth and survival.<sup>7</sup> Other modestly successful approaches include the use of modified forms of adenoviruses that are selectively replicative and initiate their lytic cycles only when found within a tumor cell and not in normal non-transformed cells.<sup>8</sup> Thus although promising, gene therapy has yet to truly make an significant impact in cancer therapy.

The *mda-7* gene (recently renamed Interleukin 24, IL-24) was isolated from human melanoma cells induced to undergo terminal differentiation by treatment with fibroblast interferon and mezerein.<sup>9</sup> The RNA and protein expression of MDA-7/IL-24, a member of the interleukin-10 (IL-10) gene family,<sup>10,15-18, 22-26</sup> is decreased in advanced melanomas,

with nearly undetectable levels in metastatic disease.<sup>27-29</sup> Enforced expression of MDA-7/IL-24, in tumor cells, by use of a recombinant adenovirus Ad.*mda-7*, inhibits growth and kills a broad spectrum of cancer cells, without exerting any harmful effects in normal human epithelial or fibroblast cells.<sup>14-18,22,23</sup> In view of the potent cancer-specific, apoptosis-inducing and tumor growth-suppressing properties of MDA-7/IL-24 in human tumor xenograft animal models, *mda-7*/IL-24 has been evaluated in a Phase I clinical trial in patients with advanced cancers.<sup>15,16,18,24-26</sup> This study indicated that Ad.*mda-7* injected intra-tumorally was safe and with repeated injection, manifested noteworthy clinical activity in 44% of the treated patients. This is particularly notable because the patients in this trial had already been exposed to multiple different chemotherapies and would be predicted to have a high inherent level of resistance to any additional therapeutic.

The apoptotic pathways by which Ad.*mda-7* leads to cell death in tumor cells are not fully understood. However, current data suggests an intrinsic complexity and a contribution of proteins central for the onset of growth inhibition and apoptosis, including BCL-XL BCL-2 and BAX.<sup>14-18,22,23</sup> In human melanoma cell lines, but not in normal melanocytes, Ad.*mda-7* infection induces a significant decrease in both BCL-2 and BCL-XL levels, with only a modest up regulation of BAX and BAK expression.<sup>27</sup> This data supports the hypothesis that Ad.*mda-7* increases the ratio of pro-apoptotic to anti-apoptotic proteins in cancer cells, thereby facilitating induction of apoptosis.<sup>15-18,22,23,27</sup> The ability of Ad.*mda-7* to promote apoptosis in DU-145 prostate cancer cells, which do not produce BAX, indicates that MDA-7/IL-24 can initiate apoptosis in tumor cells through a BAX-independent pathway.<sup>15-18,22</sup> In prostate cancer cells, overexpression of either BCL-2 or

BCL-XL protects cells from Ad.*mda-7*-induced toxicity in a cell type-dependent fashion.<sup>28</sup> In a single ovarian cancer cell line, MDA-7/IL24 was reported to kill via the extrinsic apoptosis pathway.<sup>29</sup> Accordingly, MDA-7/IL-24 toxicity appears to occur by multiple distinct pathways in different cell types, but in all of these studies cell killing is associated with a profound induction of mitochondrial dysfunction.<sup>30</sup>

More recently, MDA-7/IL-24 toxicity has been coupled with alterations in endoplasmic reticulum stress signaling.<sup>31</sup> In these studies; MDA-7/IL-24 physically associates with BiP/GRP78 and nullifies the protective actions of this ER-chaperone protein. In addition to virus-administered *mda-7*/IL-24, cancer-specific killing is retained by delivery of this cytokine as a bacterially expressed GST fusion protein, GST-MDA-7.<sup>32</sup> In addition, selective ER localization and similar signal transduction changes in cancer cells is also seen.<sup>31</sup> We have found that a high concentration of GST-MDA-7 kills primary human glioma cells and does so in a PERK-dependent fashion that is dependent upon elevated levels of autophagy and mitochondrial dysfunction.<sup>34-36</sup>

The ability of MDA-7/IL-24 to modulate cell-signaling processes in transformed cells has been examined by several laboratories.<sup>22-40</sup> Prior work by our group has shown, using bacterially synthesized GST-MDA-7 protein,<sup>32</sup> that in the 0.25– 2.0 nM concentration range GST-MDA-7 primarily produces growth arrest with minimal cell killing. Whereas, at ~20-fold greater concentrations, this cytokine causes profound growth arrest and tumor cell death.<sup>32,35,36</sup> Our group have also demonstrated that Ad.*mda-7* kills melanoma cells in part by promoting p38 MAPK-dependent activation of growth arrest and DNA damage inducible genes, including GADD153, GADD45 and GADD34.<sup>38</sup>

However, in primary GBM cells, it was noted that p38 MAPK signaling provided a protective signal.<sup>28</sup> Other groups have argued that inhibition of PI3K signaling, but not ERK1/2 signaling, modestly promotes Ad.*mda-7* lethality in breast and lung cancer cells.<sup>39,40</sup> (Figure 1.1 and 1.2)

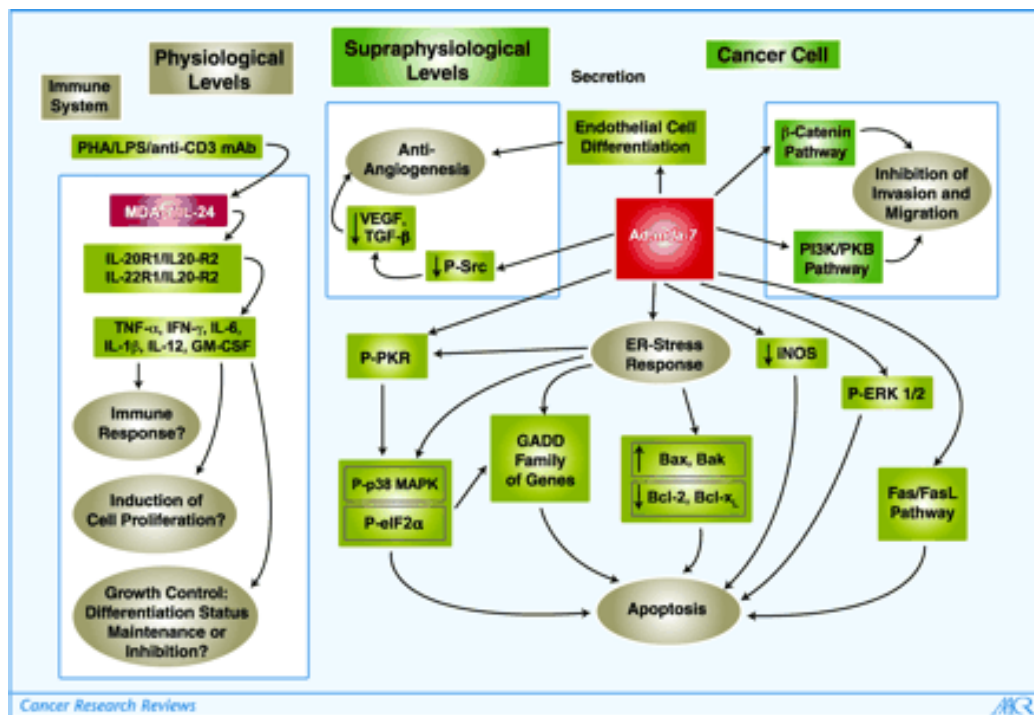
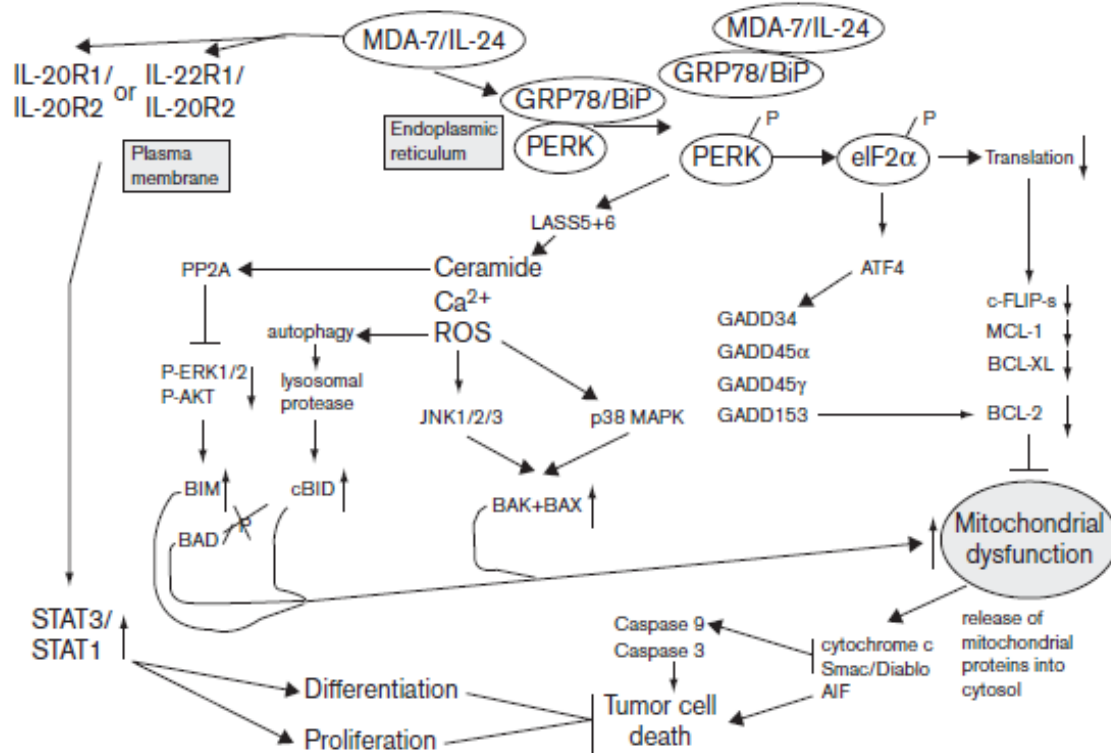


Figure 1.1 – Signaling pathways associated with Ad. *mda-7* and MDA-7/IL-24 activity.<sup>17</sup>





**Figure 1.2 – Signaling pathways associated with MDA-7/IL-24.**<sup>154</sup>

Although promising, the delivery of therapeutic genes using a serotype 5 (Ad.5) virus vector has shown limitations in treating GBMs. This limited potential is due to the dependence of the adenoviruses on expression of the Coxsackie adenovirus receptor (CARs) for virus entry. Multiple groups have shown that the use of a tropism-modified adenovirus that e.g. uses a serotype 3 modification of the viral knob protein, can better facilitate the delivery of *mda-7/IL-24* in a CAR-independent manner (Ad.5/3 vector).<sup>41,42</sup> A tropism modification, may provide a means of developing an improved therapy for GBM, a currently consistently fatal cancer.

### 1.5 Raf/MEK/ERK Mitogen-activated protein kinase (MAP) pathway

Targeted-based therapies are considered to be the future of cancer treatment and much attention has been focused on the development of inhibitors of the Raf/MEK/ERK MAP kinase pathway. The Raf/MEK/ERK MAP kinase pathway is commonly dysregulated in cancer cells.<sup>43-45</sup> There are four well characterized MAPKs. Each cascade consists of three proteins that act as a relay mainly by phosphorylation signaling. There is a MAPK kinase kinase (MAPKKK, MAP3K), a MAPK kinase (MAPKK, MAP2K), and a MAPK. The terminal serine/threonine kinases (MAPKS) comprises, ERK1/2, c-Jun NH<sub>2</sub>-terminal kinase (JNK1/2), p38, and ERK5 (Figure 1.3). Activation of the ERK1/2 pathway is often associated with cell survival, whereas JNK, p38, and ERK5 are activated by stress and growth factors.<sup>45,46</sup> Although the mechanisms by which ERK1/2 activation promote survival are not fully characterized, a number of anti-apoptotic effector proteins have been identified, including increased expression of anti-apoptotic proteins such as c-FLIP, Bcl-xL, XIAP, and Mcl-1.<sup>44,47-51</sup>

In the ERK MAPK module, Ras is a small GTP-binding protein which acts as the molecular switch that controls this signaling pathway. There are four Ras proteins, namely H-Ras, N-Ras, Ki-Ras 4A and Ki-Ras4B. Ras is mutationally activated in a variety of cancers, though not in GBM, and this leads to persistent activation of downstream effectors.<sup>52</sup> In normal quiescent cells, Ras is inactivated (GDP-bound). Extracellular stimuli (i.e. EGF), induce the exchange of guanosine diphosphate (GDP) for guanosine triphosphate (GTP) which converts Ras into its active conformation. In many tumors that express wild type Ras proteins, the wild type protein is often constitutively active due to

the upstream actions of receptor tyrosine kinases e.g. expression of EGFR vIII. This process relies on the recruitment of GDP/GTP exchange factors to the cell membrane. Guanine nucleotide exchange factors (GEFs; i.e. Sons of Sevenless, SOS) promote formation of active Ras-GTP, whereas GTP activating proteins (GAPS) stimulate GTP hydrolysis and formation of inactive Ras-GDP.<sup>45</sup> Ras activation leads to the recruitment and activation of the MAPKKK (MAP3K), Raf serine/threonine kinases (c-Raf-1, B-Raf, and A-Raf). Activation of Raf kinases is a multistep process that involves dephosphorylation of inhibitor sites by protein phosphatases 2A (PP2A) as well as phosphorylation of activating sites by PAK (p21 activated kinase). The regulatory mechanisms of various isoforms differ in that A-Raf and C-Raf-1 require additional phosphorylation reactions for activity whereas B-Raf has a much higher level of basal kinase activity. B-Raf is mutated in many cancers making it constitutively active.<sup>45</sup> Raf kinases phosphorylate and activate MAPKKs, MEK1/2. MEK1/2 then phosphorylates and activates ERK1/2 MAPKs.<sup>53,54</sup> Active ERKs phosphorylate numerous cytoplasmic and nuclear targets regulating processes such as proliferation, differentiation, and survival (Figure 1.4).<sup>45</sup>

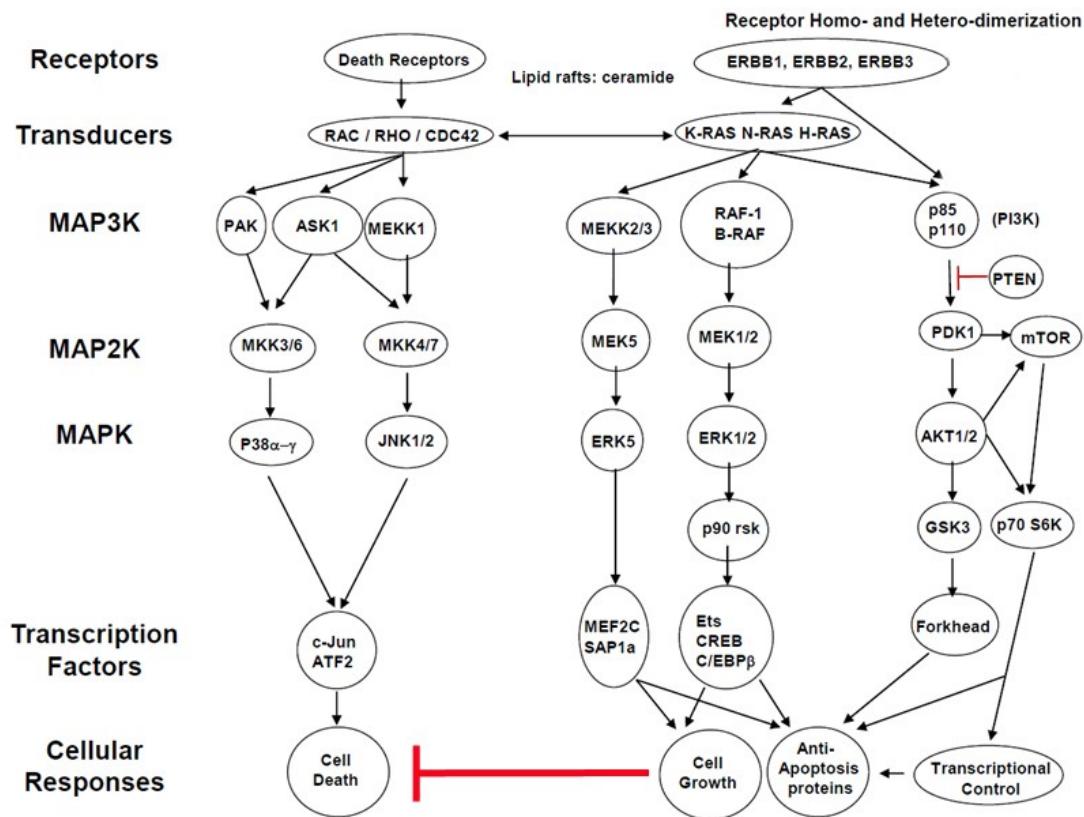


**Figure 1.3. Mammalian MAPK cascades.** There are four major mammalian protein kinase cascades; each consists of a MAPKKK, MAPKK, and MAPK. The ERK1/2 pathway is the activated by growth factors, whereas the JNK and p38 pathways are activated by environmental stressors such as ionizing radiation.<sup>45</sup>

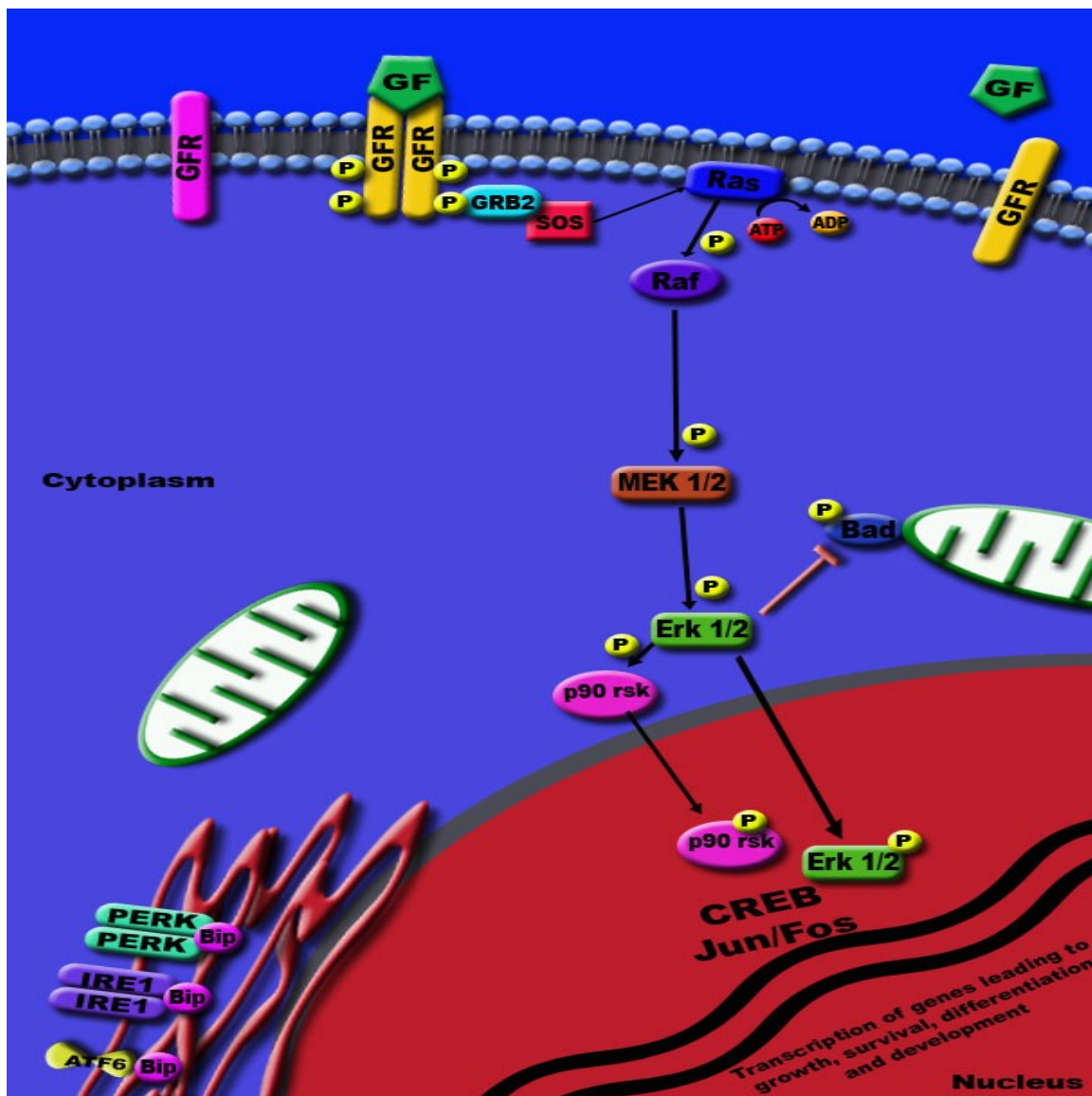


**Figure 1.4. Activation of the Raf/MEK/ERK Mitogen-activated protein kinase (MAP) pathway.** The binding of a growth factor to a growth factor receptor induces receptor dimerization and autophosphorylation on tyrosine residues. These phosphotyrosines are docking sites for signaling molecules which include Grb2-SOS complex. This complex activates the small G-protein Ras by stimulating the exchange of guanosine diphosphate (GDP) for guanosine triphosphate (GTP). Ras undergoes a conformational change which enables it to recruit Raf-1 from the cytosol to the cell membrane and bind to it where Raf-1 becomes active. Activated Raf-1 phosphorylates and activates MEK1/2 which in turn will phosphorylate and activate ERK1/2. Activated ERK may translocate to the nucleus to control gene expression of transcription factors promoting growth, differentiation, and cellular development.<sup>45,53,55</sup>

## 1.6 JNK1/2 MAPK Pathway

JNK1/2 pathway signaling often causes apoptosis. JNK activation is much more complex than that of the ERK1/2 pathway owing to inputs by a greater number of MAPKKs (at least 13, including MEKK1 (MAP/ERK Kinase-Kinase-1)-MEKK4 (MAP/ERK Kinase-Kinase-4), ASK (Apoptosis Signal-regulating Kinase), and MLKs (Mixed-Lineage Kinases), which are activated by upstream Rho-family GTPases. These phosphorylate and activate MAPKKs MEK4 (MAPK/ERK Kinase-4) and MEK7 (MAPK/ERK Kinase-7), which further phosphorylate and activate JNKs. JNK activation requires dual phosphorylation of tyrosine and threonine residues. The JNK family consists of JNK 1, 2, and 3 (also known as SAPK $\gamma$ , SAPK $\alpha$ , and SAPK $\beta$ , respectively). JNK 1 and 2 are ubiquitously expressed, whereas JNK 3 is restricted to the brain, heart, and testis.<sup>56</sup>

JNKs (MAPKs) are primarily activated in response to cytokines, UV irradiation, DNA-damaging agents, growth factor deprivation, and to a lesser extent, serum, and G-protein coupled receptors. The JNKs are able to translocate to the nucleus following stimulation. JNKs are generally thought to be involved in inflammation, proliferation and apoptosis. Accordingly, its substrates are transcription factors and pro- and anti-apoptotic proteins. One well known substrate of JNK is the transcription factor c-Jun. Others include Elk1, p53, ATF2 (Activating Transcription Factor-2), NFAT4 (Nuclear Factor of Activated T-Cell-4), and NFAT1 (Nuclear Factor of Activated T-Cell-1). JNK mediates apoptosis not only through its effects on gene transcription, but also through a transcriptional-independent mechanism. For example, JNK1 directly phosphorylates Bcl-2

(B-Cell CLL/Lymphoma-2) in vitro, co-localizes and collaborates with Bcl-2 to mediate cell death. JNK can also phosphorylate the pro-apoptotic protein Bim and Bmf to promote their pro-apoptotic effects.<sup>57</sup> JNK cascade can also phosphorylate and activate HSF1 (Heat Shock Factor-1) and JNK-mediated phosphorylation of HSF1 selectively stabilizes the HSF1 protein and confers protection to cells under conditions of severe stress.<sup>45</sup> Thus, JNKs have opposing roles in promoting proliferation and transformation and inducing apoptosis.

### **1.7 p38 MAPK Pathway**

In a similar manner to that of the JNK1/2 pathway, the p38 MAPK pathway is activated by numerous cellular stresses. The p38 module consists of several MAPKKKs; these include TAK1, ASK1/2, DLK, MEKK1-4, MLK2 and -3, and Tpl-2. The MAPKKKS phosphorylate and activate MAPKKs, MEK3 and MEK6. These MAPKKs show a high degree of specificity toward p38 as they do not activate JNK or ERK1/2. MEK4 however, activates both JNK and p38 and can thus be seen as a site of integration for the p38 and JNK pathways.<sup>45</sup> The MAPKKs phosphorylate and activate MAPK p38 pathway. There are four isoforms of p38,  $\alpha$ ,  $\beta$ ,  $\gamma$ , and  $\delta$ . p38 $\alpha$  and p38 $\beta$  are ubiquitously expressed while p38 $\gamma$  and p38 $\delta$  are differentially expressed in certain tissues. All p38 kinases have dual phosphorylation sites. MEK6 activates all p38 isoforms, but MEK3 selectively phosphorylates the p38  $\alpha$  and p38 $\beta$  isoforms.<sup>58</sup>

The p38 MAPK pathway has a diverse role in the signaling of cellular responses that varies with cell type and stimulus. Transcription factors that regulate inflammatory

gene expression are phosphorylated and activated by p38. A protein kinase termed MAP kinase-activated protein kinase 2 (MAPKAP2) is phosphorylated by p38 and is also involved in many cellular processes including stress and inflammatory responses, nuclear export, gene expression regulation and cell proliferation. Heat shock protein HSP27 (a chaperone) was shown to be one of the substrates of this kinase *in vivo*. Other substrates of p38 include p53, involved in tumor suppression and cell cycle regulators such as CDC25A, B, and C. p38 has also been implicated in other cellular responses such as cell death, development, and cell differentiation.<sup>59</sup>

### 1.8 PI3-Kinase/Akt Pathway

The phosphatidylinositol 3'-kinase (PI3-K)/ Akt signaling is regarded as a pro-survival pathway in cells. PI3Ks are a family of intracellular lipid kinases that phosphorylate the 3'-hydroxyl group of phosphatidylinositols and phosphoinositides. PI3Ks are heterodimeric kinases that are composed of a regulatory and catalytic subunit that are encoded by different genes. PI3Ks are classified into three groups, class I, II, and III based on structure and function.<sup>60</sup>

Class I PI3Ks phosphorylate the lipid phosphatidylinositol 4, 5, bisphosphate (PIP<sub>2</sub>) to generate the second messenger phosphatidylinositol 3, 4, 5, trisphosphate (PIP<sub>3</sub>). The class I PI3Ks can be further subdivided according to the signaling receptors that activate them. Class IA PI3Ks are activated by growth factor receptor tyrosine kinases (RTKs), and class IIB PI3Ks are activated by G-protein coupled receptors (GPCRs). The regulatory subunit of class IA is p85 (with three isoforms: p85 $\alpha$ , p85 $\beta$ , p55 $\gamma$ ). The catalytic subunit



of class IA is p110 (also with three isoforms:  $\alpha$ ,  $\beta$ ,  $\gamma$ ). Class IB members consist of a p101 regulatory subunit and a p110 $\gamma$  catalytic subunit.<sup>60</sup> Class II and class III PI3Ks phosphorylate phosphatidylinositol (PI) to generate PIP<sub>3</sub>. Class II PI3Ks bind clathrin coated pits and may function in membrane trafficking or receptor internalization.<sup>61</sup> VPS34 is the only mammalian class III PI3K and acts as a sensor signaling to mammalian target of rapamycin (mTOR) to regulate cell growth and autophagy in response to low nutrient pools.<sup>62</sup> Class IA however, is the only PI3K class that has been demonstrated to be clearly involved in oncogenesis.<sup>60</sup>

Upon ligand binding to RTKs, RTKs dimerize and autophosphorylate at tyrosine residues. This allows them to interact with Src homology 2 (SH2) domain containing molecules. PI3K can be activated by three independent pathways. In one activation pathway, PI3K p85 regulatory subunit binds directly to tyrosine motifs within the RTK triggering activation of PI3Ks catalytic subunit. Another pathway consists of the adapter protein GRB2 which binds preferentially to phosphotyrosine motifs in the RTK. GRB2 can bind to the scaffolding protein GAB (GRB2-associated binding protein), which can bind to p85. GRB2 can also bind to SOS and activate RAS. RAS can activate p110 independently of p85.<sup>63</sup> When PI3K is activated it results in the generation of PIP<sub>3</sub>. 3'-phosphoinositide dependent kinase 1 (PDK1) and Akt preferentially bind to PIP<sub>3</sub> (by recruitment to the membrane) which lead to Akt activation depending on its phosphorylation at Ser473 or Thr308 sites by PDK1. Phosphatase tensin homolog (PTEN), a protein frequently absent in GBM cells, is a negative regulator of PI3-K pathway that converts PIP<sub>3</sub> back to PIP<sub>2</sub>.<sup>5,60,63</sup> Akt (also known as protein kinase B, PKB)

phosphorylates Bad at Ser136 preventing cytochrome c release. Akt also phosphorylates caspase 9 at Ser196, causing a conformational change that results in the inhibition of its proteolytic activity (Figure 1.5). The overall result is protection from apoptosis and increased proliferation, events that favor tumorigenesis.<sup>64</sup>

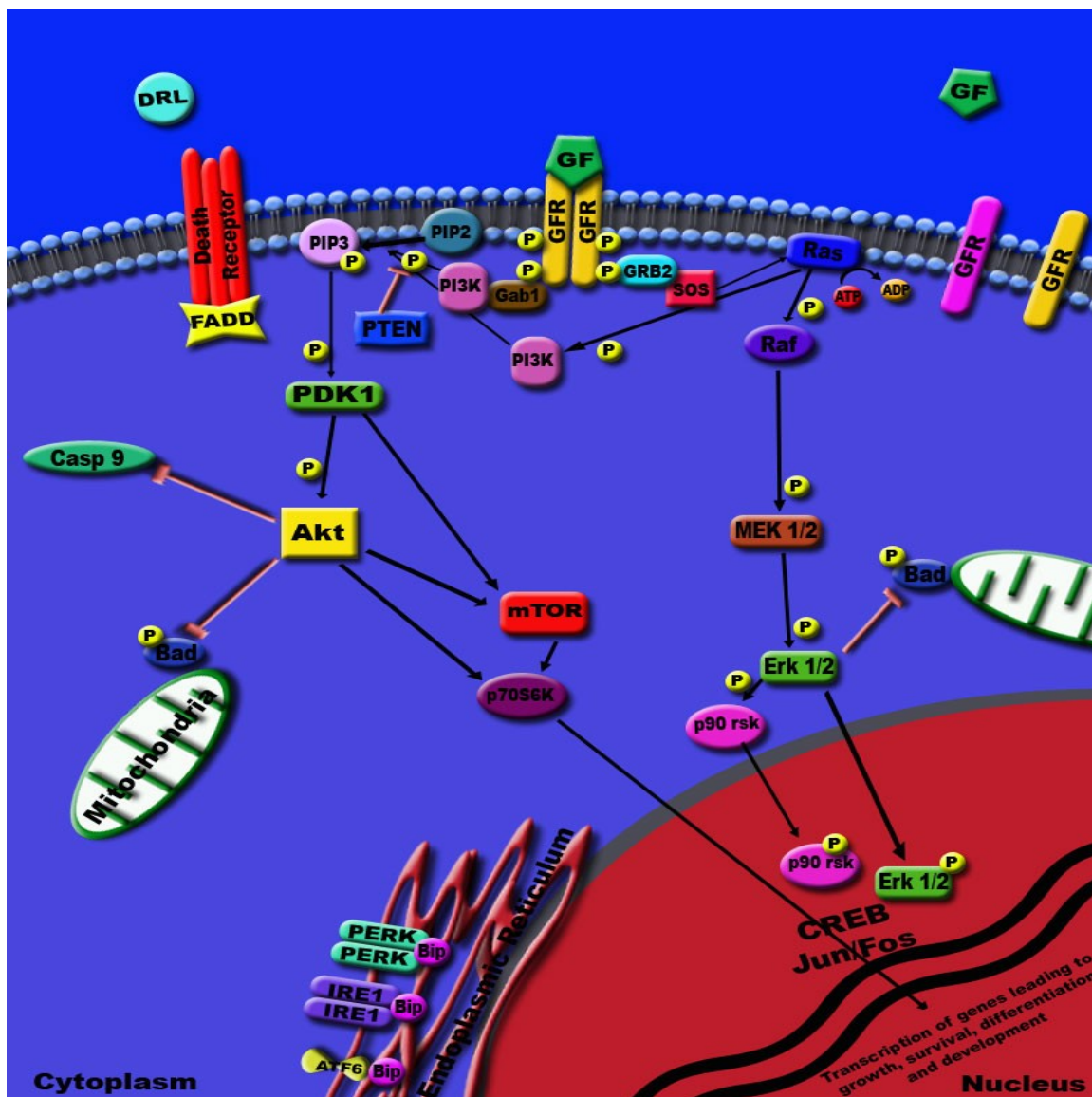


**Figure 1.5. Model of PI3K/Akt Pathway Activation.** In response to extracellular stimuli (i.e. growth factors), the catalytic subunit of PI3K (p110) is recruited to receptor tyrosine kinases (RTKS) at the membrane through its regulator subunit (p85). PI3K phosphorylates phosphatidylinositol 4, 5, bisphosphate (PIP<sub>2</sub>) to generate the second messenger phosphatidylinositol 3, 4, 5, trisphosphate (PIP<sub>3</sub>). PIP<sub>3</sub> recruits serine/threonine Akt and 3-phosphoinositide dependent kinase (PDK1) to the membrane. Membrane bound Akt is rendered fully active through its phosphorylation by PDK1. Activated Akt may phosphorylate a variety of substrates thereby activating growth and pro-survival proteins or inhibiting targets important for cellular growth control and apoptotic responses.<sup>60,64,65</sup>

### **1.9 Receptor Tyrosine Kinases - ERBB receptor family proteins:**

This family of proteins consists of four members: ERBB1 (EGFR), ERBB2 (Her2), ERBB3 and ERBB4; upon ligand binding, these proteins can homo- or heterodimerize and autophosphorylate tyrosine residues found on their cytosolic domains. These residues serve as docking sites for SH2 domain proteins that feed into the ERK1/2 and Akt pathways, molecules that can act as mediators of downstream intracellular signaling pathways.<sup>66</sup> Once activated these molecules lead to the propagation of survival signaling as well as the down regulation of pro-apoptotic BH3 domain proteins: BIM, BAD and BAK. ERBB1 receptor over expression is found in over 60% glioblastoma multiforme patients.<sup>70</sup> Deregulation of ERBB receptor signaling in many forms of aggressive cancer cells, justifies the current NIH funded studies directed at controlling and inhibiting these receptors as therapeutic cancer treatment schemes. Clinical techniques geared towards the inhibition of ERBB receptor activation include: 1) monoclonal antibodies (Trastuzumab) that prevent ligand binding and subsequent activation;<sup>67</sup> 2) quinazoline-derived small-molecule inhibitors that prevent ATP binding to the kinase domains of receptors, preventing downstream signaling protein activation; and 3) siRNA knockdown of receptor gene expression.<sup>66,71,72</sup> Lapatinib has been shown to inhibit ligand receptor binding to ERBB1/2 receptors while Sorafenib not only inhibits growth factor receptors, but also downstream activated intracellular proteins i.e. Raf family kinases.

### **1.10 Apoptosis: Extrinsic and Intrinsic Pathways**

Apoptosis is an energy-dependent process involving the transcription of specific proteins leading to a controlled form of cell death. The induction of apoptosis signaling can occur via the activation of either the extrinsic pathway, a receptor-mediated form of cell death, or the intrinsic pathway, a mitochondrially-mediated form of cell death. In many cancers, the up-regulation of pro-survival receptor tyrosine kinases and their unregulated activation can serve as major mechanisms of promoting drug resistance by way of up-regulation of pro-survival BCL-2 family proteins and down regulation of pro-death BH3-only proteins.<sup>73</sup>

Both extrinsic and intrinsic pathways have a common group of cysteine dependent aspartate specific proteases called procaspases, which require activation to become full caspases and carry out the cleaving of cellular substrates that result in biochemical and morphological changes. Biochemical processes include the externalization of phosphatidylserine on the cell surface. The morphological changes during apoptosis include chromatin condensation, cytoplasmic shrinkage, membrane blebbing, and phagocytosis of the cell or the cell breaks apart forming apoptotic bodies.<sup>74</sup>

The extrinsic pathway involves engagement of death receptors that belong to the tumor necrosis factor receptor (TNF-R) family. Death receptors are activated by their natural ligands, TNF family. Members of the TNF receptor family share similar cysteine-rich extracellular domains and have a cytoplasmic domain called the “death domain”. Death receptors include CD95 (Fas), TRAIL-R1 (APO-2, DR4), TRAIL-R2 (DR5,

KILLER, TRICK2), TNF-R1 (CD120a), and DR3 (APO-3, LARD, TRAMP, WSL1). Among these receptors, CD95 is the best characterized death receptor.<sup>75</sup>

Fas is a 45-kDa Type I transmembrane protein, which, like many members of the TNF/NGF superfamily, contains a number (three in the case of Fas) of cysteine-rich repeats in its extracellular domain. Such cysteine repeats serve as recognition sites for respective ligands, disruption of these repeats leads to the loss of ligand binding and effector signaling. The Fas receptor is ubiquitously expressed on a variety of normal cells, including activated T- and B-cells, hepatocytes, and ovarian epithelial cells, although regulated expression has been reported in various systems. High levels of Fas expression have also been detected on solid tumors of the breast, ovary, colon, prostate, and liver. In contrast, FasL is a Type II cell surface glycoprotein of 40 kDa, which has a cytosolic N-terminus and an extracellular C-terminus. FasL expression is limited, but has been detected on activated T-cells, natural killer cells, Sertoli cells of the testis, and the corneal epithelium and the retina of the eye. Some tumors also express FasL, which may be a mechanism to escape immune surveillance. Metalloproteinase-mediated shedding of membrane-bound FasL as a soluble form from effector cells, is believed to serve as a mechanism of turning off apoptosis in bystander cells.<sup>75</sup>

Ligation of Fas with FasL (expression of which can be on the same or different cells) triggers the combination of Fas monomers into trimeric Fas-complexes. Trimer formation is critical for effector function. The intracellular domain of Fas contains a stretch of 80 amino acids known as the death domain (DD). The DD enables the recruitment and construction of a multi-protein death-inducing signaling complex (DISC), following Fas

trimerization. DISC formation appears to be required for Fas-mediated apoptosis, as it both serves as a central relay station to downstream signaling proteins and more importantly, provides docking sites for critical effectors in the Fas-death pathway. Immediately following Fas/FasL ligation, there is recruitment of the serine-phosphorylated adapter Fas-associated DD (FADD)/MORT1. Fas/FADD interaction is co-ordinated through the highly conserved DD motifs found in both proteins. The presence of a functional FADD is critical for Fas-mediated apoptosis, whereby the expression of a dominant-negative FADD completely abrogates Fas-induced cell death. Moreover, *in vivo* studies have revealed a substantial attenuation of lymphocyte death in mice lacking FADD. FADD serves as a bridge between Fas and downstream molecules, such as Fas-like interleukin (IL)-1 $\beta$  converting enzyme (FLICE)/procaspase-8 $\alpha/\beta$ . FADD is a true adapter protein in that it harbors an N-terminal DD along with a C-terminal death effector domain (DED). Its unique structure enables FADD to proximally bind Fas on one end, while being able to distally recruit FLICE on the other.<sup>76</sup> The caspases that are recruited to the DISC are caspase 8 and caspase 10, which are the initiator caspases. Once these are activated, caspase 8 can cleave Bid and the intrinsic pathway is initiated, or caspase 8 can directly lead to the activation of executioner caspases (caspase 3, 6, and 7). The active executioner caspases cleave death substrates leading to apoptosis (**Figure 1.6**).<sup>74</sup>

The intrinsic apoptotic pathway involves non-receptor mediated stimuli that produce mitochondrial initiated events. Examples include radiation, hypoxia, free radicals, and hyperthermia. All of these stimuli cause changes in the inner mitochondrial membrane that result in mitochondria permeability.<sup>74</sup> The members of the Bcl-2 family regulate the

intrinsic pathway. Bcl-2 family members are divided into three subfamilies based on their function and structure: (1) anti-apoptotic proteins (Bcl-2, Bcl-xL, Bcl-w, Mcl-1, A1/Bfl1, Boo/Diva, NR-13) that have four BCL-2 homology domains, (2) pro-apoptotic members of the Bax subfamily that have three BH domains (Bax, Bak, Bok/Mtd) and (3) the BH-3 only pro-apoptotic proteins (Bik, Bad, Bid, Blk, Hrk, MimL, BNIP3, NOXA, PUMA). The BH-3 domain is present in all members and is essential for heterodimerization among members and is the minimum domain required for apoptotic function.<sup>77</sup> Activation of the mitochondrial pore formation and release of cytochrome c is by the Bcl-2 family member, Bid. Bid is cleaved by active caspase 8 and translocates to the mitochondria. Bid inserts into the membrane and activates Bax and Bak leading to mitochondrial membrane permeabilisation and release of cytochrome c. Cytochrome c binds the apoptotic protease activating factor 1 (Apaf-1) to form the apoptosome. At the apoptosome, the initiator caspase, caspase 9 is activated. This activation leads to the cleavage and activation of executioner caspases converging to the final common pathway leading to cell death **(Figure 1.6).**<sup>78</sup>



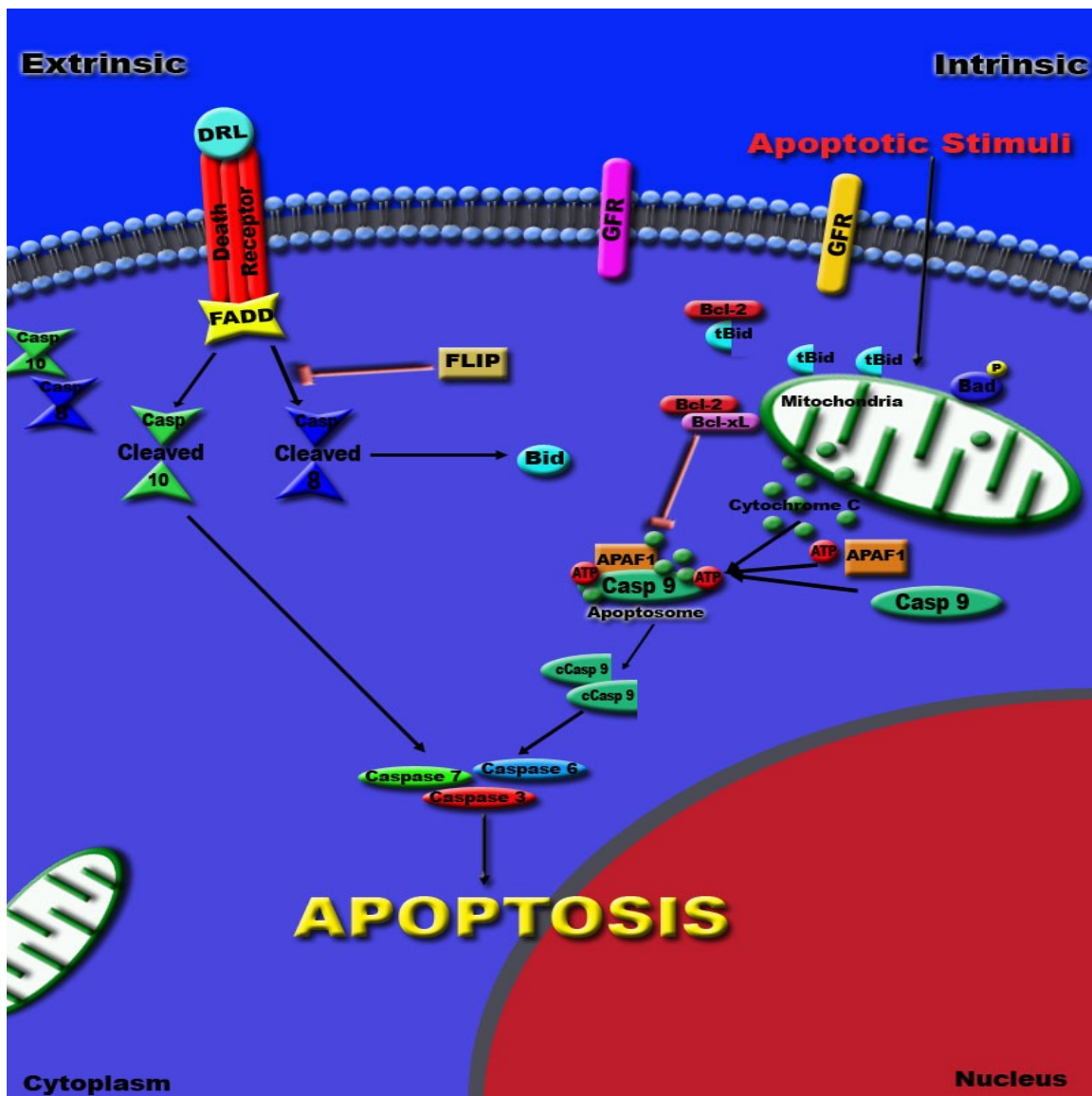


**Figure 1.6. The Apoptosis Signaling Pathways.** Apoptosis can be initiated by two pathways, the extrinsic pathway through death receptors or the intrinsic pathway through the mitochondria. In both pathways, induction of apoptosis leads to the activation of an initiator caspase (caspase 8 or 10 for the extrinsic pathway, and caspase 9 for the intrinsic pathway), and activation of executioner caspases, leading to the common pathway of cell death.

### 1.11 Regulation of Apoptosis Signaling

Death receptor mediated apoptosis can be inhibited by a protein named c-FLIP (FADD-like interleukin-1  $\beta$ -converting enzyme-like protease). Three splice variants have been identified in humans. One termed v-FLIP is found only at the mRNA level, whereas the long form (FLIP<sub>L</sub>) and a short form (FLIP<sub>S</sub>) are found at the protein level and share structural homology with procaspase-8, but lack catalytic activity. This structural homology can allow FLIP to bind to FADD and caspase 8, rendering them ineffective.<sup>76</sup>

Anti-apoptotic member, Bcl-2 suppresses cytochrome c release, thereby enhancing cell survival. Bcl-xL interacts with Apaf-1 to prevent the activation of executioner caspases and subsequent apoptosis. Bak is maintained in an inactive state on the surface of the mitochondria by binding of Mcl-1 or Bcl-xL until an apoptotic stimulus occurs. The depletion of Mcl-1 in some cells permits Bak oligomerization, activation, and apoptotic cell death.<sup>79</sup>

Inhibitor of apoptosis (IAP) proteins directly bind and inhibit caspases 3, 7, and 9. There are eight mammalian members of the IAP family which include: XIAP, c-IAP1, c-IAP2, NAIP, ILP-2, survivin and ML-IAP. There are three proteins that are negative regulators of IAP proteins, which include, XIAP-associated factor (XAF1), Second mitochondrial activator of caspases/direct IAP binding protein with low pI (Smac/DIABLO), and Omi/HtrA2. These proteins can bind to IAPs and abolish their anti-apoptotic function. XAF1 accumulates in the nucleus and can sequester XIAP from the cytosol. Smac/Diablo and Omi/HtrA2 are located in the mitochondria and are released into the cytosol upon apoptotic stress.<sup>80</sup>

### 1.12 Autophagy: Function and Process

Autophagy is a process of lysosomal protein degradation in which the cell “eats” itself. Autophagy serves as an evolutionary conserved survival mechanism in virtually all eukaryotic cells by providing a way for cells to dispose of damaged or aging organelles and proteins and allow for the recycling of molecules. However, autophagy can become deleterious to cells when upregulated and may play a role in cell death, commonly referred to as type II programmed cell death.<sup>81</sup> Autophagy can be separated into three types, macroautophagy, microautophagy, and chaperone-mediated autophagy. The focus of the work in this study will be on macroautophagy (hereafter termed autophagy) because this is the most characterized and best understood form of autophagy.<sup>82</sup>

The first stage of autophagy is vesicle nucleation and begins with a crescent shaped double membrane vesicle forming that appears in the cytoplasm. This membrane continues to elongate, entering the elongation stage, while gathering cytoplasmic cargo until it closes forming an autophagosome. The formation of the autophagosome constitutes the completion stage. The docking and fusion stage occurs when the autophagosome targets the lysosome and fuses with it allowing the captured material and the inner membrane to be degraded (Figure 1.5). The molecular mechanism(s) of autophagy involve genes termed autophagy related genes (ATG) and its products, Atg, first found in yeast cells. The Atg proteins function at distinct stages in the autophagy process, most of which have been identified in mammalian cells.<sup>81</sup>

The assembly of the pre-autophagosome (PAS) is referred to as nucleation (Figure 1.7). This step begins with Atg17. Atg17 recruits Atg13 and Atg9, which together

activate the phosphoinositide 3-kinase (PI3K) class III complex to include Atg14, Atg15, and vacuolar protein sorting-associated (VPS),<sup>82</sup> or its mammalian counterpart p150. Atg6, Beclin 1 in mammals, and UV-irradiation resistance-associated tumor suppressor gene (UVRAG) also associate with the PI3K complex. Under conditions of nutrient starvation, Atg13 interacts with Atg1 and the PI3K complex to recruit Atg18 and Atg2. Atg18 and Atg2 are involved in retrograde transport of Atg9 to the periphery of the cell where they aid in membrane recycling.<sup>83</sup>

Elongation of the autophagosome is generated by two ubiquitin-like conjugation systems, Atg12-Atg5 and Atg8-phosphatidylethanolamine (PE). The class III PI3K complex is required for the localization of both systems. In addition, both systems are similar to the ubiquitination system, consisting of three enzymes: a ubiquitin-activating enzyme (E1), a ubiquitin-conjugating enzyme (E2) and a ubiquitin-protein ligase (E3).<sup>84</sup> Atg12 is activated by Atg7 functioning as an E1 enzyme. Atg10 acts as an E2 enzyme, forming a new thioester bond and Atg7 is released. The last step is the covalent linkage of Atg12 to a lysine residue of Atg5 and the release of Atg10. This Atg12-Atg5 complex interacts with Atg16L in mammals (where Atg16L only binds to Atg5), forming an 800 kDa structure on the outer membrane necessary for the elongation of the PAS. Once the autophagosome is complete, this conjugate system dissociates and thus is not a part of the mature autophagosome.<sup>85</sup> The second ubiquitination system is Atg8-PE. Atg8 is a soluble cytoplasmic protein that conjugates with PE and becomes attached to the pre-autophagosome, as well as the mature autophagosome, and the autophagic bodies.<sup>84</sup>

The mammalian ortholog of Atg8, is microtubule-associated protein 1 light chain 3 (LC3) and this protein is one of two credible markers to detect autophagy in mammalian cells. LC3 is detected in two forms, LC3 I (18 kDa) and LC3 II (16 kDa). LC3 I becomes active when it is cleaved by Atg4 also known as autophagin. Next, with the catalysis of Atg7 and Atg3, LC3 I undergo ubiquitination-like reactions and is modified to LC3 II. LC3 II is tightly bound to the PAS as well as the autophagosome whereas LC3 I is located in the cytoplasm. Thus, the relative amount of LC3 II reflects the abundance of autophagosomes present in cells.<sup>84,86</sup> Another marker, p62, also named sequestosome 1 (SQSTM1) is a more recent protein that may be used to detect autophagy. This protein is a common component of polyubiquitinated protein aggregates that are degraded by autophagy. The C-terminal part of p62 contains an ubiquitin-associated (UBA) domain, which binds to ubiquitin non-covalently. The p62 protein also recognizes LC3 on the autophagosome. Positive p62 structures are degraded via autophagy and this protein can be recognized along with LC3.<sup>87</sup>

After the formation of the autophagosome, the fusion with the lysosome follows. This structure is commonly referred to as the autolysosome or autophagolysosome.<sup>88</sup> There are several factors involved in autophagosome fusion, these include the SNARE proteins (i.e. SEC17, SEC18, and YPT7). Degradation of the autophagosome once fused requires a low pH, proteinase B (PRB1), and the lipase Atg15. PRB1 is a hydrolase involved in the activation of vacuolar zymogens which indirectly affects the vesicle breakdown whereas, Atg15 functions directly in vesicle breakdown.<sup>84</sup>

### 1.13 Autophagy: Regulation

There are a number of pathways involved in the regulation of autophagy. A critical player in autophagy regulation is the mammalian target of rapamycin kinase (mTOR). mTOR is a serine/threonine kinase that is involved in the control of multiple cellular processes in response to changes in nutrient conditions.<sup>81</sup> It exerts an inhibitory signal on autophagy, remaining active when the supply of amino acids and other nutrients are ample. In an active form, mTOR can phosphorylate proteins that are important for cell growth. When a cell is deprived of nutrients, mTOR is inactivated, allowing proteins that are required for cell survival to be translated.<sup>86</sup> Autophagy is therefore the attempt to provide an alternate source of nutrients for cell survival. Treatment of cells with rapamycin, an inhibitor of mTOR, blocks cell cycle progression and triggers autophagy. mTOR also appears to affect Atg proteins, resulting in interference with autophagosome formation. Under nutrient-rich conditions, activated mTOR causes hyperphosphorylation of Atg13, thereby preventing the association of Atg13 with Atg1 (Figure 1.7 and 1.8).<sup>88</sup>

Another signaling pathway involved in the regulation of autophagy are class I PI3Ks. Evidence that PI3K was involved in autophagy stems from the use of 3-methyladenine (3MA), a PI3K inhibitor, that inhibits the autophagic process. Other PI3K inhibitors (i.e. wortmannin and LY294002) have also been shown to inhibit autophagy.<sup>89</sup> There are three classes of PI3Ks in mammalian cells. Activation of class I PI3K inhibits autophagy in HT29 colon cancer cells.<sup>90</sup> Class II PI3K does not appear to have an effect on autophagy. Class III PI3K plays a significant role in the early steps of autophagy.<sup>83</sup> In

addition, the class III PI3K product, phosphatidylinositol 3-phosphate (PIP<sub>3</sub>), plays a role in the induction of autophagy.<sup>90</sup>

### **1.14 Autophagy and Cancer**

Autophagy can be activated in response to extra- or intracellular stimuli such as starvation, hormone treatment, growth factor deprivation, ER stress and infection. Often regarded as a cell survival mechanism, autophagy can play a significant role in cancer cell survival and resistance to treatment. However, other studies have shown that autophagy may also have a role in cell death.<sup>82</sup>

One of the key proteins involved in the induction of autophagy, beclin 1, displays tumor suppressor activity. Beclin 1 is mono allelically deleted in 40-75% of human breast, ovarian, and prostate cancers. Mice with heterogeneous disruption of beclin 1 are more prone to developing spontaneous tumors and show a decrease in autophagy.<sup>91</sup> Beclin 1 was originally isolated as a Bcl-2 interacting protein. Furthermore, Bcl-2 downregulation stimulates autophagy. Consequently, beclin 1 mutations that abolish the interaction with Bcl-2 or Bcl-xL confer a gain-of-function phenotype with respect to autophagy. Similarly, mutations in Bcl-xL that prevent its binding to beclin 1 also eliminate its capacity to antagonize autophagy induction. The autophagy inducing activity of beclin 1 is also inhibited by Mc1-1.<sup>92</sup> PTEN, a tumor suppressor which dephosphorylates class I PI3K products, is shown to prevent autophagy.<sup>91</sup> Thus, autophagic signaling is tightly linked to oncogenic signaling. Currently, the variability of autophagic signaling in cancer cells is at the forefront of discussion in cancer therapy.

**Figure 1.7. The Cellular Aspect of Autophagy.** The cellular process of autophagy follows distinct stages: vesicle nucleation (formation of the isolation membrane), vesicle elongation (growth of the membrane from the preautophagosomal structure to the mature autophagosome), docking and fusion of the autophagosome with the lysosome to form an autolysosome, and lastly breakdown of the autolysosome and the degradation of its contents.



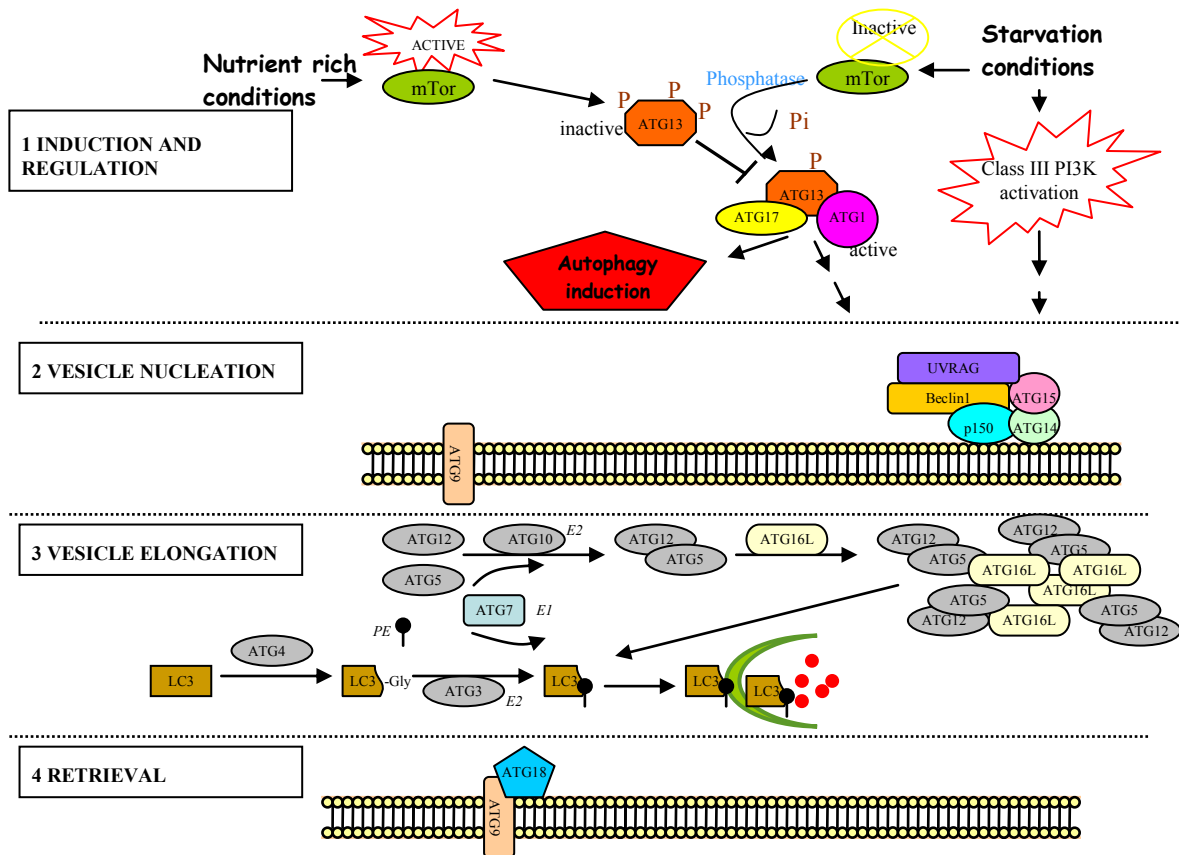


**Figure 1.8. The Molecular Aspect of Mammalian Autophagy.** Regulatory steps of autophagy, as seen in response to starvation. (Dent et al.)

### 1.15 Molecular Chaperones in Protein Folding

Protein folding is the physical process by which a polypeptide folds into its characteristic three-dimensional structure. Protein structure can be described at four levels. The primary structure consists of the amino acid sequence and this determines the three-dimensional structure. The secondary structure refers to the polypeptide chain folding into a regular structure (i.e. alpha helix, beta sheet, and turns and loops). The tertiary structure is the compact, asymmetric structure in which all proteins have the common features of interior amino acids with a hydrophobic side chain and hydrophilic amino acids that can interact with the aqueous environment. The quaternary structure refers to the assembly of multi subunit structures. The correct structure of the protein is essential for its function. Thus, incorrect folding usually produces inactive proteins. The process of folding *in vivo* begins co-translationally so that the protein's N-terminus begins to fold while the C-terminus is still being synthesized on the ribosome.<sup>93</sup>

Molecular chaperones also known as heat shock proteins (hsps) are ubiquitous in nature and act to maintain proper protein folding within the cell or proteasome-mediated degradation in the case of damaged proteins.<sup>93</sup> These proteins facilitate the correct folding *in vivo* but they do not contain steric information regarding the correct folding. Instead, they prevent incorrect interactions within non-native polypeptides increasing the yield but not the rate of folding reactions.<sup>93</sup> The demand upon these heat shock proteins increases after environmental stress (i.e. drugs, toxic chemicals, and extreme temperatures), non-stress conditions, and disease states (i.e. Cancer, Alzheimer's disease and cystic fibrosis).<sup>94</sup>

Heat shock proteins are classified by molecular weight into six major hsp families to include the small hsps (20-25 kda), and hsp40, hsp60, hsp70, hsp90, and hsp100.<sup>95</sup> The small hsps bind to partially denatured proteins and are responsible for protecting proteins from irreversible aggregation via an energy independent process. Once suitable conditions are restored for renewed cellular function, protein release and refolding are mediated by ATP-dependent chaperones such as hsp70.<sup>96</sup> The small hsps also function to maintain the integrity of membranes via specific lipid interactions under physiological conditions.<sup>97</sup> Hsp40, hsp60, and hsp70 are all involved in nascent protein folding.<sup>93</sup> Additionally, hsp40 is considered a co-chaperone for hsp70, playing a vital role in the stimulation of conformational changes in the ATPase domain of hsp70.<sup>98</sup> In addition to stabilization processes, Hsp70 is also important in the degradation of misfolded proteins.<sup>93</sup> The hsp100 family of chaperones, function to disaggregate proteins and some members of this family target specific classes of proteins for degradation.<sup>99</sup> Hsp90 however, seems to be more important in cancer progression, stabilizing a number of signaling proteins involved in cancer progression and is it not required for de novo protein synthesis.<sup>100</sup> (Figure 1.9)

### **1.16 Hsp90 Structure and Function**

Hsp90 is a heat shock protein that conserves the folding of newly translated protein.<sup>101</sup> It is distinctly different from other chaperones in that most of its substrates are signaling proteins. Classic examples include steroid hormone receptors and signaling kinases.<sup>102,103</sup> Thus, disruption of Hsp90 in tumor cells has been shown to induce improper folding of many proteins, including Raf-1, B-Raf, Akt, and ERBB family receptors

culminating in their proteosomal degradation.<sup>104</sup> Hsp90 is a constitutive homodimer and has 3 domains, a 25 kDa N-terminal domain, a charged linker domain, and a 55 kDa C-terminal domain. The N-terminal domain binds ATP and other purine analogues,<sup>105</sup> while the C-terminal domain is responsible for dimerization and is required for biologic activity.<sup>106,107</sup> Hsp90 consists of two isoforms, alpha and beta. Hsp90 $\alpha$  is elevated under stress conditions whereas hsp90 $\beta$  is constitutively expressed. The proteins are encoded on two separate genes, chromosome 14 for Hsp90 $\alpha$  and chromosome 6 for hsp90 $\beta$ .<sup>108</sup> Although there are some functional differences between the two the isoforms,<sup>109</sup> they are usually not distinguished from each other.<sup>110</sup> However, a knockout mouse strain for hsp90 $\beta$  is embryonic lethal.<sup>111</sup>

Hsp90 genes are regulated by a family of transcription factors known as heat shock factors (HSFs). Hsp90 genes contain heat shock-responsive elements in their promoters, which are bound by the HSFs to initiate transcription. There are 4 HSF proteins that include HSF1, 2, and 4 which are ubiquitous in nature, and HSF3 which has been characterized in avian species.<sup>94</sup> Of the HSFs, HSF1 is the principal stress-induced transcription factor.<sup>112</sup>

HSFs consist of four conserved structural domains. The DNA binding domain is characterized by a helix-turn-helix motif. There is also a hydrophobic repeat domain essential for trimer formation and a carboxy-terminal transactivation domain.<sup>114</sup> Under unstressed conditions, HSF1 exists as a cytosolic monomer in complexes containing hsp70 and hsp90. Upon exposure to stress, HSF1 is activated and binds to the heat shock promoter element (HSE) in hsp promoters. HSF1 forms a phosphorylated homotrimer in

the nucleus that activates a program of transcription, including the upregulation of HSP production.

The transcriptional regulation of HSF1 is controlled in part by heat shock proteins. It has been shown that the binding of hsp70 to HSF1 at the hydrophobic carboxy-terminus suppresses the function of HSF1.<sup>115</sup> When there is accumulation of non-native proteins during a stressful event, these may compete with HSF1 for binding to chaperone hsp70. Unbound HSF1 could then homotrimerize and be available for transcription.<sup>116</sup> Similarly, hsp90 can form a complex with HSF1 and repress its function as well. Additionally, geldanamycin, an inhibitor of hsp90, activates HSF1 in vitro.<sup>117</sup>

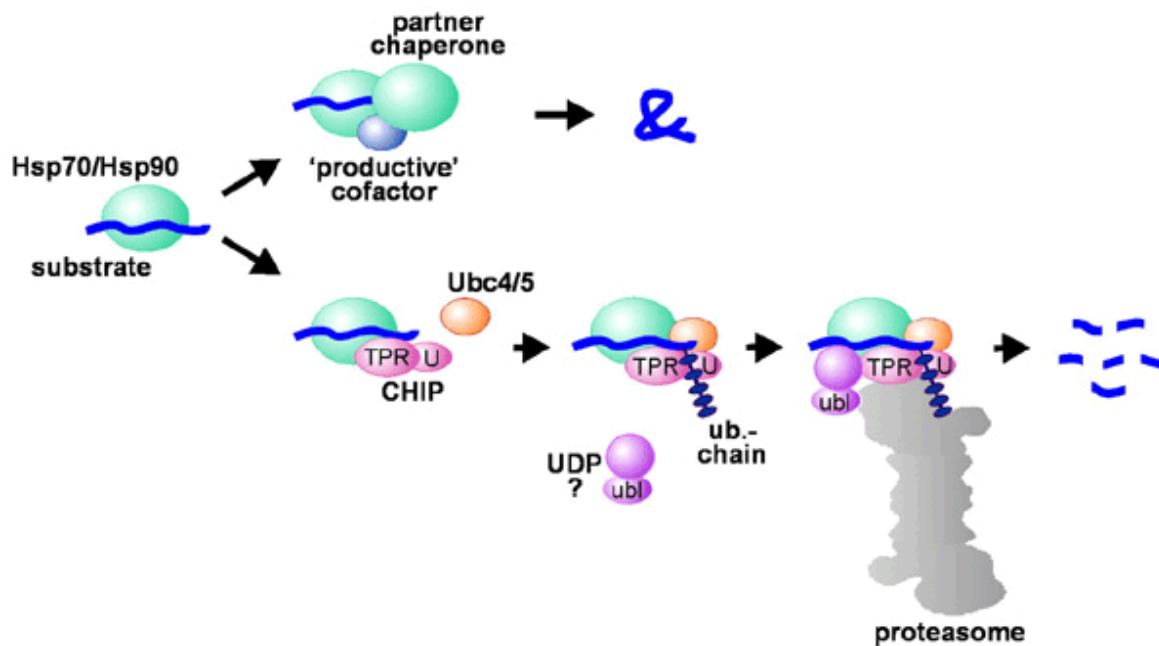
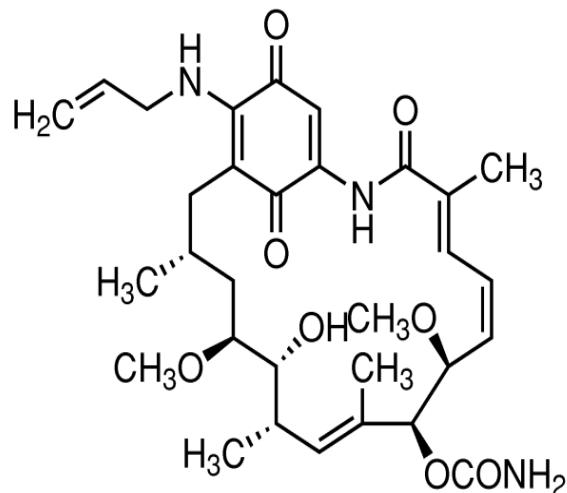


Figure 1.9 Hsp70 and Hsp90 protein folding and degradation.<sup>81</sup>

### 1.17 Hsp90 inhibitors

The highly conserved N-terminal domain of hsp90 is the binding site for geldanamycin (GA), an ansamycin drug which specifically targets hsp90,<sup>118</sup> inhibits the hsp90 ATPase with nanomolar affinity. This drug occupies the nucleotide-binding cleft within in the N-terminal domain.<sup>105</sup> GA acts like a nucleotide that locks hsp90 in an ADP-bound state, ultimately leading to the inhibition of the two chaperone proteins; p23-hsp90 interacting with each other.<sup>120</sup> Like many chemotherapeutic agents, GA has a dose-dependent selectivity for tumor cells. In

cancer cells, Hsp90 has a higher affinity for N-terminal ligands than in normal cells.<sup>119,121</sup> Thus, GA would preferentially target cancer cells rather than normal cells since it binds the N-terminus of hsp90. Unfortunately, studies have shown GA drug toxicity in



**Figure 1.10 - 17-AAG**

the liver, which has precluded further clinical development.<sup>122</sup> 17-allylamino-17-demethoxygeldanamycin (17-AAG), a derivative of GA, is a reversible Hsp90 inhibitor, and has been shown to have potential anti-tumor activity and is currently undergoing clinical phase I trials. 17-AAG seems to undergo extensive metabolism that can result in the generation of toxic species<sup>123</sup> and ultimately increased levels of ER stress.

### 1.18 ER Stress: The Unfolded Protein Response

The endoplasmic reticulum (ER) is a membranous network found throughout the cytoplasm of eukaryotic cells. Serving as the main site of protein biosynthesis, the ER is responsible for the folding, assembly and glycosylation of membrane bound and secretory proteins. Homeostasis within the ER is contingent on the levels of ER stress that can arise due to improper folding/processing of proteins. The pathways, known collectively as the unfolded protein response (UPR), are important for normal cellular homeostasis and organism development and may play key roles in the pathogenesis of many diseases.<sup>124</sup> The UPR is mediated by three ER membrane associated proteins, PERK (PKR-like eukaryotic initiation factor 2 $\alpha$  kinase), IRE1 (inositol requiring enzyme 1), and ATF6 (activating transcription factor-6). In a “stress-free” ER, these proteins are inactive due to binding by an ER localized HSP70 family chaperone, BiP/GRP78, in their intra-lumenal domains, amino-terminal of IRE1 and PERK and carboxy-terminal of ATF6. When the accumulation of misfolded proteins occurs within the ER, BiP/Grp78, dissociates from PERK, IRE-1 and ATF6, to assist in protein folding, as a result of depletion of ER chaperone reserves. The dissociation of BiP/GRP78 from PERK enables its dimerization, which in turn leads to its autophosphorylation and subsequently, triggers the phosphorylation of eukaryotic transcription initiation factor alpha (eIF2 $\alpha$ ) at serine 51.<sup>124</sup> Eif2 $\alpha$  is required to recruit the initiator methionyl-transfer RNA (Met-tRNA<sub>i</sub>) to the 40S ribosome. Thus, when eif2 $\alpha$  is phosphorylated, it loses its ability to exchange GDP for GTP and thus prevents the 40S ribosome and the 60S ribosomal unit from forming the 80S initiation complex necessary for translation. As a result of activated eif2 $\alpha$ , inhibition of

both translation and cell cycle progression occurs.<sup>125</sup> In addition, the activating transcription factor 4 (ATF4) is translated after eif2 $\alpha$  is phosphorylated and is responsible for the activation of genes involved in amino acid metabolism, transport, oxidative-reduction reactions, and ER stress-induced apoptosis. One of these proteins, C/EBP homologous transcription factor (CHOP) is implicated in both growth arrest and cellular apoptosis.<sup>124,125</sup>

In combination with an induction of pro-survival autophagy, this mechanism can enable the cell to recover from the accumulation of misfolded proteins. This UPR has also been shown to play a role in the increased production of pro-survival proteins; however, under prolonged stress conditions it also has the potential of inducing a toxic form of autophagy, and an ATF4-induced expression of CHOP activating caspase 3 and ultimately apoptosis.<sup>125,127</sup>

Prior to the initiation of apoptosis, a cell will co-ordinate itself with the ER associated degradation (ERAD) system, allowing the misfolded proteins to be degraded. XBP1 is responsible for increasing the expression of genes encoding proteins required for ERAD. Recent data has shown, that, under prolonged UPR, ER calcium homeostasis is significantly disrupted, and caspase 4 is activated.<sup>126</sup> Caspase 4 activation then leads to the cleavage and processing of caspases 9 and 3 into their active cleaved counterparts, ultimately leading to apoptosis (**Figure 1.11**).



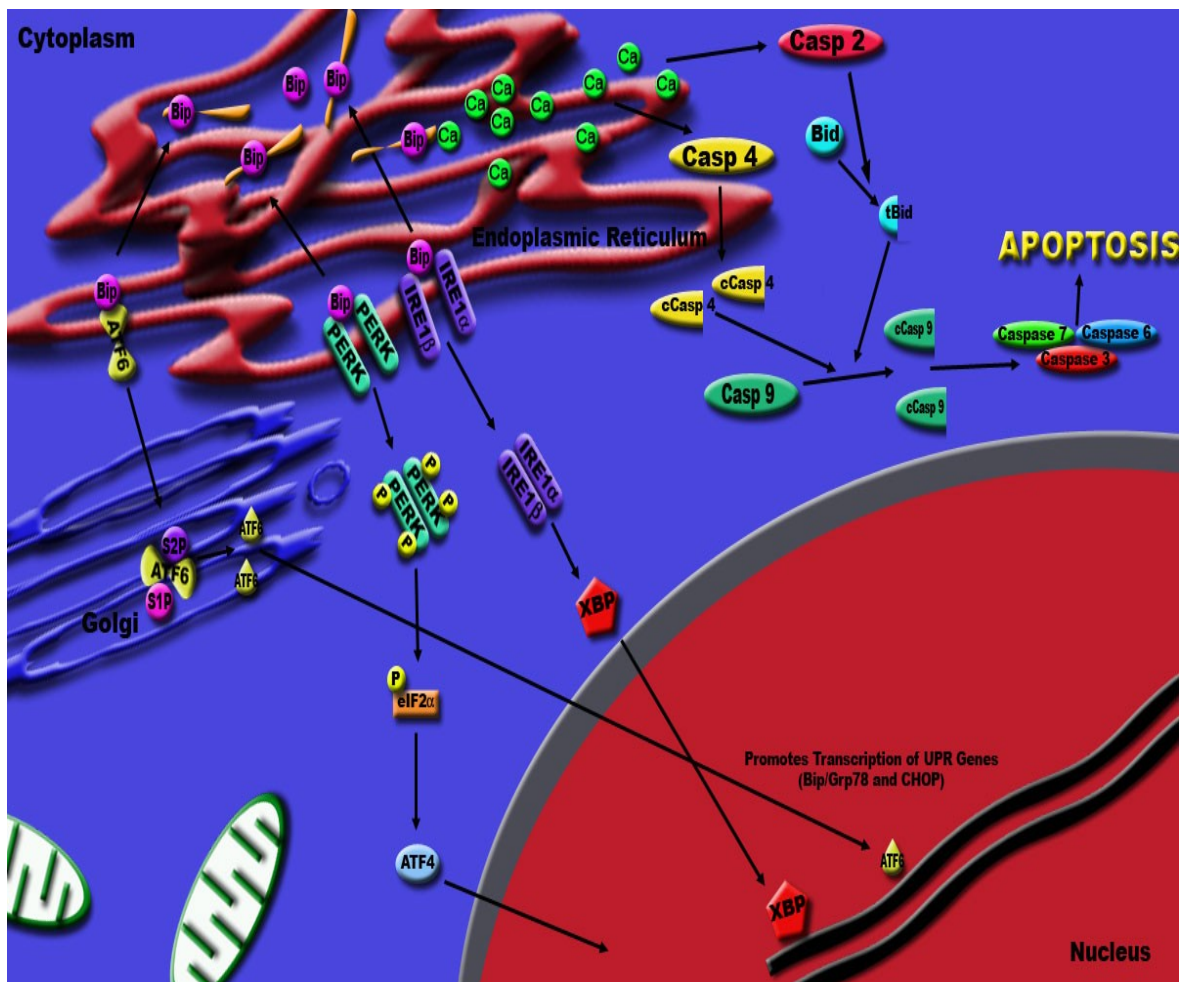
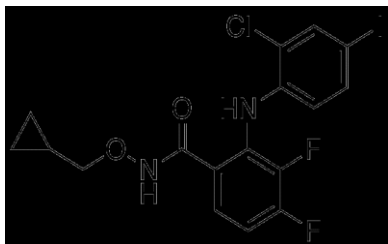


**Figure 1.11** Upon accumulation of misfolded or unfolded proteins in the ER lumen, Bip/Grp78 dissociates from UPR sensors PERK, IRE1 and ATF6.

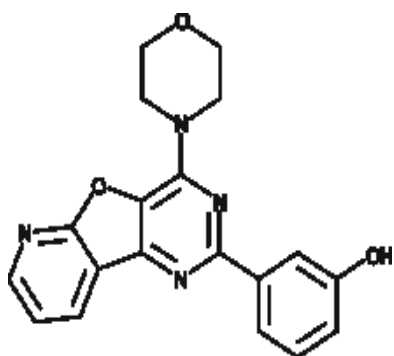
### 1.19 Small Molecule Inhibitors/Drugs used in this study:

**Figure 1.12 - PD184352 (CI-1040):**

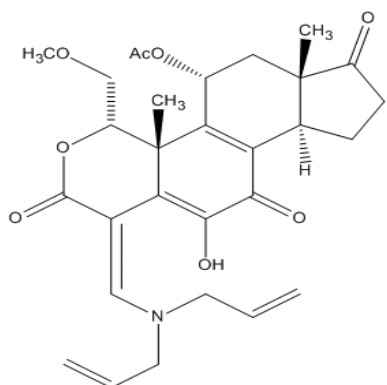


PD184352 (also called CI-1040) is a second generation MEK1/2 inhibitor with enhanced bioavailability. Acting as an allosteric inhibitor by not competing with ATP for its binding site, binding of PD184352 outside the ATP and ERK1/2 binding sites on MEK1/2 inhibits the activation of MEK1 in cells by greater than 50% at 2nM, a concentration 100 fold lower than that which completely inhibits MEK 1 activity *in vitro*. This drug is also highly specific for MEK 1/2 and has shown to reduce levels of DNA synthesis in U87 gliomas.<sup>128</sup>

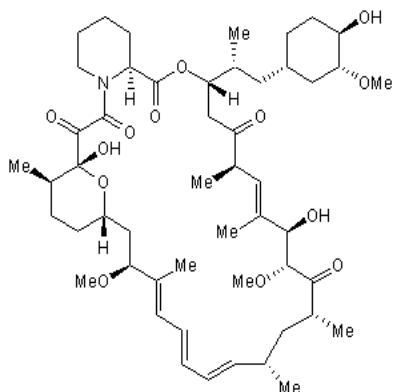
**Figure 1.13 - PI-103:**



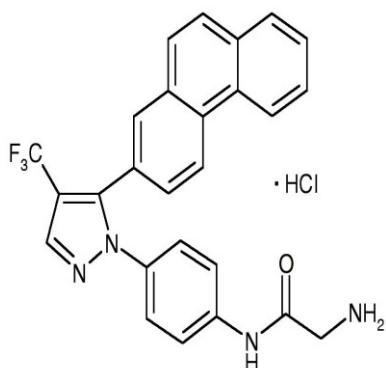
Pyridnylfuranopyrimidine Inhibitor, PI-103, is a multi-kinase inhibitor of PI3K/Akt-mediated signaling. Recently, PI-103 has been shown to enhance the efficacy of DNA-damaging chemotherapeutic agents, in the treatment of GBMs. This sensitivity is generated by way of inhibition of growth and survival cascades as well as the down-regulation of mTOR, necessary for the production of protective BCL-2 family proteins.<sup>130</sup>

**Figure 1.14 - PX-866:**

A more specific PI3K inhibitor, PX-866 has been shown inhibit tumor cell growth in U87 and U251 glioma cells. Much like its counter-part, PI-103, this specific inhibitor of PI3K down regulates the product of survival proteins, affording the opportunity for a combinatorial approach to increase drug efficacy.<sup>130</sup>

**Figure 1.15 - Rapamycin:**

The mammalian target of rapamycin, mTOR is crucial in regulating the proliferation of cancer cells. Inhibitors of mTOR, such as rapamycin have been shown to have tumor cell killing ability in vivo in U87 glioma cells. Originally synthesized as an antifungal and immunosuppressant agent, rapamycin complexes with FKBP-12 and binds to and inhibits mTOR, leading to inhibition of IL-2 induced activation of p70 S6 kinase. Unfortunately, if the tumor is re-occurrent, the inhibitory attributes of rapamycin are greatly diminished.<sup>131</sup>

**Figure 1.16 - OSU-03012 (AR-12):**

OSU-03012 is a derivative of Celecoxib, a COX2 inhibitor. Although, OSU-03012 does not inhibit COX2, it has an order of magnitude greater effect at killing tumor cells than Celecoxib. Recently, our studies have shown that OSU-03012 induced cell death in GBM cells, as a result of down regulation of BiP/GRP78. This interaction

prevents Bip from aiding in the proper folding of proteins transported into the ER, ultimately leading to an ER stress induced autophagic response, which has a high potential for activating apoptotic signaling.<sup>132</sup>

**Figure 1.17 - Temozolomide (TMZ):**

An alkylating chemotherapeutic agent that is orally administered and can pass the blood brain barrier. Studies have shown TMZ to have cytotoxic effects through the methylation of DNA, specifically at the O<sub>6</sub> position of guanine, resulting in mispairing with thymine during the

next round of cell cycle DNA replication and ultimately mis-match repair mechanisms eliciting an apoptotic response.<sup>6,134</sup>

## CHAPTER 2: MATERIALS AND METHODS

### 2.1 Materials

Phosphate-buffered saline solution (PBS), Dulbecco's Modified Eagle's Medium (DMEM), RPMI medium, trypsin-EDTA, and penicillin-streptomycin were purchased from GIBCOBRL (Invitrogen-GIBCOBRL Life Technologies, Grand Island, NY). Dr. C.D. James, (UCSF) very generously supplied primary human GBM cells (GBM6, GBM12, GBM14) and information on the genetic background of such cells. Dr. S. Spiegel (VCU) supplied the plasmid to express LC3-GFP. Trypan blue solution, formaldehyde, 6-Diamidino-2-Phenylidole (DAPI), and dimethyl sulfoxide (DMSO) were all obtained from Sigma Chemical (St. Louis, MO). Anti-GAPDH (37 kDa, 1:1000, mouse monoclonal), phospho-PERK (125 kDa, 1:500, rabbit polyclonal), phospho-/total ERK1/2 (42, 44 kDa, 1:1000, mouse monoclonal), phospho-/total-Akt (60 kDa, 1:1000, rabbit polyclonal), phospho-/total-JNK1/2 (46, 54 kDa, 1:1000, rabbit polyclonal), anti-Bcl-xL (30 kDa, 1:1000, rabbit polyclonal), anti-Mcl-1 (40 kDa, 1:1000, rabbit polyclonal), phospho-/total-p38 $\alpha/\beta$  MAPK (38 kDa, 1:1000, rabbit polyclonal), anti-LC3 (17/19 kDa, LC3II/LC3I, rabbit polyclonal) antibodies were purchased from both Cell Signaling Technologies (Worcester, MA), Santa Cruz Biotechnology (Santa Cruz, CA) and Novus Biologicals (Littleton, CO). All of the secondary antibodies (anti-rabbit-HRP, anti-mouse-HRP, and anti-goat-HRP) were obtained from Santa Cruz Biotechnology (Santa Cruz, CA). The JNK inhibitor peptide was supplied by Calbiochem (San Diego, CA) as a powder, dissolved in sterile dimethyl sulfoxide, and stored frozen under light-protected conditions

at  $-80^{\circ}\text{C}$ . MDA-7/IL-24 antibody (35 kDa, Human IL-24 Antibody, 1:500 Rabbit Polyclonal) was purchased from GenHunter (Nashville, TN). Other reagents were of the highest quality commercially available.<sup>35,36,134</sup>

## **Methods:**

### **2.2 Generation of Ad.5-*mda-7* or Ad. 5/3-*mda-7***

Recombinant serotype 5 and serotype 5/3 adenoviruses to express MDA-7 (Ad.5-*mda-7* and Ad.5/3-*mda-7*) and control empty vector (Ad.*cmv*) were generated using recombination in HEK293 cells.<sup>18,22,23,135</sup>

### **2.3 Synthesis of GST-MDA-7**

A bacterial expression vector containing a 3'-end open reading frame, was fused to the glutathione S-transferase (GST) open reading frame in a GST-4T2 vector (Amersham Pharmacia) by introducing restriction enzymes BamH1 and Not1 into the *mda-7* gene via polymerase chain reaction (PCR). To verify the expression of MDA-7 protein, a culture of HEK293 cells were subjected to an overnight inoculation of GST-MDA-7 (1:100 dilution) followed by incubation at  $25^{\circ}\text{C}$  until an absorbance of 0.4-0.6 at  $A_{600\text{nm}}$  was obtained (ref 12-18-20,24-28,32). Next, the culture was exposed to  $0.1\ \mu\text{M}$  isopropyl-1-thio- $\beta$ -D-galactopyranoside for two hours. The cells were collected by centrifugation and sonicated in PBS. The solution was again centrifuged to obtain soluble protein. The lysate was then bound to a glutathione-agarose column (Amersham Pharmacia) for two hours at  $4^{\circ}\text{C}$ . The column was washed with 50 ml vol/vol of PBS and 10 ml vol/vol of PBS containing

500nM sodium chloride. The bound protein was eluted by passing 20mM reduced glutathione through the column, while collecting 1 mL fractions. The fractions were analyzed by gel electrophoresis to determine the presence of bound GST-MDA-7, and positive samples were dialyzed in the presence of 1000  $\mu$ l vol/vol of PBS for four hours, at which time the PBS was replaced, and the dialysis repeated for a further four hours. Final, protein concentration was determined by coomassie blue staining, as well as gel electrophoresis using an anti-GST-MDA-7 antibody (50 kDa, 1:3000, rabbit polyclonal) generated in rabbits by using gel-purified fragments of GST-MDA-7.

## 2.4 Cell Culture

GBM6/GBM12/GBM14 glioma cell lines were originally derived from patients at the Mayo Clinic (Rochester, MN). GBM6/GBM12/GBM14 cells were cultured in Dulbecco's modified Eagle's medium supplemented with 5% (vol/vol) fetal calf serum and 100  $\mu$ g/ml (1% vol/vol) penicillin and streptomycin. Cells were incubated in a humidified atmosphere of 5% (vol/vol) CO<sub>2</sub> at 37 °C. For short-term cell killing assays and immunoblotting, cells were plated at a density of  $3 \times 10^3/\text{cm}^2$  for 36 hours prior to treatment with MDA-7/IL-24 and/or various drugs, as indicated.

Cell Line	Media	Characteristics
GBM6	5% DMEM	Mutant Variant - ERBB1 vIII
GBM12	5% DMEM	Expresses mutant active full length ERBB1
GBM14	5% DMEM	Mutant PTEN
GL261	5% DMEM	Mouse Glioma Cells

**Table 2.1 Cell Line Information.**

## **2.5 *In vitro* Exposure of Cells to GST-MDA-7, Recombinant Adenoviral Vectors and all other drugs**

Cells were treated with various GST-MDA-7 concentrations, as indicated in the figure legends. *In Vitro* small molecule inhibitor treatments were from a 100 mmol/l stock solution of each drug, the maximal concentration of vehicle (dimethyl sulfoxide) in media was 0.02% (vol/vol). Recombinant adenoviruses to express constitutively activated and dominant negative (dn) AKT and MEK1 proteins, dn-caspase 9, XIAP, c-FLIP-s, CRM A, and BCL-XL were purchased from Vector Biolabs, (Philadelphia, PA). Monolayer cell cultures were washed in PBS prior to infection with specific virus in serum-free growth medium at a m.o.i. (multiplicity of infection) of 50 (m.o.i. = # of virus particles per cell). Cells were incubated for 24 hours to ensure adequate expression of transduced gene product prior to drug exposure. For Ad.*mda-7* or Ad.*cmv* infections, cells were infected 12 hours after plating and a further 12 hours was allowed for expression of the recombinant viral transgene before any additional experimental procedure was performed. Cells were not cultured in reduced serum media during any study.<sup>23,24</sup>

## **2.6 Assessment of Cell Viability**

Cells were harvested by trypsinization with trypsin/EDTA for ~10 minutes at 37°C. Apoptotic/dead cells detached from the culture substratum into the medium were also collected. Both fractions were pelleted by centrifugation at 1,500 rpm for 5 minutes. The pooled cell pellets were resuspended and mixed with the vital stain trypan blue. Incorporation of trypan blue stain into the cell cytoplasm was used as an indicator of cell



death. A haemocytometer mounted on a light microscope was used to count a total of 500 cells from randomly selected fields per experimental point. The percentage of dead cells was expressed as a percentage of the total number of cells counted. For confirmatory purposes, the presence of apoptotic cells was evaluated by assessing Hoechst and terminal deoxynucleotidyl transferase dUTP nick-end labeling stained cytopsin slides for each experimental point, under fluorescent light microscopy and determining the number of cells exhibiting the “classic” morphological features of apoptosis and necrosis. For each condition, 10 randomly selected fields per slide were evaluated, encompassing at least 1,500 cells. Alternatively, the Annexin V/propidium iodide assay to determine cell viability was performed as per the manufacturer’s instructions (BD PharMingen, San Diego, CA), using a Becton Dickinson FACScan flow cytometer (Mansfield, MA).<sup>23,24</sup>

## **2.7 Colony Formation Assay for Cell Survival**

Cells were plated from a single cell suspension, (250-500 cells/well) in a 6 cm dish. Twenty four hours after plating, cells were treated as specified in the figures, 48 hours after treatment, the drug-containing media was carefully removed, and fresh media lacking drugs was carefully added. The cells were cultured for an additional 10 to 14 days. Upon control group colony formation, the medium was removed and the cells washed in 1X PBS. The cells were then fixed on to the dish by adding 100% methanol for 10 minutes. The methanol was removed and 0.1% (vol/vol) crystal violet stain (Sigma-Aldrich) was added to the dish for 1 h. Colonies containing more than 50 cells were then counted and normalized to the control cell survival sample. The survival data shown

includes individual assays performed at multiple dilutions of cells with a total of three dishes per data point, repeated for a total of three experiments.

## **2.8 Western Blot Analysis for Protein Expression**

Cells were plated in 10 cm<sup>3</sup> dishes for 24 hours prior to treatment. Twenty four or 48 h after drug exposure cells were applied to sodium dodecyl sulfate–polyacrylamide gel electrophoresis (SDS-PAGE) and immunoblotting. The cells were lysed in either a nondenaturing lysis buffer, and prepared for immunoprecipitation or were washed in PBS and then scraped off the plate by using whole-cell lysis buffer (0.5 M Tris-HCl, pH 6.8, 2% (w/v) SDS, 10% (v/v) glycerol, 1% (v/v)  $\beta$ -mercaptoethanol, 0.02% (w/v) bromophenol blue). A 1:20 dilution of protease inhibitor cocktail (Roche) and a 1:100 dilution of phosphatase inhibitor cocktail (Roche) was also added to the lysis buffer. When whole cell lysis buffer was used, the samples were vortexed to dislodge the pellet, heated at 95-100°C for 5 minutes and placed immediately on ice. Nondenaturing lysis buffer was used, after immunoprecipitation, samples were also boiled in whole-cell lysis buffer. 50-100  $\mu$ g aliquots of boiled samples (depending on the protein analyzed) were loaded onto 10–14% SDS-PAGE apparatus and electrophoresed. Proteins were electrophoretically separated and then transferred onto 0.22  $\mu$ m nitrocellulose for 4 hours on ice at 450 mA in transfer buffer (5.8g Tris-base, 2.9g glycine, milli-Q water to 800 ml, 1.8 ml 20% (w/v) SDS, 200 ml methanol.), and then immunoblotted with appropriate primary antibodies against the specific proteins.<sup>23,24</sup>

The membrane containing transferred proteins was blocked in TBS-tween (TBST) buffer containing 5% (w/v) non-fat dry milk for 30 minutes. Following removal of the blocking solution, the desired primary antibody was added at a certain dilution to fresh blocking solution. After overnight exposure to primary antibody at 4°C with orbital shaking, the antibody-blocking solution was removed and the membrane was washed with TBST (3 x 15 minutes). The membrane was then incubated with the corresponding goat anti-mouse or rabbit secondary antibody for 2 hours at room temperature with orbital shaking. Following this incubation, the secondary antibody was removed and the membrane washed with TBST (3 x 15 minutes). All immunoblots were visualized using an Odyssey Infrared Imager (LI-COR Biosciences, Lincoln, NE) with associated Image Studio software. For presentation, immunoblots were opened in PhotoShop CS2 (Adobe Systems, Mountain View, CA); the color was removed, and figures were generated in PowerPoint (Microsoft Corp., Redmond, WA).

## **2.9 Plasmid and siRNA Transfections**

Plasmid DNA (0.5 µg/total plasmid transfected) was diluted into 50 µl of RPMI growth media that lacked supplementation with fetal bovine serum or penicillin–streptomycin and was incubated in solution for 5 minutes at room temperature. Lipofectamine 2000 reagent (1 µl) (Invitrogen, Carlsbad, CA) was diluted into 50 µl growth media that lacked supplementation with fetal bovine serum or penicillin–streptomycin and incubated in solution for 5 minutes at room temperature. The two solutions were then mixed together and incubated at room temperature for 30 minutes. The

total mix was added to each well (4-well glass slide or 12-well plate) containing 200  $\mu$ l growth media that lacked supplementation with fetal bovine serum or penicillin–streptomycin. The cells were incubated for 4 hours at 37 °C, after which time the media was replaced with RPMI growth media containing 5% (vol/vol) fetal bovine serum and 1% (vol/vol) penicillin–streptomycin.

RNA interference or gene silencing for down-regulating the expression of specific mRNA was performed using validated target sequences designed by Ambion (Austin, TX). Specified siRNA's were used at 10 nM concentration of the annealed siRNA or the negative control, siSCR (a "scrambled" sequence with no significant homology to any known gene sequences from mouse, rat, or human cell lines) were used. The siRNA molecules were transfected into cells according to the manufacturer's instructions, similar to plasmids above.

## **2.10 Microscopy for LC3-GFP Expression**

Where indicated LC3-GFP transfected cells, 12 hours after transfection, were infected with either “Ad.*cmv*” (empty vector) or Ad.*mda-7*, then cultured for 24 hours prior to treatment with specified drug. Cells were then stained with LysoTracker Red Dye (Invitrogen) at the indicated time points for 20 minutes. LysoTracker Red Dye stained cells were visualized immediately after staining on a Zeiss Axiovert 200 microscope (Carl Zeiss, Wake Forest, NC) using a rhodamine filter. LC3-GFP transfected cells were visualized at the indicated time points on the same microscope using the FITC filter.

### 2.11 Intracerebral Inoculation of GBM cells

Athymic female NCr-nu/nu and C57 BL/6 mice (NCI-Fredrick) weighing ~20 g, were used for these studies. Mice were maintained under pathogen-free conditions in facilities approved by the American Association for Accreditation of Laboratory Animal Care and in accordance with current regulations and standards of the US Department of Agriculture, Washington, DC, the US Department of Health and Human Services, Washington, DC, and the National Institutes of Health, Bethesda, MD. GBM6/GBM12/GBM14 glioma cell lines were originally derived from patients at the Mayo Clinic (Rochester, MN).<sup>34</sup> GBM6/GBM12/GBM14 cells were cultured in Dulbecco's modified Eagle's medium supplemented with 5% (vol/vol) fetal calf serum and 100 µg/ml (1% vol/vol) penicillin–streptomycin. Cells were incubated in a humidified atmosphere of 5% (vol/vol) CO<sub>2</sub> at 37 °C. Mice were anesthetized *via* intraperitoneal administration of (ketamine, 40 mg/kg; xylazine, 3 mg/kg) and immobilized in a stereotactic frame (David Kopf Instruments, Tujunga, CA). A 24-gauge needle attached to a Hamilton syringe was inserted into the right basal ganglia to a depth of 3.5-mm and then withdrawn 0.5-mm to make space for tumor cell accumulation. The entry point at the skull was 2-mm lateral and 1-mm dorsal to the bregma. Intracerebral injection of  $0.5 \times 10^6$  GBM6/GBM12/GBM14 glioma cells (~40 mice per cell line per separate experiment) in 2 µl of DMEM (lacking supplementation with fetal bovine serum or with penicillin–streptomycin) was performed over 10 minutes. The skull opening was enclosed with sterile bone wax and the skin incision was closed using sterile surgical staples. Adenoviral vectors, Ad.*mda-7*, Ad.*5/3-mda-7*, or Ad.*cmv* were administered 14 days after tumor cell

implantation *via* stereotactic injection into the intracerebral tumor using the same anesthesia procedure and stereotactic frame coordinates, as described above. Viral vectors (Ad.*mda-7*, Ad.*5/3-mda-7*, or Ad.*cmv*,  $1 \times 10^8$  plaque-forming units) suspended in 2  $\mu$ l of PBS were delivered by slow infusion over a 6-minute period. For animal studies in chapter 4, we performed the experiment twice ( $n = 2$ ) with 5 animals/group. For animal studies in chapter 7, we performed the experiment twice ( $n = 2$ ) and 5 and 6 animals per group.

## 2.12 *Ex Vivo* Manipulation of Tumors

Animals were euthanized by CO<sub>2</sub> and placed in a BSL2 cell culture hood on a sterile barrier mat. The bodies of the mice were soaked in 70% (vol/vol) EtOH and the skin around skull removed using small scissors, forceps and a disposable scalpel. These implements were flame sterilized between removal of the outer and inner layers of skin. A piece of the tumor (~50% by volume) was removed and placed in a 10-cm dish containing 5 ml of RPMI cell culture media, on ice. In parallel, the remainder of the tumor was placed in 5 ml of Streck tissue fixative (Fisher Scientific, Middletown, VA) in a 50-ml conical tube for fixation. The tumor sample that had been placed in RPMI was minced with a sterile disposable scalpel into the smallest possible pieces then placed in a sterile disposable flask. The dish was rinsed with 6.5 ml of RPMI medium, which was then added to the flask. A 10 $\times$  solution of collagenase (Sigma, St Louis MO; 2.5 ml, 28 U/ml final concentration), 10 $\times$  of enzyme mixture containing DNase (Sigma; 308 U/ml final concentration), and pronase (EMD Sciences, San Diego, CA; 22,500 U/ml final concentration) in a volume of 1 ml was added to the flask. The flasks were placed into an

orbital shaking incubator at 37 °C for 1.5 hours at 150 rpm. Following digestion, the solution was passed through a 0.4- $\mu$ m filter into a 50-ml conical tube. After mixing, a sample was removed for viable and total cell counting using a hemacytometer. Cells were then centrifuged at 500g for 4 minutes, the supernatant removed, and fresh RPMI media containing 10% (vol/vol) fetal calf serum and 1% (vol/vol) penicillin–streptomycin was added to give a final resuspended cell concentration of  $1 \times 10^6$  cells/ml. Cells were diluted and plated in 10-cm dishes in triplicate at a concentration of  $2-10 \times 10^3$  cells/dish.

### **2.13 Immunohistochemistry and Staining of Fixed Tumor Sections**

After euthanization, tumors were fixed in Optimum Cutting Temperature (OCT) compound (Tissue Tek); cryostat sectioned (Leica, Wetzlar, Germany) as 12- $\mu$ m sections. Nonspecific binding was blocked with a 2% (vol/vol) rat sera, 1% (vol/vol) bovine sera, 0.1% (vol/vol) Triton X100, 0.05% (vol/vol) Tween-20 solution, then sections were stained for cell-signaling pathway markers: MDA-7/IL-24 (rabbit polyclonal IgG, 1:100; Gene Hunter, Nashville, TN), anti-Ki67 (mouse IgG, 1:100; Oncogene Science, Cambridge, MA), and CD31 (mouse IgG, 1:100; Biomed, Foster City, CA). For staining of sectioned tumors, primary antibodies were applied overnight, sections washed with PBS, and secondary antibodies applied for detection (as indicated in the figures): goat anti-rat Alexa 488/647 (1:500; Invitrogen); goat antimouse Alexa 488/647 (1:500; Invitrogen) secondary antibody as per the primary antibody used, or, detected by way of Diaminobenzidine (DAB) substrate Peroxidase Detection Kit (Biogenex, San Ramon, CA), as per the manufacturer's instructions. The presence of potentially senescent cells was

detected by using a  $\beta$ -galactosidase assay using established procedures. Sections were then dehydrated, cleared, and mounted with coverslips using Permount. Apoptotic cells with double-stranded DNA breaks were detected using the Upstate TUNEL Apoptotic Detection Kit (Charlottesville, VA) according to the manufacturer's instructions. Slides were applied to high-powered light/confocal microscopes (Zeiss LSM 510 Meta-confocal scanning microscope, Zeiss HBO 100 microscope with Axio Cam MRm camera) at the magnification indicated in the figures/figure legends. The proliferation zone, which included both tumor and normal peritoneal tissue, was usually selected as the site of interest, within 2-mm of, or juxtaposed to leading edge of, the tumor. Data shown are representative slides from several sections from the same tumor with multiple tumors (from multiple animals and multiple experiments) having been examined ( $n$  = at least 3–6 animals-tumors).

## **2.14 Data Analysis**

The effects of various treatments were analysed using one-way analysis of variance and a two-tailed Student's  $t$ -test. Results with a  $P$  value of  $<0.05$  were considered statistically significant. Log-rank statistical analyses between the different treatment groups were used for statistical examination of *in vivo* animal survival data. Experimental data shown are the mean values of multiple individual points from multiple experimental data sets ( $\pm$ -SEM).



## CHAPTER 3 INTRODUCTION:

### **OSU-03012 ENHANCES MDA-7/IL-24 KILLING OF GBM CELLS VIA ER STRESS AND AUTOPHAGY AND BY DECREASING EXPRESSION OF MITOCHONDRIAL PROTECTIVE PROTEINS**

MDA-7/IL-24 cellular toxicity has been shown to be coupled with alterations in endoplasmic reticulum stress signaling.<sup>31</sup> In these studies, MDA-7/IL-24 was shown to physically associate with BiP/GRP78 and nullify the protective actions of this ER-chaperone protein. In addition to virus-administered *mda-7*/IL-24, delivery of this cytokine as a bacterially expressed GST fusion protein, GST-MDA-7, retains cancer-specific killing, selective ER localization and is able to induce similar signal transduction changes in cancer cells.<sup>31,32</sup> We have demonstrated that a high concentration of GST-MDA-7 kills primary human glioma cells and does so in a PERK-dependent fashion that is dependent on elevated levels of autophagy and mitochondrial dysfunction.<sup>34-36</sup>

The ability of MDA-7/IL-24 to modulate cell-signaling processes in transformed cells has been examined by several groups.<sup>22-40</sup> Prior work by our group indicated that the use of bacterially synthesized GST-MDA-7 protein,<sup>32</sup> in the 0.25– 2.0 nM concentration range, primarily produced growth arrest with slight cell killing, whereas at ~20-fold greater concentrations, this cytokine causes profound growth arrest and tumor cell death.<sup>32,35,36</sup> Our group has also demonstrated that Ad.*mda-7* kills melanoma cells in part by promoting p38 MAPK-dependent activation of growth arrest and DNA damage inducible genes, including GADD153, GADD45 and GADD34.<sup>38</sup> However, in primary GBM cells, it was noted that p38 MAPK signaling provided a modest protective signal.<sup>36</sup>

In addition, other groups have argued that inhibition of PI3K signaling, but not ERK1/2 signaling, modestly promotes Ad.*mda-7* lethality in breast and lung cancer cells.<sup>39,40</sup>

The present studies were designed to evaluate the relative merit of enhancing autophagy in parallel with expression of MDA-7/ IL-24, using the novel drug OSU- 03012 (AR-12).<sup>136,137</sup> Presently entering Phase I trials, OSU-03012, unlike its parent drug celastrol, does not inhibit COX2 but has an order of magnitude greater toxicity towards tumor cells. Our prior studies have demonstrated that OSU-03012, like MDA-7/IL-24, is able to kill primary human GBM cells in a PERK-dependent fashion.<sup>137</sup> However, unlike MDA-7/IL-24, OSU-03012 lethality was dependent on AIF release from the mitochondrion and not on cytochrome *c* and caspases.<sup>136</sup> The present study indicates that Ad.*mda-7* induced cell killing is enhanced by OSU-03012, and that the cell death does not correlate with enhanced additional PERK phosphorylation. The induction of cell killing is nonetheless dependent on increased levels of toxic autophagy and mitochondrial dysfunction.<sup>138,139</sup>

## CHAPTER 4 RESULTS:

### **OSU-03012 ENHANCES MDA-7/IL-24 KILLING OF GBM CELLS VIA ER STRESS AND AUTOPHAGY AND BY DECREASING EXPRESSION OF MITOCHONDRIAL PROTECTIVE PROTEINS**

#### **4.1 Ad.*mda-7* lethality in GBM's is enhanced by OSU-03012**

Primary human GBM cells (GBM6, 12 and 14) were plated in 12-well plates ( $\sim 2.5 \times 10^4$  cells per well) for 24h, infected with 10 m.o.i. empty vector control virus (Ad.*cmv*) or virus to express MDA-7/IL-24 (Ad.*mda-7*). Twelve hours after infection, cells were treated with vehicle (DMSO) or OSU-03012 (1  $\mu$ M). Forty-eight hours after infection, cells were isolated and cell viability was determined by trypan blue exclusion assay ( $\pm$ SEM, n = 3). Results indicated that treatment of Ad.*mda-7* infected GBM cells with OSU-03012 led to a greater than additive enhancement in tumor cell killing in comparison to the individual agents alone (Figure 4.1).

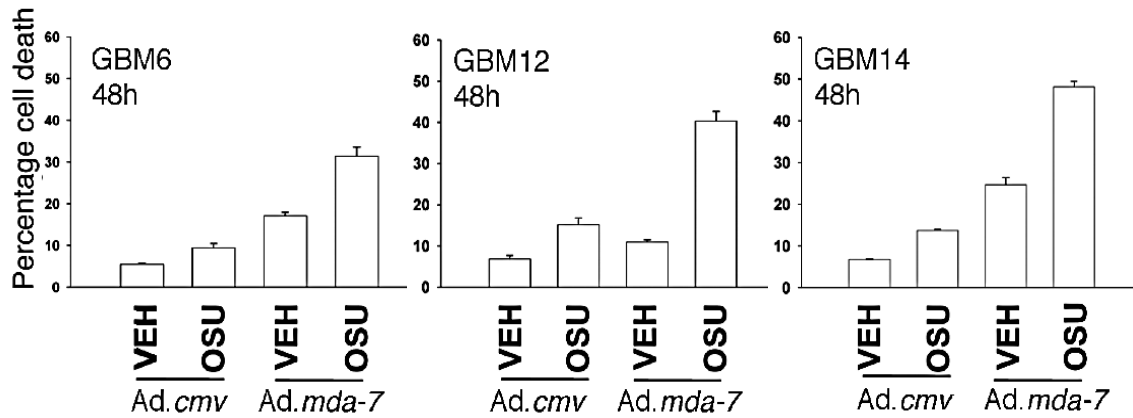


**Figure 4.1 - *Ad.mda-7* lethality is enhanced by OSU-03012.** GBM6, GBM12 and GBM14 cells were infected with empty vector control virus (*Ad.cmv*) or with virus to express MDA-7/IL-24 (*Ad.mda-7*) and 12 h after infection treated with vehicle (DMSO) or OSU-03012 (OSU, 1  $\mu$ M). Forty-eight hours after infection cells were isolated and cell viability was determined by trypan blue exclusion assay ( $\pm$ SEM, n = 3).

#### **4.2 Ad.*mda-7* and OSU-03012 synergize to kill GBM 6 cells in colony formation assays**

A single cell suspension of GBM6 cells was plated (~250 cells/well) in sextuplicate and infected with Ad.*cmv* or Ad.*mda-7*, 24 h after plating. Cells were treated with vehicle (DMSO) or OSU-03012 (1  $\mu$ M), 12 h after infection. Forty-eight hours after infection the growth media was removed and replaced with fresh media lacking drugs. Colonies of >50 cells were permitted to form over the following 10-14 days. After 10-14 days cells forming the colonies were fixed, stained and counted ( $\pm$ SEM, n = 3). Results from this study, in close agreement with the cell death assays, suggested that OSU-03012 significantly (\* p < 0.05) enhanced Ad.*mda-7* lethality in GBM6 cells, as indicated by a dramatic reduction in cell survival.

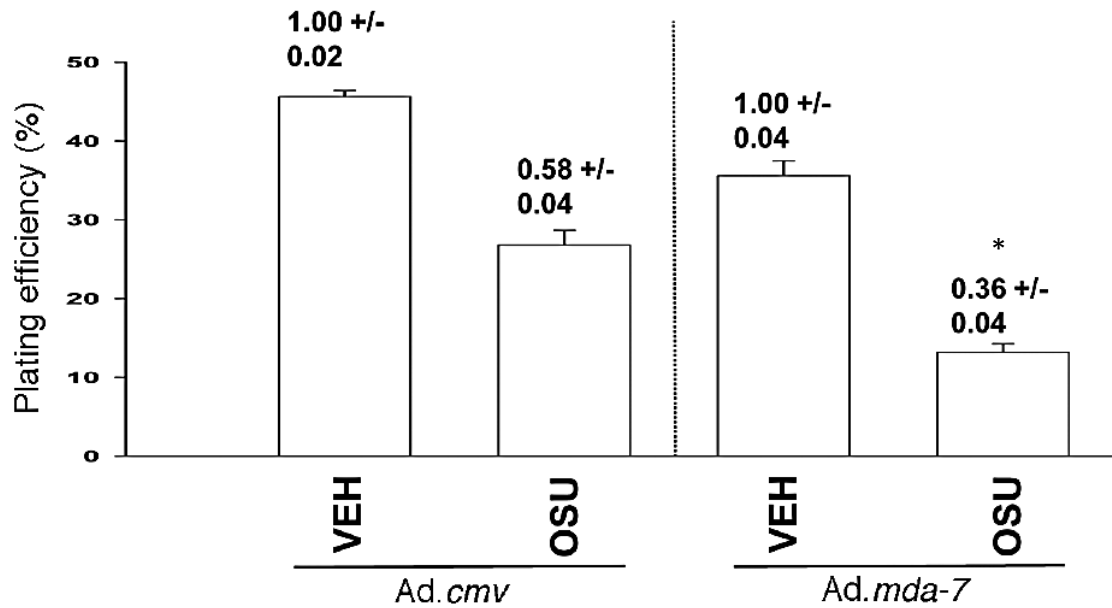


**Figure 4.2 Ad.mda-7 lethality is enhanced by OSU-03012.** GBM6 cells were plated as single cells in sextuplicate and 12 h after plating infected with Ad.cmv or Ad.mda-7 and 12 h after infection treated with vehicle (DMSO) or OSU-03012 (OSU, 1  $\mu$ M). Forty-eight hours after infection the growth media was removed and replaced with new media lacking drugs. Colonies of >50 cells were permitted to form over the following ~20 d, followed by fixing, staining and counting ( $\pm$ SEM, n = 3).

#### **4.3 Ad.*mda-7* infected GBM 6 cells treated with OSU-03012 revealed decreased levels of pro-survival proteins: BCL-XL, MCL-1 and a reduction in the phosphorylation of ERK1/2**

To further elucidate the mechanistic actions of Ad.*mda-7*/OSU-03012 combinational killing of GBM tumor cells, GBM6 cells were plated in 6 cm<sup>2</sup> dishes (~2x10<sup>6</sup> cells/dish) and infected for 24 h with Ad.*cmv* or Ad.*mda-7* prior to treatment with vehicle (DMSO) or OSU-03012 (1 µM). Twenty-four and 48 h after infection, cells were isolated and SDS PAGE performed on cell lysates to determine the expression of BCL-XL and MCL-1, as well as the phosphorylation state of ERK1/2, p38 MAPK, JNK1-3, AKT (S473) (n = 2). The results suggested that treatment of Ad.*mda-7* infected cells with OSU-03012 facilitated a MDA-7/IL-24-induced reduction in the expression of the anti-apoptotic proteins BCL-XL and MCL-1 and decreased activity of the pro-survival protein, ERK1/2 (Figure 4.3).

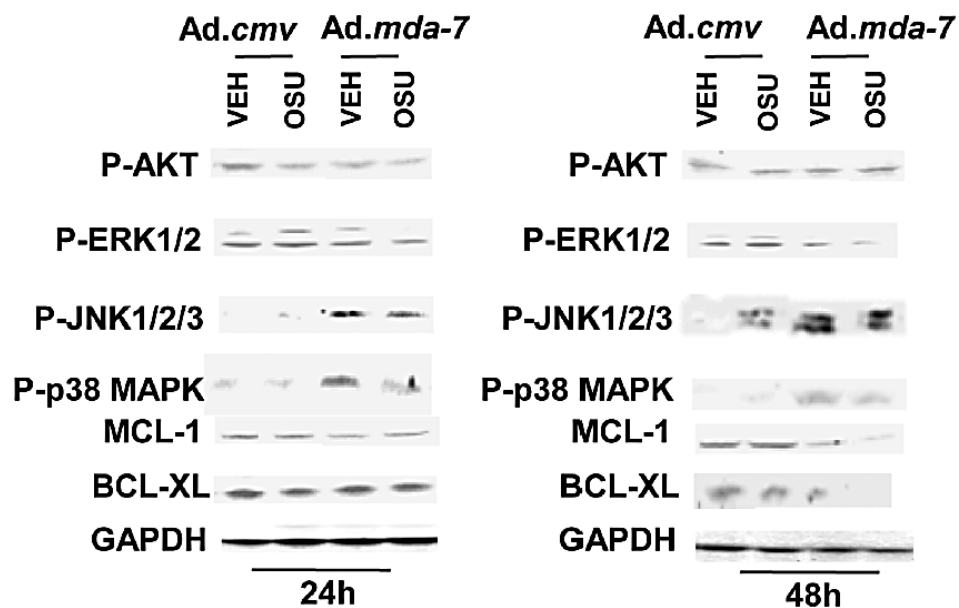


**Figure 4.3 *Ad.mda-7* inhibition of pro-survival proteins is enhanced by OSU-03012.** GBM6 cells were infected with *Ad.cmv* or *Ad.mda-7* and 12 h after infection treated with vehicle (DMSO) or OSU-03012 (OSU, 1  $\mu$ M). Twenty-four hours and 48 h after infection cells were isolated and SDSPAGE performed to determine the expression of BCL-XL and MCL-1, and the phosphorylation of ERK1/2, p38 MAPK, JNK1-3, AKT (S473) (n = 2).



#### **4.4 Overexpression of BCL-XL, or inhibition of components of the intrinsic apoptosis pathway in GBM 6 cells were shown to reduce *Ad.mda-7* or OSU-03012 toxicity as single agents or in combination**

Treatment of *Ad.mda-7* infected GBM6 with OSU-03012 was shown to profoundly affect the expression of multiple anti-apoptotic proteins, ultimately enabling the induction of apoptosis. The respective role(s) of the intrinsic and/or extrinsic pathways of apoptosis in cell death was assessed. GBM6 cells were plated in 12-well plates ( $\sim 2.5 \times 10^4$  cells per well) for 24h. Cells were then infected with (all virus infections at 10 m.o.i.) empty vector control virus (*Ad.cmv*) or virus to express MDA-7/IL-24 (*Ad.mda-7*). Twelve hours after infection cells were again infected with viruses to either express XIAP, BCL-XL, and dominant negative caspase 9 or c-FLIP-s. Twelve hours after infection, cells were treated with vehicle (DMSO), or OSU-03012 (1  $\mu$ M). Forty-eight hours after initial infection with *mda-7* or apoptotic regulatory proteins, cells were isolated and cell viability was determined by trypan blue exclusion assay ( $\pm$ SEM, n = 3). These results suggested that overexpression of the anti-apoptotic protein BCL-XL, or inhibition of components involved in the intrinsic apoptosis pathway, reduced *Ad.mda-7* or OSU-03012 toxicity when used as single agents, and abolished the enhanced cell killing seen as a result of the interaction between these agents. Inhibition of the extrinsic pathway, as judged by the overexpression of the caspase 8 inhibitor c-FLIP-s, did not alter *Ad.mda-7* or OSU-03012 lethality (Figure 4.4).

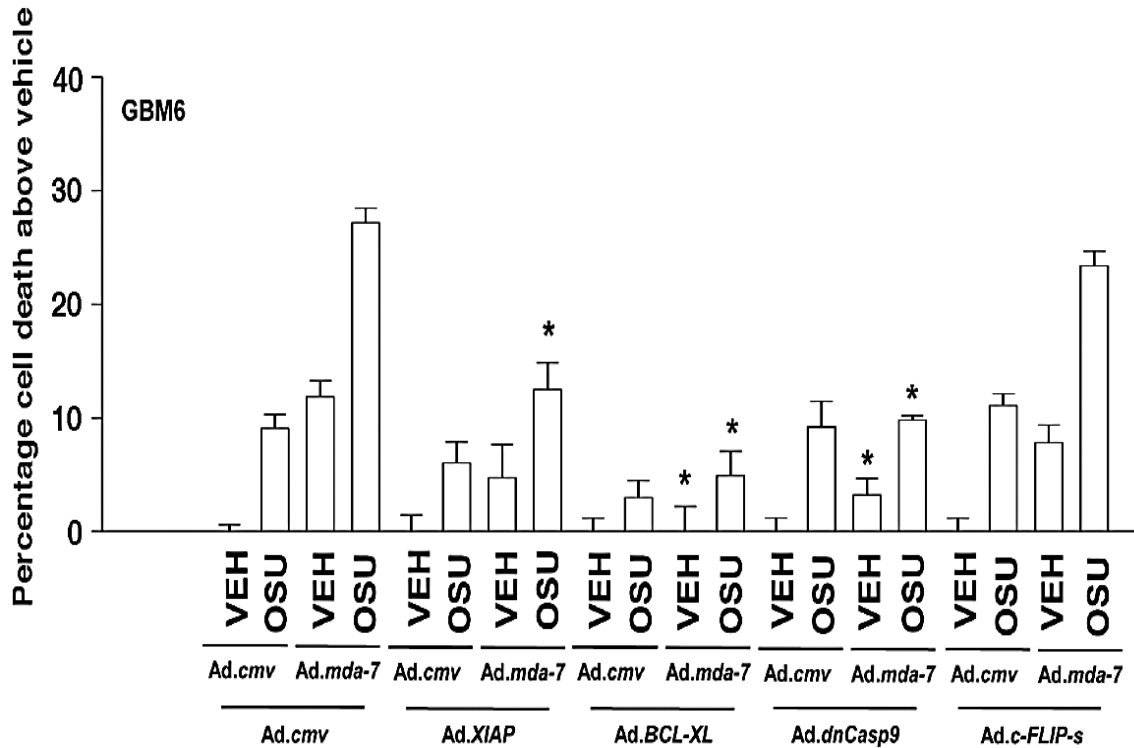


**Figure 4.4 Overexpression of BCL-XL or inhibition of components of the intrinsic apoptotic pathway reduced *Ad.mda-7* or OSU-03012 toxicity.** GBM6 cells were infected with *Ad.cmv* or *Ad.mda-7* in combination with viruses to express XIAP, BCL-XL, dominant negative caspase 9 or c-FLIP-s, and 12 h after infection treated with vehicle (DMSO), or OSU-03012 (OSU, 1  $\mu$ M). Forty-eight hours after infection cells were isolated and cell viability was determined by trypan blue exclusion assay ( $\pm$ SEM, n = 3).

#### **4.5 Activation of MEK protects GBM 6 cells from MDA-7/IL-24 and OSU-03012 toxicity**

Since our data indicated that ERK1/2 was significantly inactivated in cells treated with OSU-03012 + Ad.*mda-7*, an assessment of whether maintenance of ERK1/2 activity was able to modulate OSU-03012 + Ad.*mda-7* mediated toxicity was performed. GBM6 cells were plated and infected with (all virus infections at 10 m.o.i.) empty vector control virus (Ad.*cmv*) or with viruses to either express MDA-7/IL-24 (Ad.*mda-7*) or a constitutively active form of MEK1 (MEK1 EE). Twelve hours after infection, cells were treated with vehicle (DMSO) or OSU-03012 (1  $\mu$ M). Cells were isolated 48 h after infection and cell viability was determined by trypan blue exclusion assay ( $\pm$ SEM, n=3). Results from this study indicated that the expression of constitutively activated MEK1 EE was sufficient to maintain ERK1/2 phosphorylation, acting to also partially sustain expression of the anti-apoptotic proteins BCL-XL and MCL-1 in the presence of Ad.*mda-7*+OSU-03012 combination treatment (Figure 4.5).

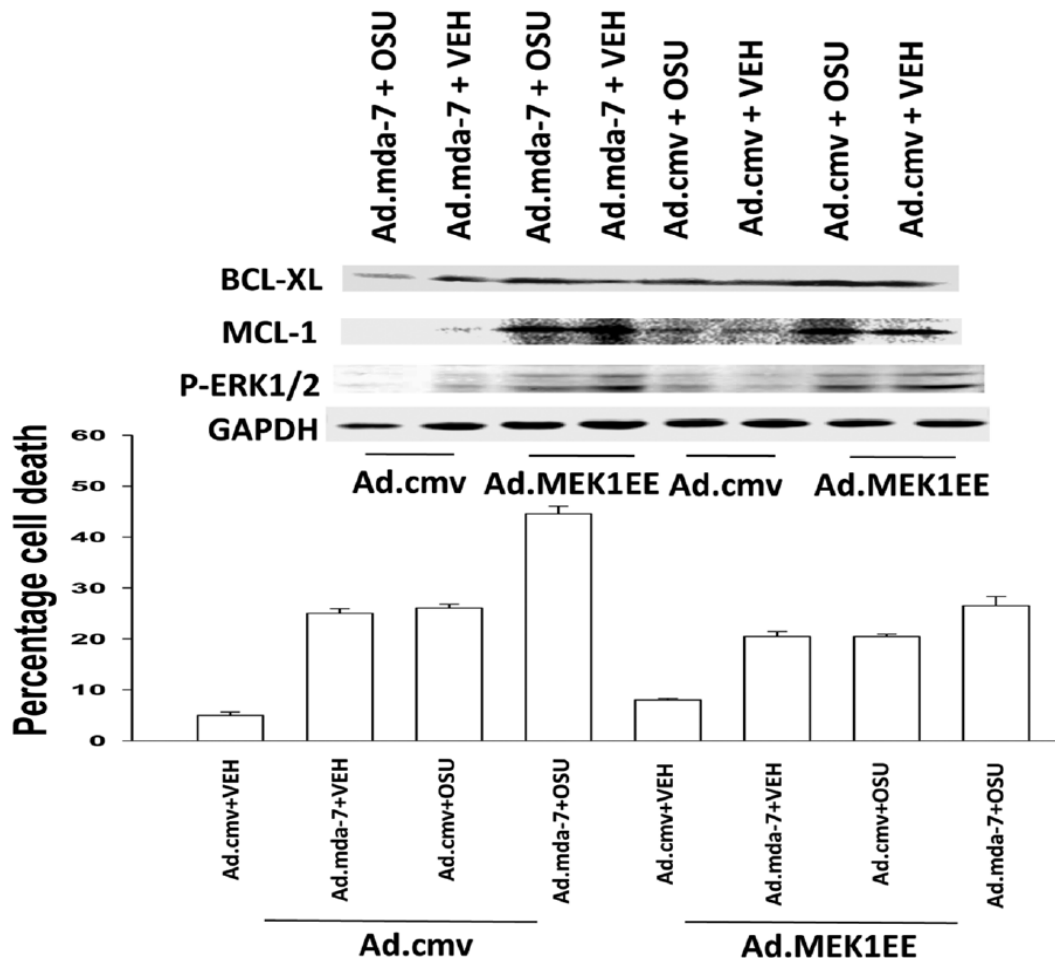


**Figure 4.5 Activation of MEK and constitutive MCL-1 expression protect GBM cells from MDA-7/IL-24 and OSU-03012 toxicity.** GBM6 cells were infected with empty vector control virus (Ad.cmv) or with viruses to express MDA-7/IL-24 (Ad.mda-7) or a constitutively active form of MEK1 (MEK1 EE). Twelve hours after infection cells were treated with vehicle (DMSO) or OSU-03012 (OSU, 1  $\mu$ M). Cells were isolated 48 h after infection and cell viability was determined by trypan blue exclusion assay ( $\pm$ SEM, n = 3).

#### **4.6 Constitutive expression of MCL-1 protects GBM 6 cells from MDA- 7/IL-24 and OSU-03012 toxicity**

Dramatic changes in the cytoprotective protein levels of Mcl-1 and not Bcl-xL were noticed. In this study, a role for OSU-03012 in enhancing *Ad.mda7* cell lethality by facilitating MDA-7/IL24 induced down regulation of specific mitochondrial protective proteins was assessed. GBM6 cells were infected with empty vector control virus (*Ad.cmv*) or with a virus to express MDA-7/IL-24 (*Ad.mda-7*) and, in parallel, transfected with either a control plasmid or a plasmid to express MCL-1. Twelve hours after infection/transfection, cells were treated with vehicle (DMSO) or OSU-03012 (OSU, 1  $\mu$ M). Cells were isolated 48 h after infection and cell viability was determined by trypan blue exclusion assay ( $\pm$ SEM, n = 3). The results indicate that overexpression of cytoprotective MCL-1 protected GBM cells from OSU-03012 + *Ad.mda-7* induced lethality (Figure 4.6).

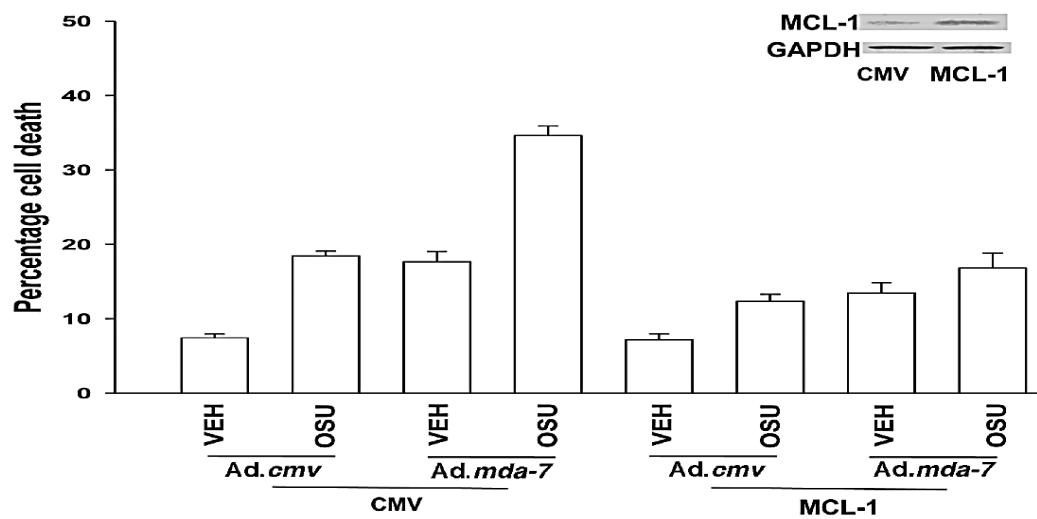


**Figure 4.6 Constitutive MCL-1 expression protects GBM cells from MDA-7/IL-24 and OSU-03012 toxicity.** GBM6 cells were infected with empty vector control virus (Ad.cmv) or with viruses to express MDA-7/IL-24 (Ad.mda-7) and in parallel transfected with a control plasmid or a plasmid to express MCL-1. Twelve hours after infection cells were treated with vehicle (DMSO) or OSU-03012 (OSU, 1  $\mu$ M). Cells were isolated 48 h after infection and cell viability was determined by trypan blue exclusion assay ( $\pm$ SEM, n = 3).

#### **4.7 OSU-03012 treatment enhances *Ad.mda-7* induced toxic autophagy but does not promote additional activation of PERK in primary human GBM cells**

In this study, GBM6 cells were infected with *Ad.cmv* or *Ad.mda-7*, and subsequently 12 h after infection, the cells were treated with either vehicle (DMSO) or OSU-03012 (1  $\mu$ M). Cells were isolated 24 and 48 h after infection and SDSPAGE and immunoblotting was performed to determine the presence of phosphorylated PERK and the conversion of LC3 to LC3-II (n = 3). Infection of primary human GBM cells with *Ad.mda-7* was shown to activate PERK however; treatment of GBM 6 cells expressing MDA-7/IL-24 with OSU-03012 did not cause additional PERK activation, instead leading to a reduction in PERK phosphorylation. OSU-03012 + *Ad.mda-7* treatment was shown to increase the processing/expression of LC3-II to a greater extent than that induced by treatment of cells with the individual agents. These results indicate that the therapeutic combination of OSU-03012 + *Ad.mda-7* is able to induce elevated levels of autophagy (Figure 4.7).

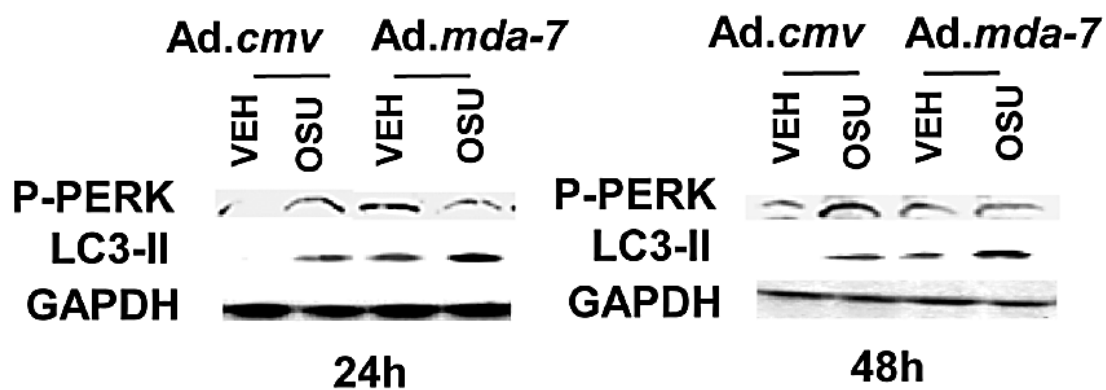


**Figure 4.7 OSU-03012 treatment enhances *Ad.mda-7*-induced toxic autophagy but does not promote additional activation of PERK.** GBM6 cells were infected with *Ad.cmv* or *Ad.mda-7* and 12 h after infection treated with vehicle (DMSO) or OSU-03012 (OSU, 1  $\mu$ M). Cells were isolated 24 and 48 h after infection, SDS-PAGE and immunoblotting was performed to assess the phosphorylation of PERK and the conversion of LC3 to LC3-II (n = 3).



#### **4.8 Expression of dominant negative PERK suppresses the lethal interaction between OSU-03012 and Ad.*mda-7* in primary human GBM cells**

This study further assessed the role of PERK in the toxicity induced by OSU-03012 + Ad.*mda-7* treatment. GBM6 cells were infected with Ad.*cmv* or Ad.*mda-7* and in parallel transfected with either an empty vector plasmid (CMV) or a plasmid to express dominant negative PERK (dnPERK). Twelve hours after infection cells were treated with vehicle (DMSO) or OSU-03012. Forty-eight hours after infection the cells were isolated and cell viability was determined by trypan blue dye exclusion assay ( $\pm$ SEM, n = 3). Although OSU-03012 + Ad.*mda-7* treatment does not further increase the expression of PERK, compared to single agent treatments, these results indicated that the expression of dnPERK was still able to suppress the lethal interactions between OSU-03012 and Ad.*mda-7*/IL-24 (Figure 4.8).

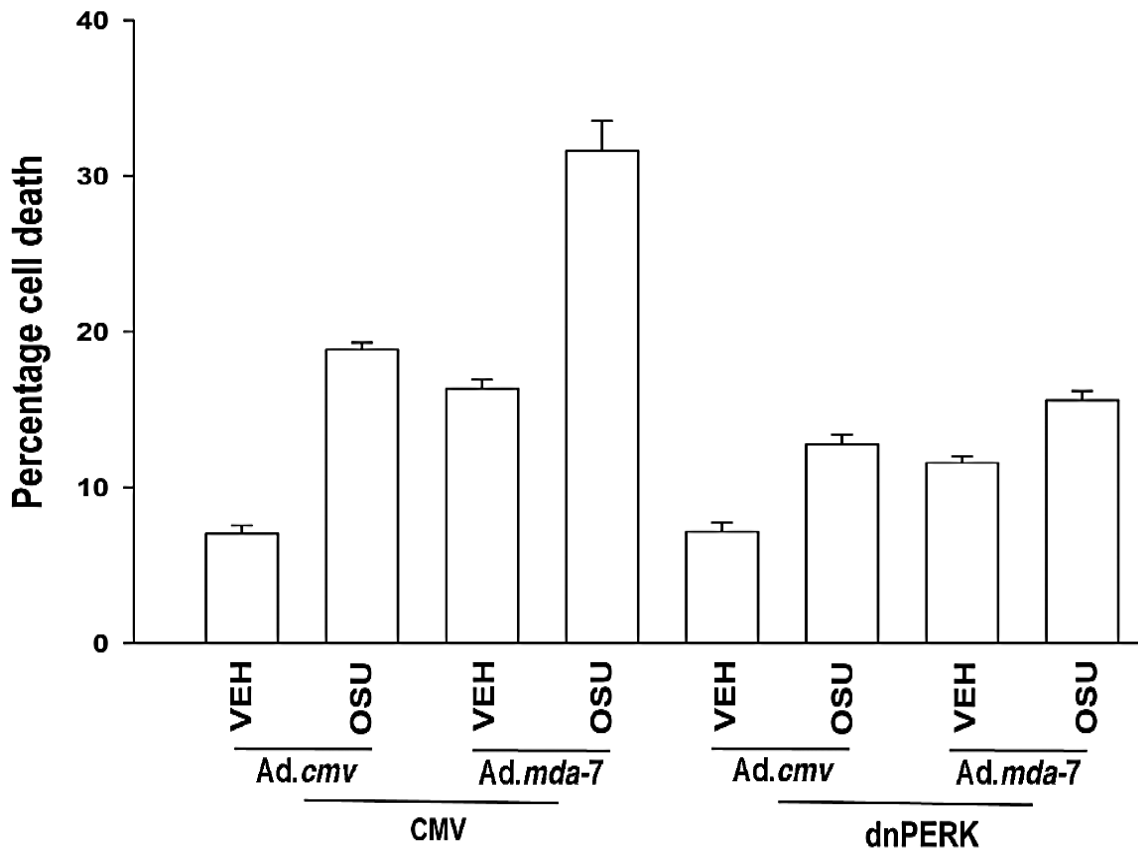


**Figure 4.8 Expression of dominant negative PERK suppresses the lethal interaction between OSU-03012 and Ad.mda-7 in primary human GBM cells.** GBM6 cells were infected with Ad.cmv or Ad.mda-7 and in parallel transfected with either an empty vector plasmid (CMV) or a plasmid to express dominant negative PERK (dnPERK). Twelve hours after infection cells were treated with vehicle (DMSO) or OSU-03012. Forty-eight hours after infection cells were isolated and cell viability was determined by trypan blue dye exclusion assay ( $\pm$ SEM,  $n = 3$ ).

#### **4.9 The additive increase of LC3-GFP vesicularization in GBM cells caused by OSU-03012 and Ad.*mda-7* is blocked by expression of dominant negative PERK**

The role of OSU-03012 + Ad.*mda-7* in cell death mediated by toxic autophagy was assessed. GBM6 cells were plated ( $2.5 \times 10^4$  cells/well) in four-well chamber slides and infected with Ad.*cmv* or Ad.*mda-7* and concurrently, cells were transfected with a plasmid to express LC3-GFP and with either an empty vector plasmid (CMV) or a plasmid to express dominant negative PERK (dnPERK). In parallel, cells were transfected with either scrambled siRNA (siSCR) or a siRNA to specifically knock down autophagy inducing protein, Beclin1 (siBeclin1). Twelve hours after infection cells are treated with vehicle (DMSO) or OSU-03012 and twelve hours after drug treatment cells were examined using a fluorescent microscope (40x magnification) for the formation of intense GFP positive stained vesicles ( $\pm$ SEM,  $n = 3$ ). The results indicated that GBM6 cells treated with OSU-03012 + Ad.*mda-7* display an additive increase in the vesicularization of a transfected LC3-GFP construct, suggesting that autophagy occurred. Further confirmation of these findings was provided through the indication that the toxic autophagic effect was blocked by expression of dominant negative PERK or by knock down of Beclin 1 (Figure 4.9).

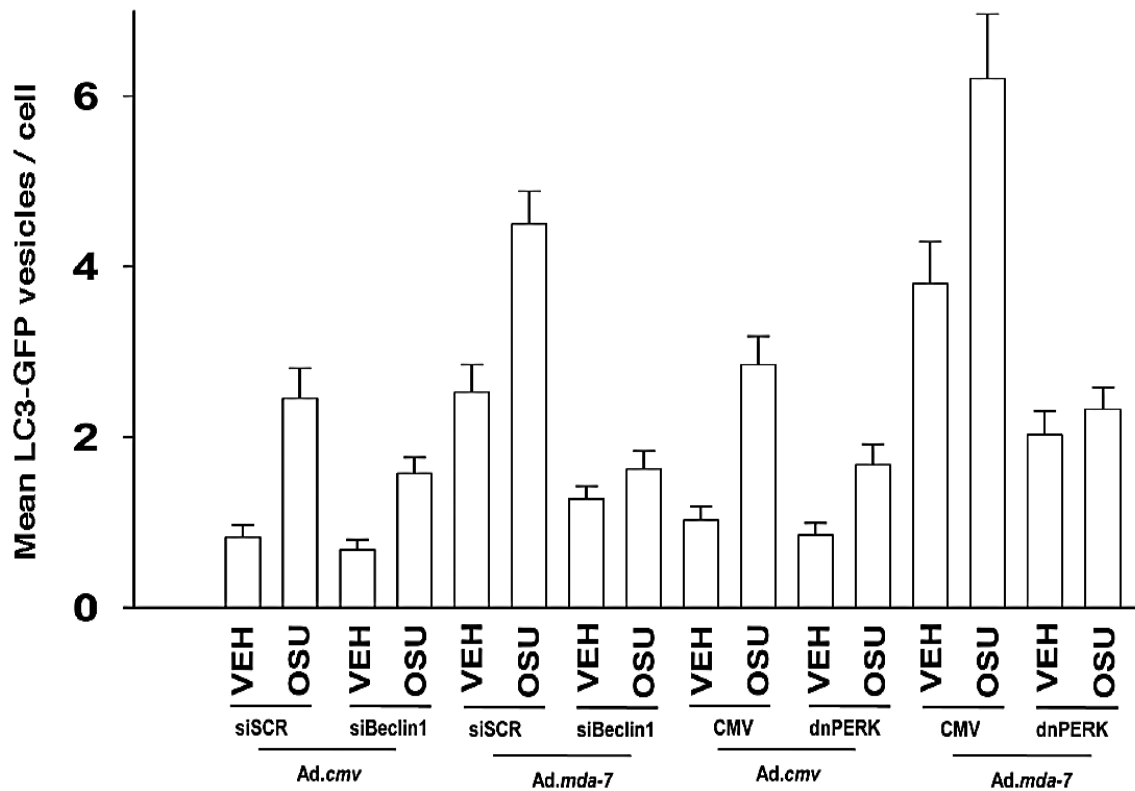


**Figure 4.9 The additive increase of LC3-GFP vesicularization in GBM cells caused by OSU-03012 and Ad.mda-7 is blocked by expression of dominant negative PERK.** GBM6 cells in four-well chambered slides were infected with Ad.cmv or Ad.mda-7 and in parallel transfected with a plasmid to express LC3-GFP and with either an empty vector plasmid (CMV) or a plasmid to express dominant negative PERK (dnPERK). Twelve hours after infection cells are treated with vehicle (DMSO) or OSU-03012. Twelve hours after drug treatment cells were examined using a fluorescent microscope (40x magnification) for the formation of intense GFP staining vesicles ( $\pm$ SEM,  $n = 3$ ).

#### **4.10 Knockdown of ATG5 or Beclin1 expression reduced the toxicity of Ad.*mda-7*, OSU-03012 or the combination in GBM cells**

To further assess the role of autophagy induced by OSU-03012 + Ad.*mda-7* treatment, GBM6 cells were simultaneously infected with Ad.*cmv* or Ad.*mda-7* and transfected with either siSCR or siRNAs to knockdown autophagy inducing proteins Beclin1 (siBeclin1) or ATG5 (siATG5). Twelve hours after infection/transfection, cells are treated with vehicle (DMSO) or OSU-03012 (1  $\mu$ M). Forty-eight hours after drug treatment the cells were isolated and cell viability was determined by trypan blue exclusion assay ( $\pm$ SEM, n = 3). These results indicated that knockdown of ATG5 or Beclin1 expression resulted in a profound reduction in the cellular toxicity of Ad.*mda-7*, OSU-03012 and combined treatment with both agents in GBM6 cells (Figure 4.10).

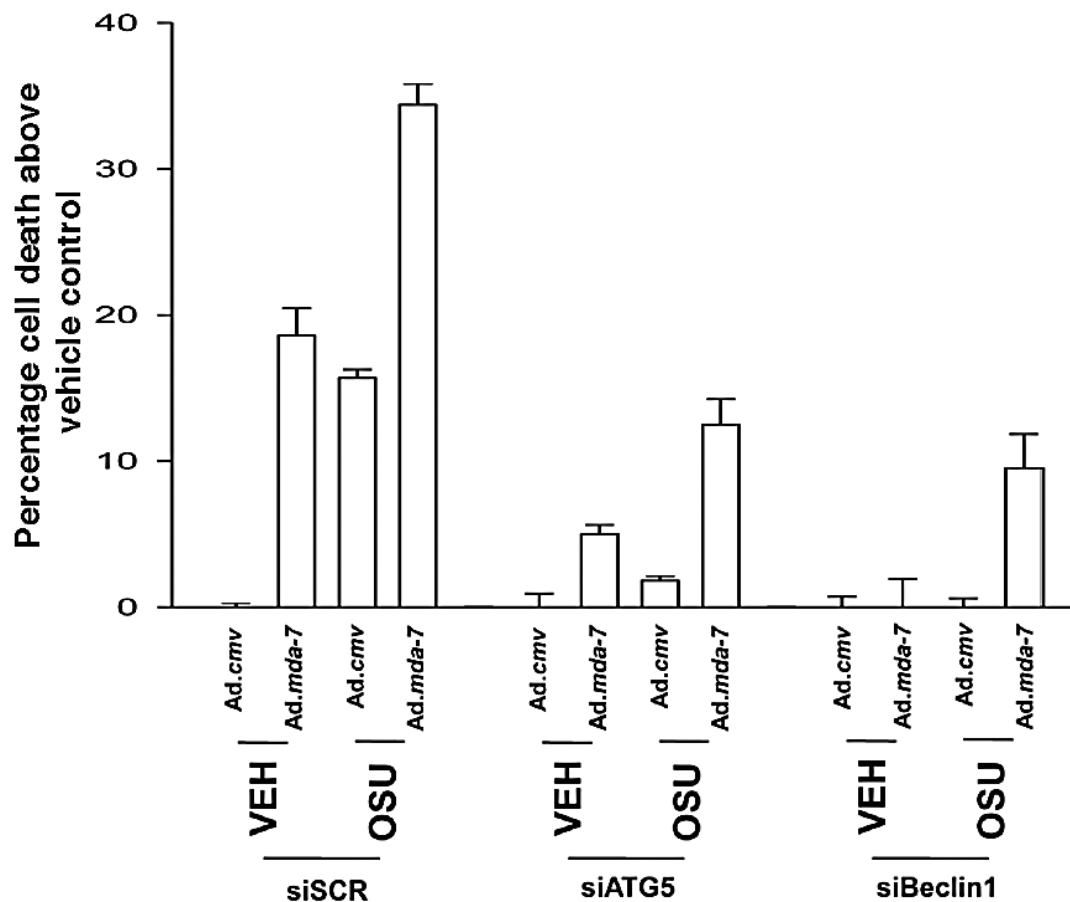


**Figure 4.10 Knockdown of ATG5 or Beclin1 expression reduced the toxicity of Ad.mda-7, OSU-03012 or the combination in GBM cells.** GBM6 cells were infected with Ad.cmv or Ad.mda-7 and in parallel transfected with either a scrambled siRNA (siSCR) or siRNAs to knockdown Beclin1 (siBeclin1) or ATG5 (siATG5). Twelve hours after infection cells are treated with vehicle (DMSO) or OSU-03012 (OSU, 1  $\mu$ M). Forty-eight hours after drug treatment cells were isolated and cell viability was determined by trypan blue exclusion assay ( $\pm$ SEM, n = 3).

#### **4.11 MDA-7/IL-24 enhances the toxicity of ionizing radiation**

In addition to a role in inducing cytotoxic autophagy and sensitization to OSU-03012, studies next investigated the effect of MDA-7/IL-24 upon radiation sensitivity and the presence of a “by-stander” cell killing capacity. GBM6 cells were infected with *Ad.cmv* or *Ad.mda-7*. Forty-eight hours after infection cells and media were collected separately. The conditioned media was placed onto uninfected GBM6 cells, and 24 h after media addition these cells were irradiated (4 Gy). Forty-eight hours after addition of the conditioned media (as described in the Methods section) to the cells, cell viability was determined by trypan blue dye exclusion assay ( $\pm$ SEM,  $n = 3$ ). These results indicate that the conditioned media from *Ad.mda-7* infected GBM cells played a role in enhancing the toxicity of ionizing radiation in uninfected GBM cells (Figure 4.11). To further establish the effect of *Ad.mda-7* on uninfected cells, conditioned media was applied and along with ionizing radiation.

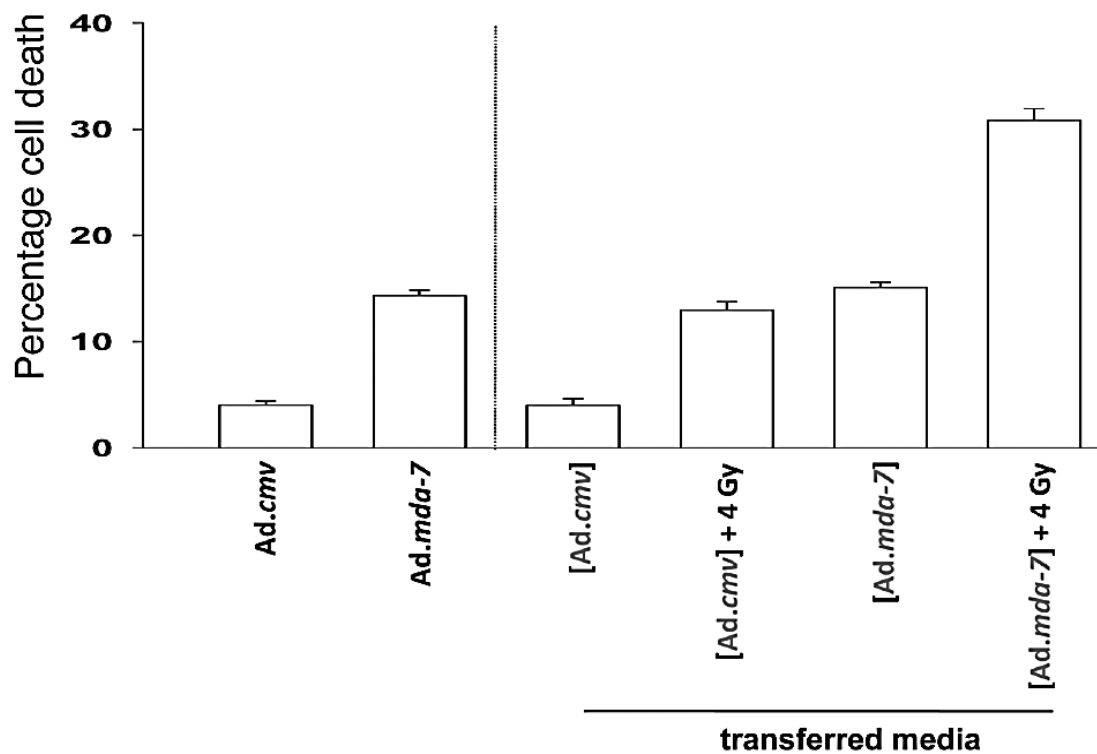


**Figure 4.11 MDA-7/IL-24 sensitizes GBM6 cells to radiation.** GBM6 cells were infected with Ad.cmv or Ad.mda-7. Forty-eight hours after infection cells and media were isolated. Cell viability was determined by trypan blue dye exclusion assay ( $\pm$ SEM,  $n = 3$ ). The media was placed onto GBM6 cells and 24 h after media addition cells were irradiated (4 Gy). Forty-eight hours after placement of conditioned media onto the cells, cell viability was again determined by trypan blue dye exclusion assay ( $\pm$ SEM,  $n = 3$ ).



**4.12 Transfection of uninfected GBM cells with siRNA to knock down MDA-7/IL-24 expression prevented conditioned media from Ad.*mda-7* infected GBM cells from increasing MDA-7/IL-24 expression, as well as enhancing the toxicity of OSU-03012 or ionizing radiation**

GBM6 cells were infected with Ad.*cmv* or Ad.*mda-7* and forty-eight hours after infection, the cells and media were isolated and cell viability was determined by trypan blue dye exclusion assay ( $\pm$ SEM, n = 3). The media was added to uninfected GBM6 cells that had previously been transfected with plasmids to either express a control shRNA (shSCR) or a shRNA to knock down MDA-7/IL-24 expression (shMDA-7). Thirty minutes after media addition cells were exposed to radiation (4 Gy) and treated with vehicle (DMSO) or OSU-03012 (1  $\mu$ M). Forty-eight hours after the addition of conditioned media to the cells, cell viability was again determined by trypan blue exclusion assay ( $\pm$ SEM, n = 3). All results imply that the conditioned media from Ad.*mda-7* infected GBM cells was able to induce expression of MDA-7/IL-24 in uninfected GBM cells. Furthermore, these cells displayed enhanced toxicity to ionizing radiation compared to control treated cells (Figure 4.12). Transfection of uninfected GBM cells with a siRNA to knock down MDA-7/IL-24 expression was shown to prevent the effects of conditioned media from Ad.*mda-7* infected GBM cells increasing MDA-7/IL-24 expression. In addition, the enhanced toxicity to OSU-03012 and ionizing radiation was also significantly reduced in these cells.

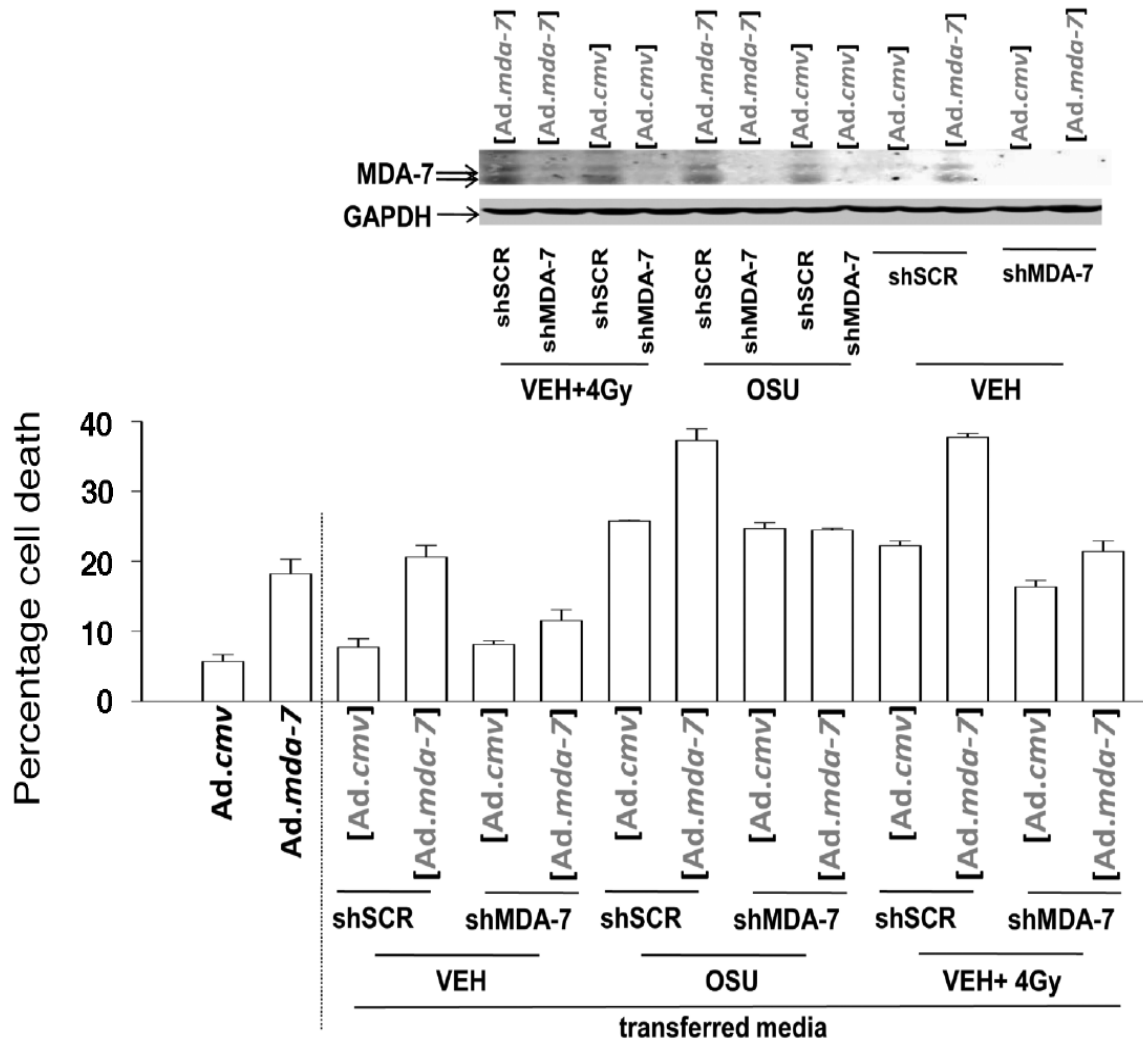


**Figure 4.12 MDA-7/IL-24 stimulates expression of MDA-7/IL-24 and increases toxicity of GBM6 cells to drug and ionizing radiation.** GBM6 cells were infected with *Ad.cmv* or *Ad.mda-7*. Forty-eight hours after infection cells and media were isolated. Cell viability was determined by trypan blue dye exclusion assay ( $\pm$ SEM,  $n = 3$ ). The media was placed onto GBM6 cells that had been transfected with plasmids to express a control shRNA (shSCR) or an shRNA to knock down MDA-7/IL-24 expression (shMDA-7) (labeled in parentheses, grey). Thirty minutes after media addition cells were treated with: (a) radiation (4 Gy) or; (b) vehicle (DMSO) or OSU-03012 (OSU, 1  $\mu$ M). Forty-eight hours after placement of conditioned media onto the cells, cell viability was again determined by trypan blue exclusion assay ( $\pm$ SEM,  $n = 3$ ). *Inset Panel:* conditioned media containing MDA-7/IL-24 induces MDA-7/IL-24 in uninfected GBM cells that is blocked by shRNA knockdown of MDA-7/IL-24.

## CHAPTER 5 DISCUSSION:

### **OSU-03012 ENHANCES MDA-7/IL-24 KILLING OF GBM CELLS VIA ER STRESS AND AUTOPHAGY AND BY DECREASING EXPRESSION OF MITOCHONDRIAL PROTECTIVE PROTEINS**

Previous studies, in both our laboratory and others, have shown that GST-MDA-7/IL-24 or Ad.*mda-7/IL-24* is able to reduce cellular proliferation and cause tumor cell-specific killing of malignant glioma cells via the induction of a toxic form of autophagy.<sup>35,36,141,142,145</sup> We have also shown that OSU-03012 also kills GBM cells through the induction of autophagy thus the data presented in Chapter 4 was designed to establish whether OSU-03012 and Ad.*mda-7/IL-24* display a cooperative action in GBM cell killing, and determine the mechanisms involved in their mutual action.

Infection of GBM cells with a 10 m.o.i dose of Ad.*mda-7/IL-24* was shown to cause modest levels of toxicity at ~48 h post drug exposure. These results closely correlated with the activation of the pro-apoptotic JNK1/2 and p38 MAPK pathways, as well as the phosphorylation of ER-stress related protein, PERK. In addition, the combination of OSU-03012 and Ad.*mda-7/IL-24* was shown to suppress the pro-growth/survival ERK1/2 and, to a lesser extent, AKT signaling cascades. Multiple studies using a number of toxic stimuli have documented that prolonged JNK1-3 and/or p38 MAPK activation in a wide variety of cell types, can lead to cell death.<sup>134,140-145</sup> It is well established that the balance between the ERK1/2 and JNK1-3 signaling plays a key role in homeostatic balance that distinguishes between cell survival versus cell death processes.<sup>140-</sup>

<sup>145</sup> Prior studies in primary human GBM cells using GST-MDA-7/IL-24, have

demonstrated that inhibition of the ERK1/2 signaling cascade represents a key pro-apoptotic effect generated by GST-MDA-7 exposure. Also, treating GBM cells with OSU-03012 as a single agent at low concentrations does not significantly modulate the activity of any of the widely examined signal transduction pathways, e.g., ERK1/2, JNK1/2, p38 MAPK or AKT.<sup>141-142</sup> In the work presented here, OSU-03012 was able to further enhance the MDA-7/IL-24-induced suppression of ERK1/2 signaling, which in turn was shown to result in a significantly reduced expression of the mitochondrial protective proteins MCL-1 and BCL-XL.

Infection of GBM cells with *Ad.mda-7/IL-24* was shown to decrease the expression of BCL-XL and MCL-1, an affect which has previously been demonstrated with GST-MDA-7. The latter case has been attributed to ER stress signaling via activation of PERK-eIF2 $\alpha$ .<sup>35,36,145</sup> Reduced MCL-1 and BCL-XL expression was able to facilitate mitochondrial dysfunction and the release of cytochrome *c* into the cytosol. In addition, we have recently published work indicating that the reduced expression of these anti-apoptotic proteins was shown to enhance the induction of autophagy by increasing the levels of free Beclin1.<sup>41,145,146</sup> Unbound Beclin1 has been shown to interact with Vps34 to promote autophagy.<sup>146</sup> We have also demonstrated that MDA-7/IL-24 mediated induction of JNK1/2 pathway signaling was able to mediate the activation of the pro-apoptotic proteins BAX and BAK. OSU-03012 was unable to further increase JNK1/2 signaling levels. Thus, the possibility exists that MDA-7/IL-24 is able to induce an increased expression of pro-apoptotic proteins and a concomitant reduction in anti-apoptotic proteins, potentially inhibiting protective signaling pathways, leading to greater levels of tumor cell death.

Prior studies have demonstrated that as single agents, the lethality of both GST-MDA-7/IL-24 and OSU-03012 seen in GBM cells, required the induction of a toxic form of autophagy and that this process was dependent upon PERK signaling.<sup>35,36</sup> A less than additive lethal interaction when *Ad.mda-7/IL-24* and OSU-03012 are used in combination to kill GBM cells would argue that both of these agents were acting upon a single molecule, e.g., PERK, in the promotion of toxic autophagy and cell death. Alternatively, if *Ad.mda-7/IL-24* and OSU-03012, when used in combination to kill GBM cells, induced a greater than additive amount of cell killing, both agents would be expected to have individual modes of action/targets. Although OSU-03012 did not further enhance MDA-7/IL-24-induced PERK activation or JNK1/2 signaling, when used in combination *Ad.mda-7/IL-24* and OSU-03012 were shown to induce an additive increase in LC3-II levels and in the vesicularization of a transfected LC3-GFP construct. The inhibition of autophagy, either at the level of PERK inhibition or by the knock down of ATG5/Beclin1, was shown to block the lethal interaction between *Ad.mda-7/IL-24* and OSU-03012.

BiP/GRP78 has been defined as a key target for MDA-7/IL-24. The binding of MDA-7/IL-24 to this chaperone protein, results in the release and subsequent activation of PERK.<sup>31</sup> Several initial reports argue that the lethality of OSU-03012 in tumor cells may be due to inhibition of the enzyme PDK-1, part of the PI3 kinase pathway, and OSU-03012, millimolar range, has been shown to suppress AKT phosphorylation and measurable inhibition of PDK-1 activity.<sup>136,137</sup> In addition, OSU-03012 interacts with multiple kinase inhibitors to kill tumor cells in a manner that appears to be caspase independent. OSU-03012 has also been shown to enhance HSP70 and decrease HSP90

expression. As a result, the key mode of action for this drug may be to alter chaperone protein function, this in turn may have an effect upon the correct processing/folding of many different proteins, including those with the ability to stabilize lysosomes and mitochondria. Indeed,<sup>132</sup> recent studies have demonstrated that OSU-03012 treatment was able to suppress expression of BiP/GRP78 and did so through reduced stability of the protein. In this work, knock down of BiP/GRP78 was shown to enhance OSU lethality and overexpression of BiP/GRP78 was shown to abolish OSU toxicity. Further detailed studies will be required to fully unravel the biological consequences and molecular basis of the actions of OSU-03012 upon cancer cells.

GBM was one of the first malignancies considered to be treatable through viral delivery of genetic-based therapeutics.<sup>41</sup> However, a problem of efficacy, exists for all gene therapy approaches, a problem that is intensified by the highly invasive and diffuse nature of GBM's as compared to other tumor cell types. This problem signifies the need for the development of a toxic 'bystander' effect in tumor cells that have not been infected by the virus during the primary infection process. By the rules of simple mass-action, i.e., with the total number of non-transformed cells within and around a GBM tumor, compared to the total number of transformed cells in a tumor and the total number of virus particles infused. Thus, it is not possible for all tumor cells in a highly invasive tumor cell type such as GBM to be infected by a non-replicative virus. Furthermore, many prior studies with GBM involving the use of gene therapeutic vectors, have often expressed intracellular proteins that are not normally expressed or secreted, which will frequently result in only the cells that have been virally infected being subjected to the actions of the therapeutic

agent. The expression of MDA-7/IL-24 overcomes this limitation associated with lack of a 'bystander' effect following gene therapeutic intervention seen in the majority of previous studies.<sup>138,139</sup> We have found that, as a cytokine, MDA-7/IL-24 is secreted from infected GBM cells into the surrounding media and this MDA-7/IL-24 conditioned media has been shown to induce apoptosis in uninfected GBM cells and to promote the toxic effects seen with either OSU-03012 or ionizing radiation.

**CHAPTER 6 INTRODUCTION:**

**INHIBITORS OF MULTIPLE PROTECTIVE SIGNALING  
PATHWAYS AND Ad.5/3 DELIVERY ENHANCES MDA-7/IL-24  
KILLING**

The ability of MDA-7/IL-24 to modulate cell-signaling processes in transformed cells has been investigated by several groups.<sup>22-41</sup> Prior work by our group has demonstrated, using bacterially synthesized GST-MDA-7 protein,<sup>32</sup> in the 0.25–2.0 nmol/l concentration in range, that GST-MDA-7 primarily caused growth arrest with little cell killing. At ~20-fold greater concentrations, this cytokine causes profound growth arrest and tumor cell death.<sup>32,35,36</sup> Our group has also demonstrated that Ad.5-*mda-7* mediated cell death in melanoma cells is in part due to promotion of p38 MAPK dependent activation of the growth arrest and DNA damage inducible genes, including GADD153, GADD45, and GADD34.<sup>38</sup> However, in primary GBM cells, p38 MAPK signaling was shown to provide a protective signal.<sup>36</sup> Other groups have argued that inhibition of PI3K signaling, but not ERK1/2 signaling, modestly promotes Ad.5-*mda-7* lethality in breast and lung cancer cells.<sup>39,40</sup> This study was designed to define more effective ways of inducing GBM cell death using *mda-7*/IL-24. This study provides data supporting the hypothesis that simultaneous inhibition of multiple cytoprotective pathways, including mammalian target of rapamycin (mTOR), PI3K, and/or mitogen-activated extracellular regulated kinase (MEK)1/2 signaling, facilitates lethality of *mda-7*/IL-24 toward GBM cells both *in vitro* and *in vivo*.



Delivery of therapeutic genes using Ad.5 has shown limitations in treating GBM, due to the need for Coxsackie adenovirus receptors (CARs) on tumor cells for virus entry. This work in this study evaluated the use of a tropism-modified adenovirus which uses a serotype 3 modification of the serotype 5 viral knob protein to facilitate delivery of *mda-7/IL-24* in a CAR-independent manner.<sup>148,147</sup> This approach resulted in augmented therapeutic activity of *mda-7/IL-24* in GBM cells, suggesting that combination of both strategies, namely inhibition of cytoprotective pathways and tropism modification, may provide a means of developing an improved therapy for GBMs.

## CHAPTER 7 RESULTS:

### INHIBITORS OF MULTIPLE PROTECTIVE SIGNALING PATHWAYS AND Ad.5/3 DELIVERY ENHANCES MDA-7/IL-24 KILLING

#### 7.1 Serotype Ad.5-*mda-7* killing was significantly enhanced with coexpression of dnMEK1 and dnAKT. Ad.5-*mda-7* lethality was almost abolished with coexpression of activated MEK1 and AKT in primary human GBM cells

As previously shown in the first section of this thesis, MDA-7/IL-24 has a profound effect, i.e. inhibition, on pro-survival signaling pathways. To further identify the potential pathways involved in the regulation of MDA-7/IL-24 toxicity, modulation of AKT and MEK1 function was performed to assess a role for the PI3K/MEK/mTOR pathways. GBM6 and GBM12 cells were plated in 12-well plates ( $\sim 2.5 \times 10^4$  cells per well) for 24h. Cells were then infected (all virus infections at 10 m.o.i.) with empty vector control virus (Ad.*cmv*) or virus to express MDA-7/IL-24 (Ad.*mda-7*). Twelve hours after initial infection cells were infected with viruses to express activated forms of AKT and MEK1 (caAKT, caMEK1), and dominant negative forms of AKT and MEK1 (dnAKT, dnMEK1). At 48 hours (GBM6) or 96 hours (GBM12) post initial infection, cells were isolated and cell viability was determined by Trypan blue exclusion assay ( $\pm$ SEM,  $n = 3$ ). Upper inset of figure 8.1.1 shows the impact of expressing caAKT, caMEK1, dnAKT, and dnMEK1 on cell signaling.

These results indicated that in primary human GBM cells, infection with a serotype 5 recombinant adenovirus to express MDA-7/IL-24 (Ad.5-*mda-7*) was able to induce cell

killing that was modestly enhanced by expression of dnMEK1 or dnAKT individually; killing was shown to be significantly enhanced by concomitant expression of these inhibitory proteins. In contrast, expression of either activated MEK1 or activated AKT alone was shown to significantly suppress Ad.5-*mda-7* cell killing and, concomitant expression of these active proteins was shown to almost abolish cell killing.

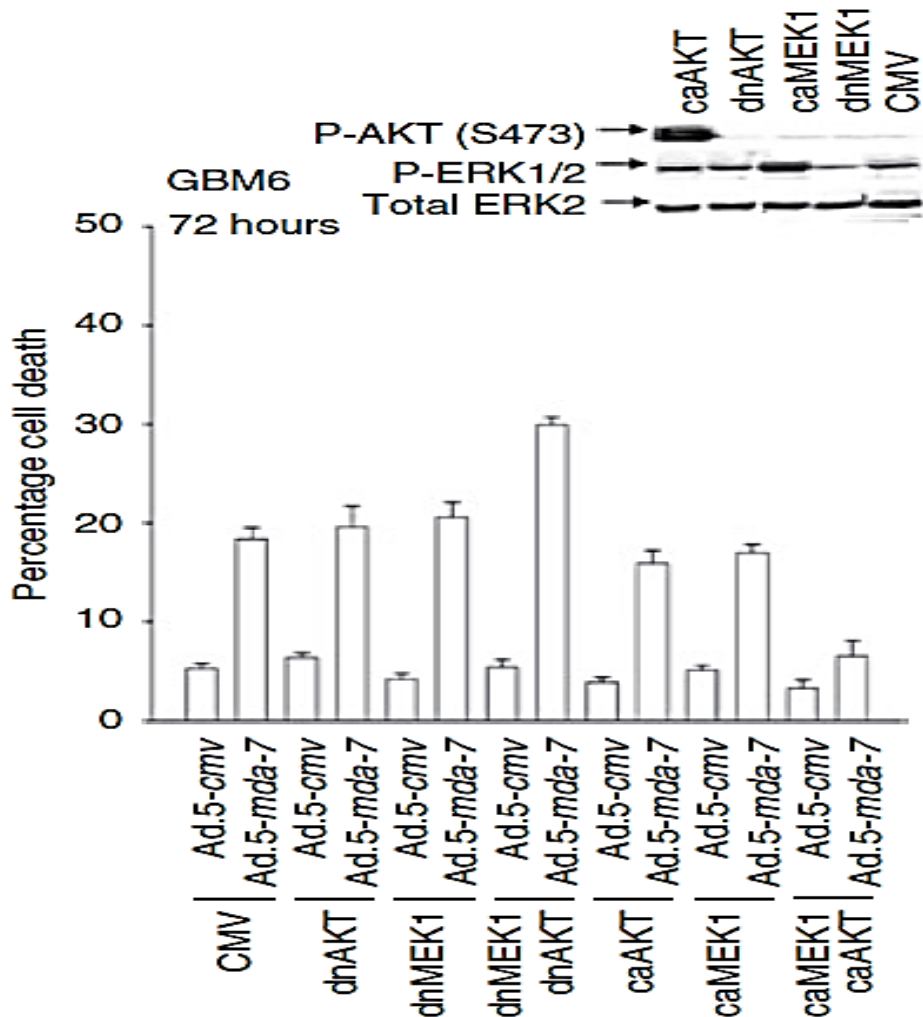


**Figure 7.1.1 Ad.5-*mda-7* lethality is enhanced by combined inhibition of PI3K/MEK/mTOR pathways in GBM 6 cells.** GBM6 cells were infected with empty vector control virus (Ad.5-*cmv*) or with viruses to express MDA-7/IL-24 (Ad.5-*mda-7*), activated forms of AKT and MEK1 (caAKT, caMEK1), and dominant negative forms of AKT and MEK1 (dnAKT, dnMEK1). At 48 hours (GBM6) or 96 hours (GBM12) after infection, cells were isolated and cell viability was determined by Trypan blue exclusion assay ( $\square$  SEM,  $n = 3$ ). Upper inset shows the impact of expressing caAKT, caMEK1, dnAKT, and dnMEK1 on cell signaling.

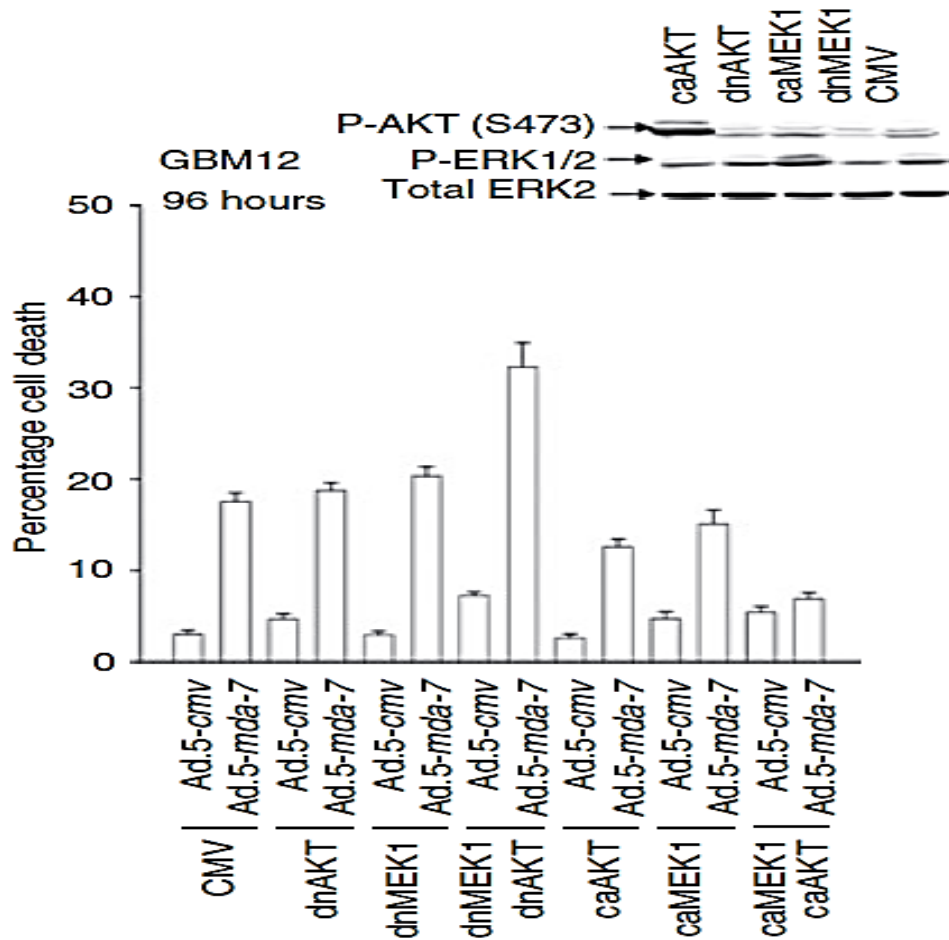
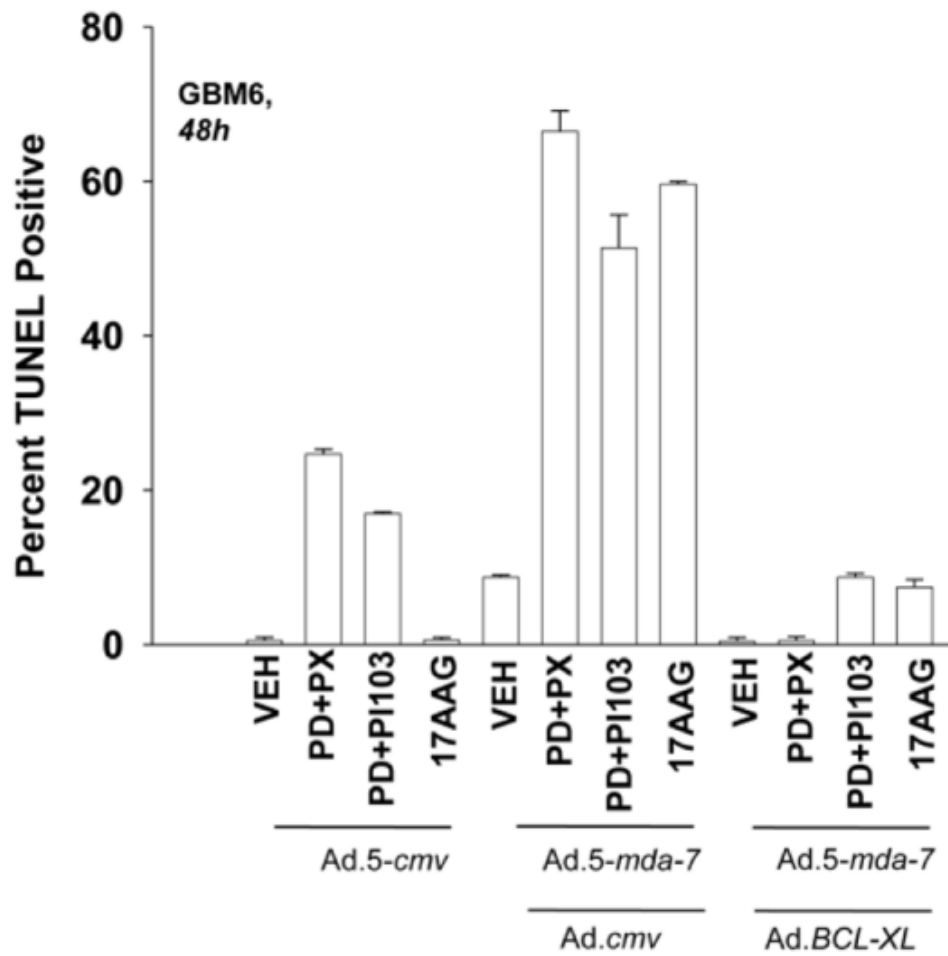


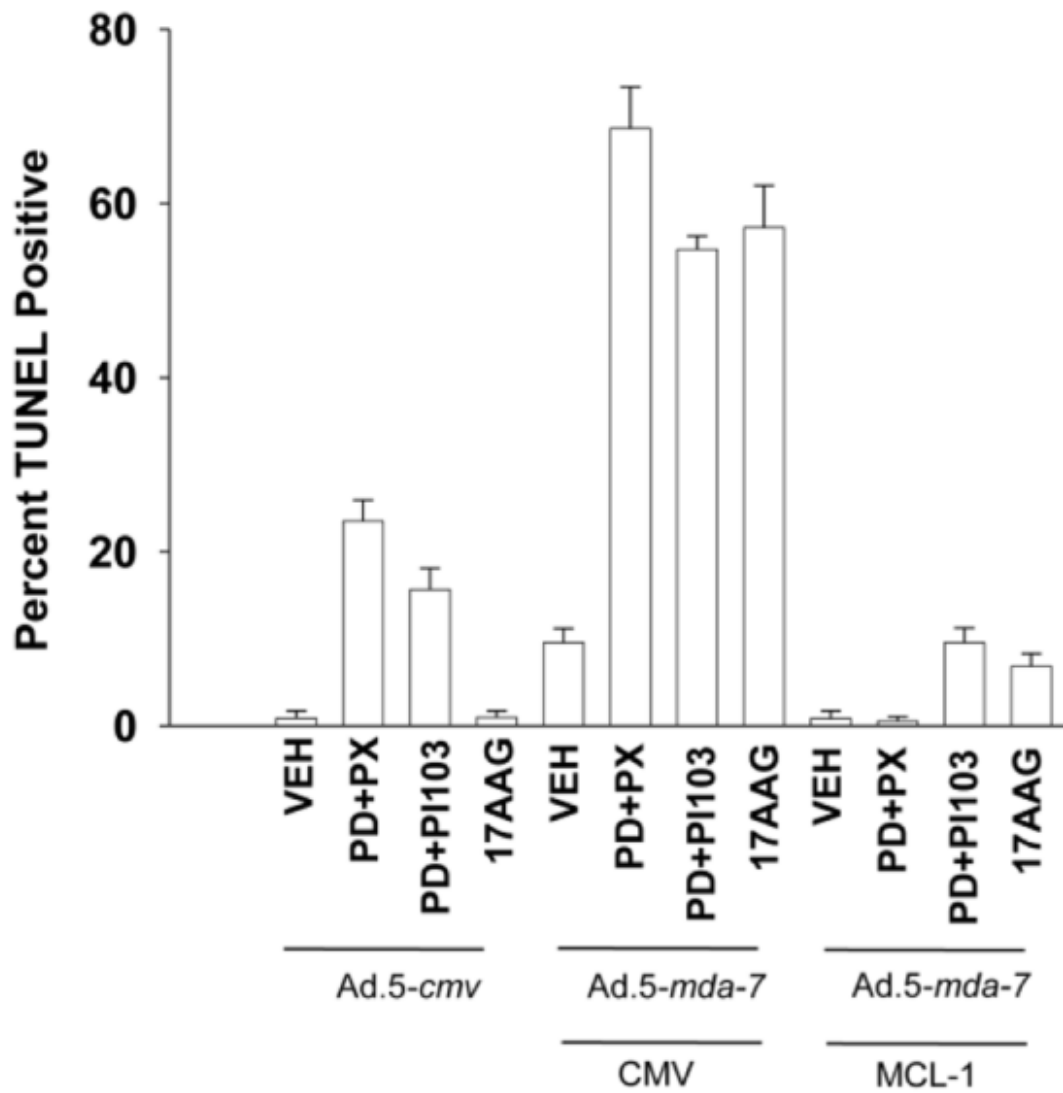
**Figure 7.1.2 Ad.5-*mda-7* lethality is enhanced by combined inhibition of PI3K/MEK/mTOR pathways in GBM 12 cells.** GBM12 cells were infected with empty vector control virus (Ad.5-*cmv*) or with viruses to express MDA-7/IL-24 (Ad.5-*mda-7*), activated forms of AKT and MEK1 (caAKT, caMEK1), and dominant negative forms of AKT and MEK1 (dnAKT, dnMEK1). At 48 hours (GBM6) or 96 hours (GBM12) after infection, cells were isolated and cell viability was determined by Trypan blue exclusion assay ( $\square$  SEM,  $n = 3$ ). Upper inset shows the impact of expressing caAKT, caMEK1, dnAKT, and dnMEK1 on cell signaling.

**7.2 17AAG, PD184352/PX866 and PD184352/PI-103 treatments all promote *Ad.5mda-7/IL-24* toxicity that is abolished by upregulation of pro-survival BCL-2 family proteins found in GBM cells.**

The expression of pro-survival proteins of the BCL2 family, are highly upregulated when MEK and AKT pathways are activated. In this study, GBM6 cells were used to assess the role of the BCL-2 family members in modulating cell death induced by *Ad.5mda-7/IL24*. Cells were plated in 12-well plates ( $\sim 2.5 \times 10^4$  cells per well) for 24h. Cells were then infected (all virus infections at 10 m.o.i.) with empty vector control virus (*Ad.cmv*) or virus to express MDA-7/IL-24 (*Ad.mda-7*). Twelve hours after initial infection cells were infected with viruses to express BCL-XL and MCL-1. Cells were treated with 17AAG, PD184352/PX866 and PI103/PD184352 twelve hours after infection. Forty-eight hours after initial infection with *Ad.mda-7*, cells were isolated and cell viability was determined by trypan blue exclusion assay ( $\pm$ SEM, n = 3). These results indicated that BCL-XL and MCL-1 over-expression led to the abolition of the cell killing potential of 17AAG (100 nmol/l), PD184352/PX866 (PD+PX - 1  $\mu$ mol/l+100 nmol/l respectively) and PI-103/PD184352 (PI103+PD - 200 nmol/l+1  $\mu$ mol/l respectively) when used as individual agents or in combination with *Ad.mda-7/IL-24* (**Figures 7.2.1 and 7.2.2**).



7.2.1 BCL-2 overexpression abolishes 17AAG, PD184352/PX866 and PD184352/PI-103 enhancement of Ad.5mda-7/IL-24 toxicity in GBM6 cells.



**7.2.2 MCL-1 overexpression abolishes 17AAG, PD184352/PX866 and PD184352/PI-103 enhancement of Ad.5mda-7/IL-24 toxicity in GBM6 cells.**



### **7.3 Knockdown of mTOR expression *in vitro* enhanced Ad.5-*mda-7* toxicity to a similar extent as expression of dnMEK1 and a dn-p85 PI3K subunit.**

Previous sections have indicated that the PI3K/MEK/mTOR pathways are involved in MDA-7/IL-24 mediated cell death. In addition, a key mechanism of MDA-7/IL-24 tumor cell killing is the capacity of this agent to induce toxic autophagy. In an attempt to demonstrate this, GBM6 cells were plated in 12-well plates ( $\sim 2.5 \times 10^4$  cells per well) for 24h. Cells were then infected (all virus infections at 10 m.o.i.) with empty vector control virus (Ad.*cmv*) or virus to express MDA-7/IL-24 (Ad.*mda-7*) for 12 h. In parallel, cells were transfected with empty vector plasmid or plasmids to express a dn-p85 PI3K subunit (dn-p85) and dnMEK1. Cells were also transfected with a nonspecific siSCR or a siRNA to specifically knockdown mTOR expression, as indicated. At 48 hours after initial infection, cells were isolated and cell viability was determined by Trypan blue exclusion assay ( $\pm$ SEM,  $n = 3$ ). Results indicated that combined expression of dnMEK1 and a dn-p85 PI3K subunit led to an enhancement of Ad.5-*mda-7* cell killing, similar to that seen for dnMEK1 or dnAKT expression (**Figure 7.3**). Knockdown of mTOR expression *in vitro* was also shown to enhanced Ad.5-*mda-7* toxicity to a similar extent to that seen for dnMEK1 and a dn-p85 PI3K subunit (**Figure 7.3**). The inhibition of mTOR/PI3K/MEK together in these cells was shown to significantly reduce GBM cell viability and strongly enhanced Ad.5-*mda-7* lethality.

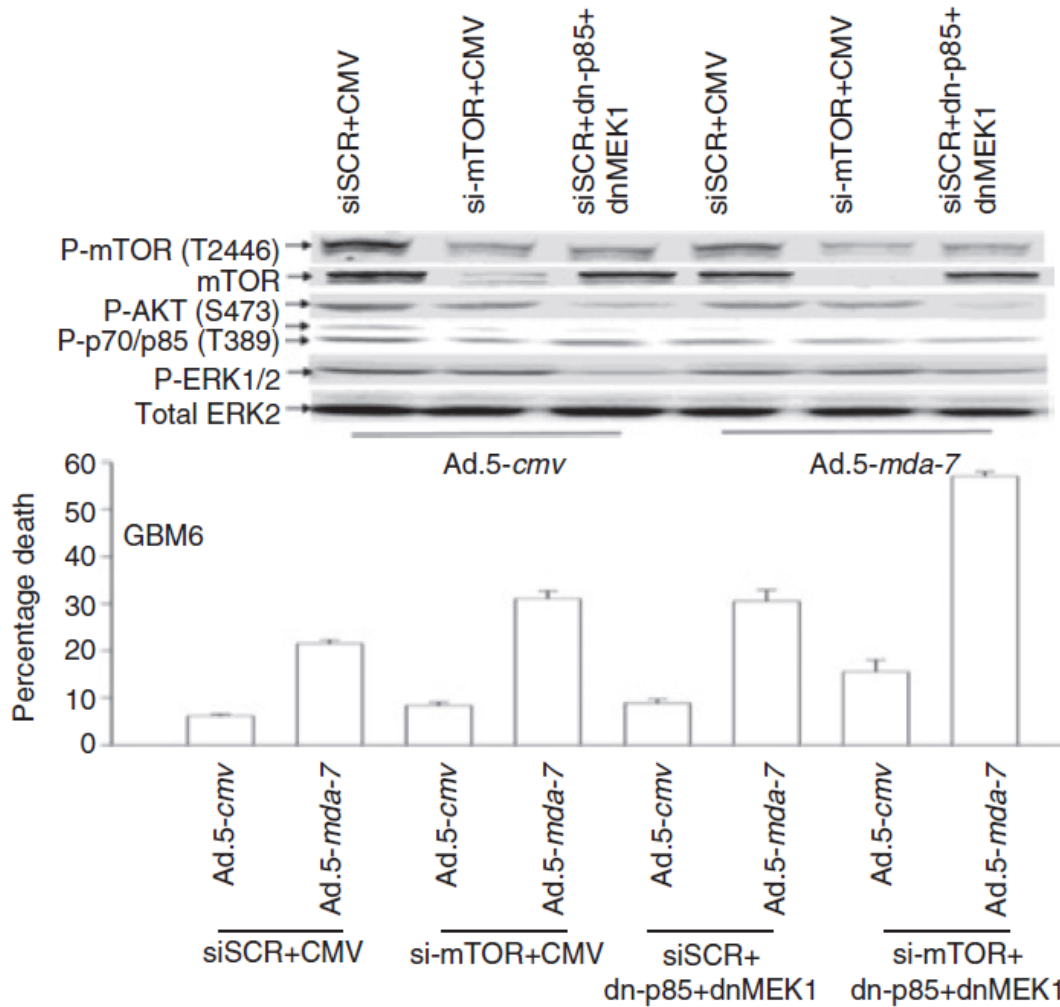


**Figure 7.3 Ad.5-mda-7 lethality is enhanced by combined inhibition of PI3K/MEK/mTOR pathways.** GBM6 cells were infected with empty vector control virus (Ad.5-cmv) or with a virus to express MDA-7/IL-24 (Ad.5-mda-7). In parallel, cells were transfected with empty vector plasmid or plasmids to express a dn-p85 PI3K subunit (dn-p85) and dnMEK1; cells were transfected with a nonspecific scrambled siRNA (siSCR) or an siRNA to knockdown mTOR expression, as indicated. At 48 hours after infection, cells were isolated and cell viability was determined by Trypan blue exclusion assay (—SEM,  $n = 3$ ).

#### **7.4 Combined inhibition of PI3K/MEK/mTOR modestly suppressed tumor growth of orthotopic GBM tumors *in vivo* and profoundly enhanced Ad.5-*mda-7* tumoricidal capability**

In order to characterize the autophagic-inducing effects of MDA-7/IL-24 on GBM cells *in vivo*, GBM6 cells stably transfected with luciferase, were infected (all virus infections at 10 m.o.i.) with empty vector control virus (Ad.*cmv*) or virus to express MDA-7/IL-24 (Ad.*mda-7*), and subsequently transfected with a siSCR and an empty vector plasmid or with an siRNA to knockdown mTOR expression and plasmids to express a dn-p85 PI3K subunit and dnMEK1. Twelve hours after transfection/infection equal numbers of viable tumor cells were implanted into the brains of athymic mice and tumor formation monitored over the following 32 days by luciferase/CCD camera imaging ( $n = 2$ ,  $\pm$ SEM). In agreement with *in vitro* findings, results indicated that the molecular inhibition of mTOR/PI3K/MEK1 signaling, but not mTOR alone, was shown to modestly suppress tumor growth of orthotopic GBM tumors *in vivo* for up to 32 days after infusion of tumor cells into mouse brains, and profoundly enhance the tumoricidal effects of Ad.5-*mda-7* (Figure 7.4).

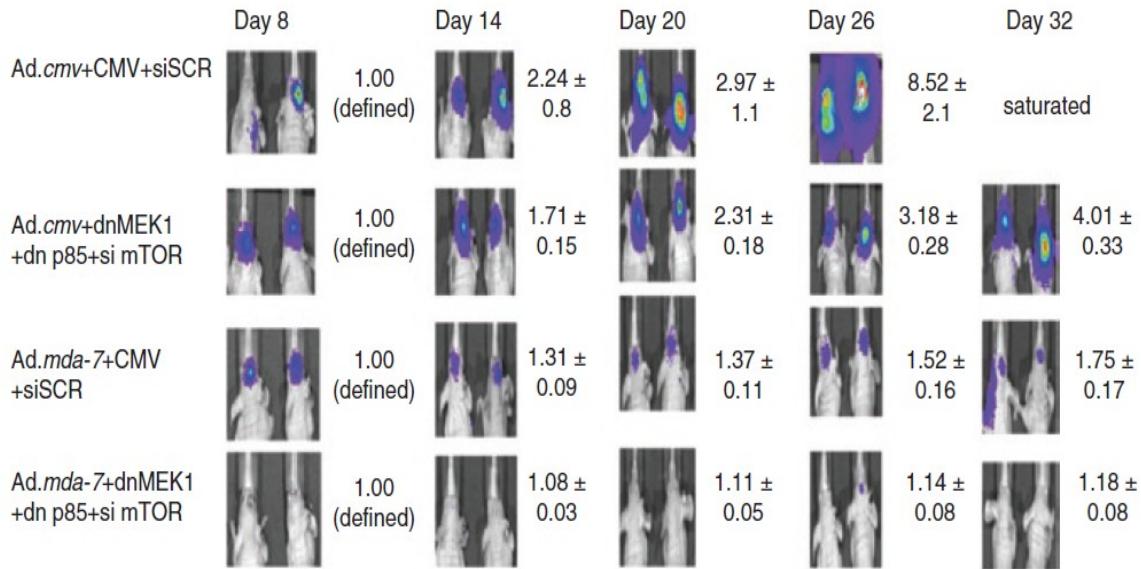


**Figure 7.4 Ad.5-*mda-7* lethality is enhanced by combined inhibition of PI3K/MEK/mTOR pathways in vivo.** GBM6-luciferase cells were infected with empty vector control virus (Ad.5-*cmv*) or with viruses to express MDA-7/IL-24 (Ad.5-*mda-7*) and in parallel transfected with a siSCR and an empty vector plasmid or with an siRNA to knockdown mTOR expression and plasmids to express a dn-p85 PI3K subunit and dnMEK1. At 12 hours after transfection/infection equal numbers of viable tumor cells were implanted into the brains of athymic mice and tumor formation monitored over the following 32 days by luciferase/CCD camera imaging ( $n = 2$ , —SEM). CMV, cytomegalovirus; dn, dominant negative; ERK, extracellular regulated kinase; GBM, glioblastoma multiforme; MEK, mitogen-activated extracellular regulated kinase.

**7.5 Small molecule inhibitors of mTOR, PI3K and MEK1/2 signaling: 17AAG, PX866 and PD184352 respectively, enhanced Ad.5-*mda-7* toxicity in primary human GBM cells. This correlated closely with enhanced JNK1/2 activation and reduced expression of BCL-XL and MCL-1**

Known small molecular inhibitors of pro-survival signaling cascades were used to further confirm previous results using molecular tools. GBM6, 12 and 14 cells were infected (all virus infections at 10 m.o.i.) with empty vector control virus (Ad.*cmv*) or virus to express MDA-7/IL-24 (Ad.*mda-7*). Twelve hours after infection, cells were treated with vehicle (DMSO), PD+PX, 1  $\mu$ mol/l + 100 nmol/l respectively), 17AAG (100 nmol/l). Twenty four and 48 hours after infection, cells were isolated and SDS-PAGE was performed to determine the expression of BCL-XL and MCL-1, and the phosphorylation of ERK1/2, p38 MAPK, JNK1-3, AKT (S473) ( $n = 2$ ). At 48 hours after infection, cells were isolated and cell viability was determined by Trypan blue exclusion assay ( $\pm$ SEM,  $n = 3$ ). These results indicated that in GBM6 cells (expressing ERBB1 vIII), GBM12 cells (expressing mutant active full length ERBB1), and GBM14 cells (expressing mutant PTEN (phosphatase and tensin homologue on chromosome 10)), the individual drugs had modest (GBM6) to significant (GBM14) effects as single agents on cell viability (**Figure 7.5**, graphical panels). In all GBM cell isolates tested, PD+PX and 17AAG were shown to enhance the toxicity of Ad.5-*mda-7* in a greater than additive fashion. In GBM6 cells infected with Ad.5-*mda-7*, inhibition of the MEK1/2 and PI3K signaling pathways led to enhanced JNK1/2, but not p38 MAPK activation, and to more tumor cell killing *in vitro* (**Figure 7.5**, blotting panels). Inhibition of signaling pathways and enhanced cell killing

was also closely correlated with reduced expression of the BCL-2 family proteins BCL-XL and MCL-1.

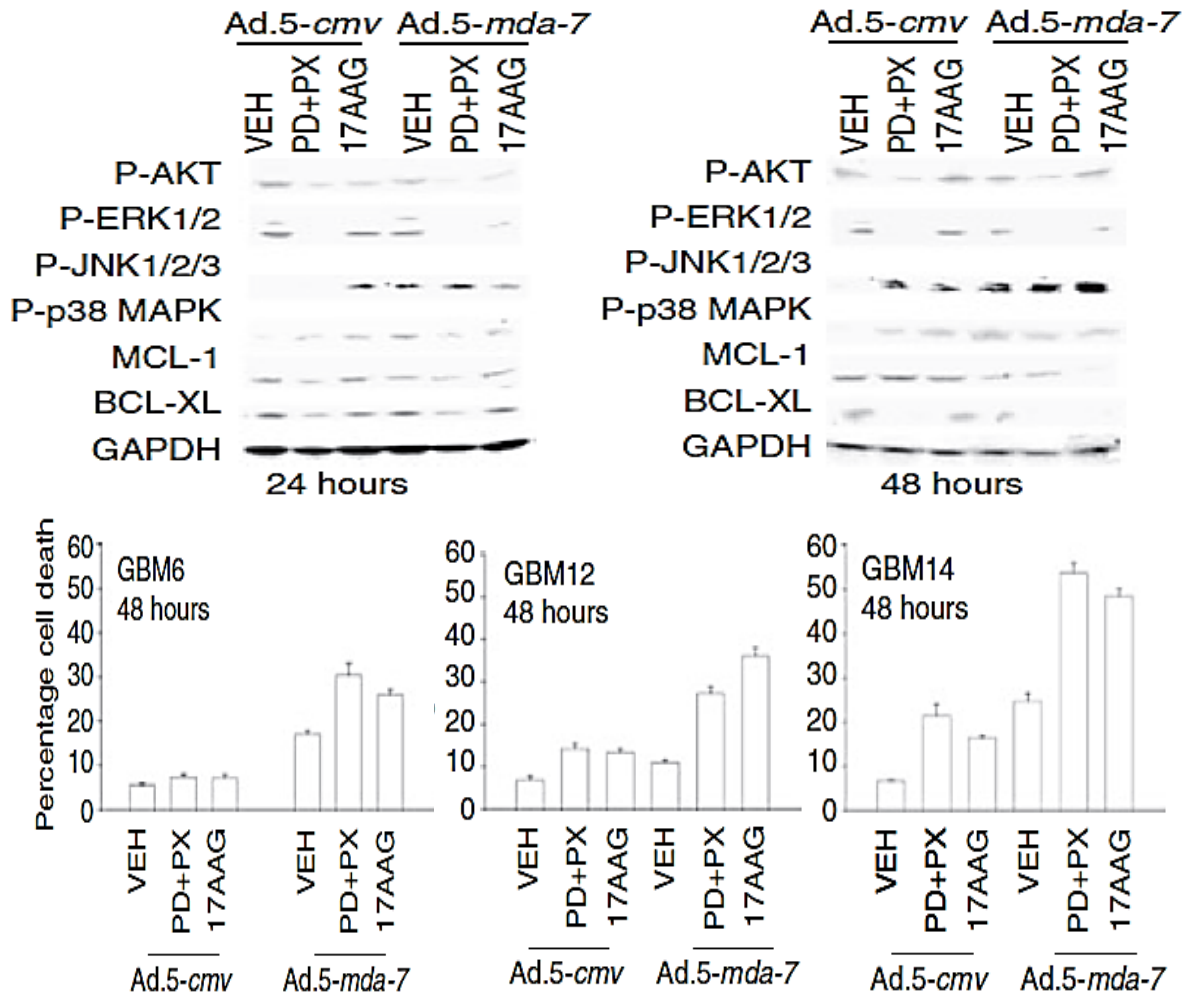


**Figure 7.5 Inhibition of mTOR, PI3K, and MEK1/2 signaling enhances Ad.5-mda-7 lethality in GBM cells.** GBM6 cells were infected with Ad.5-cmv or Ad.5-mda-7 and 12 hours after infection treated with vehicle (DMSO), 17AAG (100 nmol/l), or PD184352 (PD, 1  $\mu$ mol/l) and PX866 (100 nmol/l) (PD+PX). At 24 and 48 hours after infection, cells were isolated and sodium dodecyl sulfate–polyacrylamide gel electrophoresis (SDS-PAGE) was performed to determine the expression of BCL-XL and MCL-1, and the phosphorylation of ERK1/2, p38 MAPK, JNK1-3, AKT (S473) ( $n = 2$ ). GBM cells were infected with empty vector (Ad.5-cmv) or to express MDA-7/IL-24 (Ad.5-mda-7) and 12 hours after infection treated with vehicle (VEH) dimethyl sulfoxide (DMSO)], PD184352+PX866 (PD+PX, 1  $\mu$ mol/l + 100 nmol/l), 17AAG (100 nmol/l). At 48 hours after infection, cells were isolated and cell viability was determined by Trypan blue exclusion assay (—SEM,  $n = 3$ ).

**7.6 Treatment of GBM6 cells with multi-PI3K inhibitor PI-103 in combination with PD184352, had a greater killing effect than PD184352 in combination with PX866, without further activation of JNK1-3**

In this study, GBM6 cells were plated as single cells in sextuplicate, 12 hours after plating; cells were infected with Ad.5-*cmv* or Ad.5-*mda-7*. Twelve hours after initial infection, cells were treated with vehicle (DMSO), PD184352 (1  $\mu\text{mol/l}$ ) + PI-103 (200 nmol/l) (PD+PI), PD (1  $\mu\text{mol/l}$ ) + PX866 (100 nmol/l), PD+PX, or 17AAG (100 nmol/l). Forty eight hours after initial infection, the growth media was removed from treated cells and replaced with fresh media lacking drugs. Colonies of >50 cells were permitted to form over the following ~20 days, followed by fixing, staining, and counting ( $\pm\text{SEM}$ ,  $n = 3$ ). In conjunction with this work, GBM6 cells were plated in 12-well plates ( $\sim 2.5 \times 10^4$  cells per well) for 24h and then infected (all virus infections at 10 m.o.i.) with empty vector control virus (Ad.*cmv*) or virus to express MDA-7/IL-24 (Ad.*mda-7*). Twelve hours after infection, cells were treated with vehicle (DMSO), rapamycin (rap, 100 nmol/l), PI-103 (200 nmol/l), PD (1  $\mu\text{mol/l}$ ), or PI-103+PD. Forty eight hours after initial infection, cells were isolated and cell viability was determined by Trypan blue exclusion assay ( $\pm\text{SEM}$ ,  $n = 3$ ) (**Figure 7.6.1**). In addition, GBM6 cells were infected with Ad.5-*cmv* or Ad.5-*mda-7* and 12 hours after infection treated with vehicle (DMSO), rap (100 nmol/l), or PD (1  $\mu\text{mol/l}$ ) and PI-103 (200 nmol/l) (PI-103 + PD). Twenty four hours after infection, cells were isolated and SDS-PAGE performed to determine the expression of BCL-XL and MCL-1, and the phosphorylation of ERK1/2, p38 MAPK, JNK1-3, AKT (S473), mTOR (S2446), and p70 S6K (T389) ( $n = 2$ ) (**Figure 7.6.3**).



Treatment of GBM6 cells with PI-103+PD was shown to induce a significantly greater decrease in tumor cell viability/growth than was observed using PD+PX in a colony assay (**Figure 7.6.2**). PI-103+PD treatment was shown to inhibit the phosphorylation of AKT, mTOR, and p70 S6K but unlike PD+PX treatment, did not cause further activation of JNK1-3 (**Figure 7.6.3**).

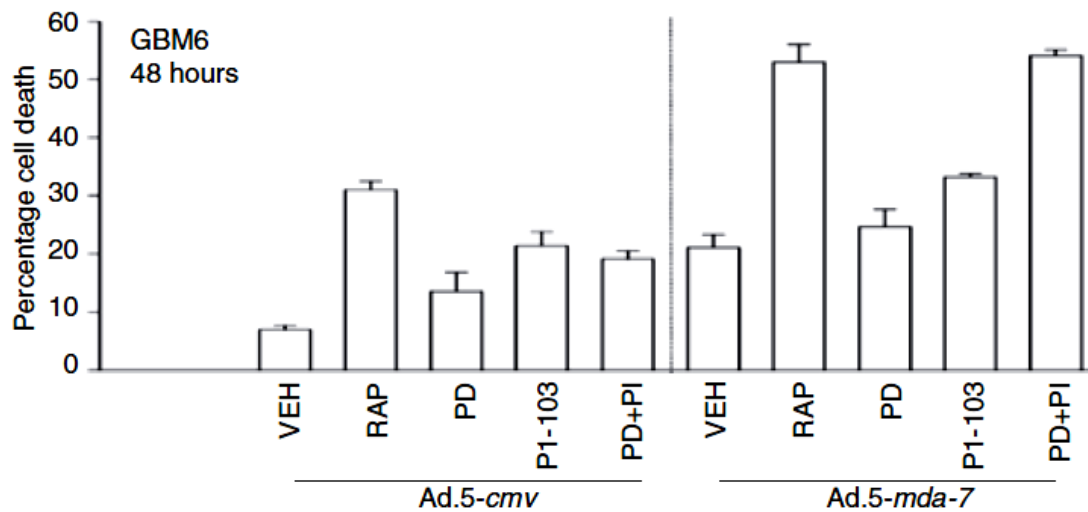


**Figure 7.6.1 Inhibition of mTOR, PI3K, and MEK1/2 signaling enhances Ad.5-*mda-7*-induced inhibition of growth/survival in GBM cells – Trypan Blue Assay.** GBM6 cells were infected with Ad.5-*cmv* or Ad.5-*mda-7* and 12 hours after infection treated with vehicle (DMSO), rapamycin (rap, 100 nmol/l), PI-103 (200 nmol/l), PD184352 (PD, 1  $\mu$ mol/l), or PI-103+PD. At 48 hours after infection, cells were isolated and cell viability was determined by Trypan blue exclusion assay (—SEM,  $n = 3$ ).

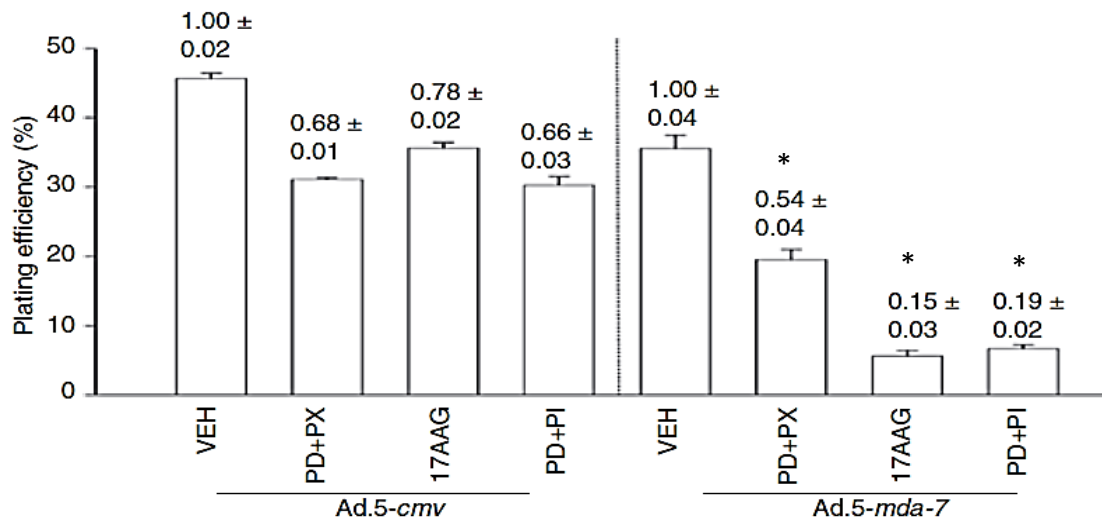


**Figure 7.6.2 Inhibition of mTOR, PI3K, and MEK1/2 signaling enhances Ad.5-*mda-7*-induced inhibition of growth/survival in GBM cells – Colony Formation Assay.** GBM6 cells were plated as single cells in sextuplicate and 12 hours after plating were infected with Ad.5-*cmv* or Ad.5-*mda-7*. At 12hour(s) after infection cells were treated with vehicle (DMSO), PD184352 (PD, 1  $\mu\text{mol/l}$ ) + PI-103 (200 nmol/l) (PD+PI), PD184352 (PD, 1  $\mu\text{mol/l}$ ) + PX866 (100 nmol/l) (PD+PX), or 17AAG (100 nmol/l). At 48 hours after infection, the growth media was removed and replaced with new media lacking drugs. Colonies of >50 cells were permitted to form over the following ~20 days, followed by fixing, staining, and counting (—SEM,  $n = 3$ ).

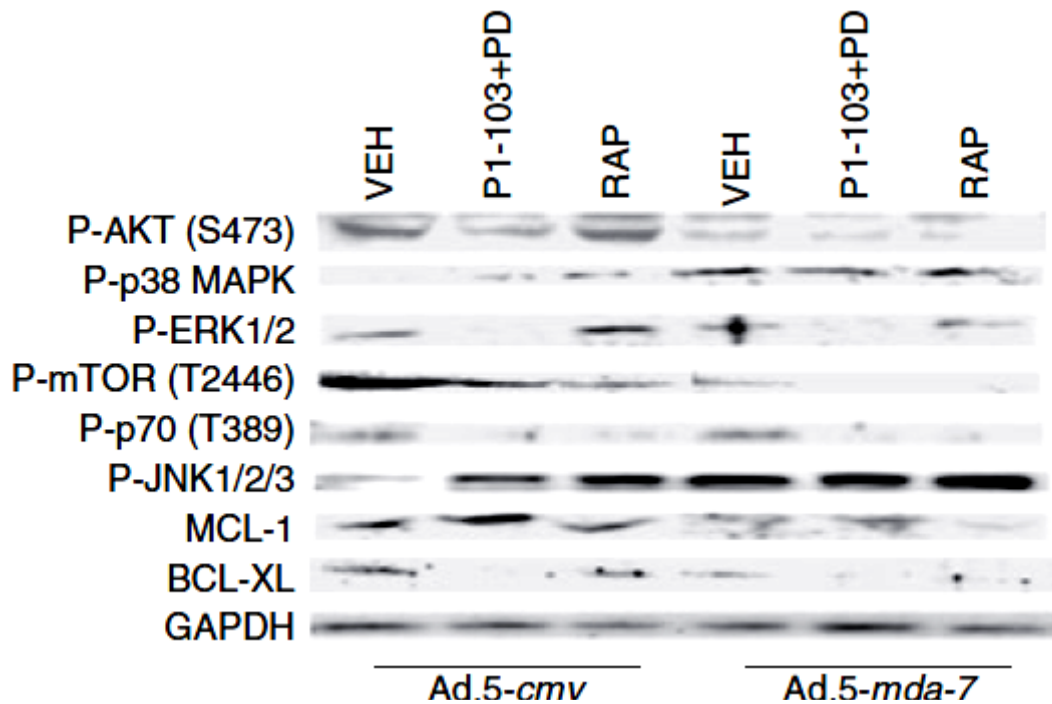


**Figure 7.6.3 Inhibition of mTOR, PI3K, and MEK1/2 signaling enhances Ad.5-mda-7 lethality in GBM cells.** GBM6 cells were infected with Ad.5-cmv or Ad.5-mda-7 and 12 hours after infection treated with vehicle (DMSO), rapamycin (rap, 100 nmol/l), or PD184352 (PD, 1  $\mu$ mol/l) and PI-103 (200 nmol/l) (PD+PI-103). At 24hour(s) after infection cells were isolated and SDS-PAGE performed to determine the expression of BCL-XL and MCL-1, and the phosphorylation of ERK1/2, p38 MAPK, JNK1-3, AKT (S473), mTOR (S1221), and p70 S6K (T389) ( $n = 2$ ).

### **7.7 Inhibition of JNK1-3 blocks MDA-7/IL-24 toxicity and inhibited the promotion of cell death by small molecule kinase inhibitors**

Previous results had suggested that JNK1-3 activation plays a key role in MDA-7/IL-24-induced lethality. To further expand upon these findings GBM6 cells were plated in 12-well plates ( $\sim 2.5 \times 10^4$  cells per well) for 24h. Cells were then infected (all virus infections at 10 m.o.i.) with empty vector control virus (Ad.*cmv*) or virus to express MDA-7/IL-24 (Ad.*mda-7*) and 12 hours after infection treated with vehicle (DMSO) or JNK inhibitory protein (JNK-IP). Thirty minutes after treatment with the JNK-IP, cells were treated with vehicle (DMSO), PD+PX (1  $\mu\text{mol/l}$ +100 nmol/l respectively), PI-103+PD (200 nmol/l+1  $\mu\text{mol/l}$  respectively) or 17AAG (100 nmol/l). Forty eight hours after initial infection, cells were isolated and cell viability was determined by TUNEL assay ( $\pm$ SEM,  $n = 3$ ). These results indicated that the inhibition of JNK1-3 was able to block MDA-7/IL-24 mediated toxicity, in addition to blocking the enhancement of MDA-7/IL-24 toxicity by the small molecule kinase inhibitors (**Figure 7.7**).

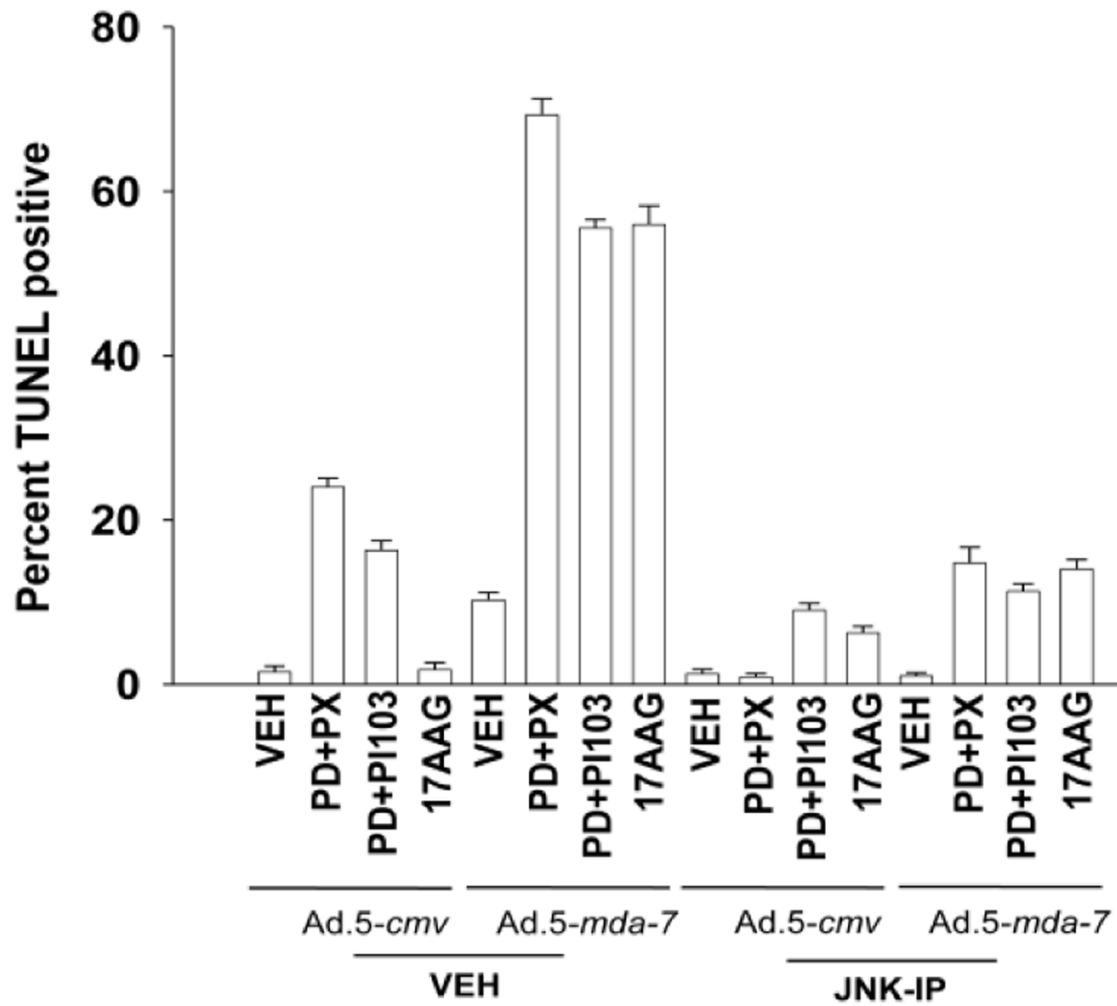


**Figure 7.7** Inhibition of JNK1-3 blocks MDA-7/IL-24 toxicity and any promotion of toxicity by small molecule kinase inhibitors.

## **7.8 17AAG, Rapamycin, PD184352/PX866 and PD184352/PI-103 treatments all promote Ad.5mda-7/IL-24 toxicity through the intrinsic apoptotic pathway in GBM cells**

MDA-7/IL-24 treated GBM cells, in combination with the molecular inhibitors used, was shown to enhance MDA-7/IL-24-induced downregulation of pro-survival proteins (BCL-XL, MCL-1 and AKT1/2) as well as inducing the upregulation of stress induced signaling cascades (JNK1-3, p38-MAPK), leading to cell death. A potential role for apoptosis (Intrinsic/Extrinsic pathway(s)) in cell death was investigated. GBM6 cells were infected with Ad.5-*cmv* or Ad.5-*mda-7* in combination with viruses to express XIAP, BCL-XL, dominant negative (dn) caspase 9, or c-FLIP-s. Twelve hours after infection, cells were treated with vehicle (DMSO), or PD (1  $\mu$ mol/l) + PX (100 nmol/l) (PD+PX) (**Figure 7.8.1**); 17AAG (100 nmol/l) (**Figure 7.8.2**); rap (100 nmol/l), or PI-103 (200 nmol/l) + PD (1  $\mu$ mol/l) (PI-103+PD) (**Figure 7.8.3**). Forty eight hours after initial infection cells were isolated and cell viability was determined by Trypan blue exclusion assay ( $\pm$ SEM,  $n = 3$ ). The results from this study indicated that inhibitors of the intrinsic pathway of apoptosis (XIAP, BCL-XL, dn caspase 9) induced less cell death in the presence of *Ad.mda-7/IL-24*, when compared to cell death seen in response to inhibition of proteins involved in the extrinsic pathway of apoptosis (c-FLIP-s) (**Figures 7.8.1-7.8.3**).

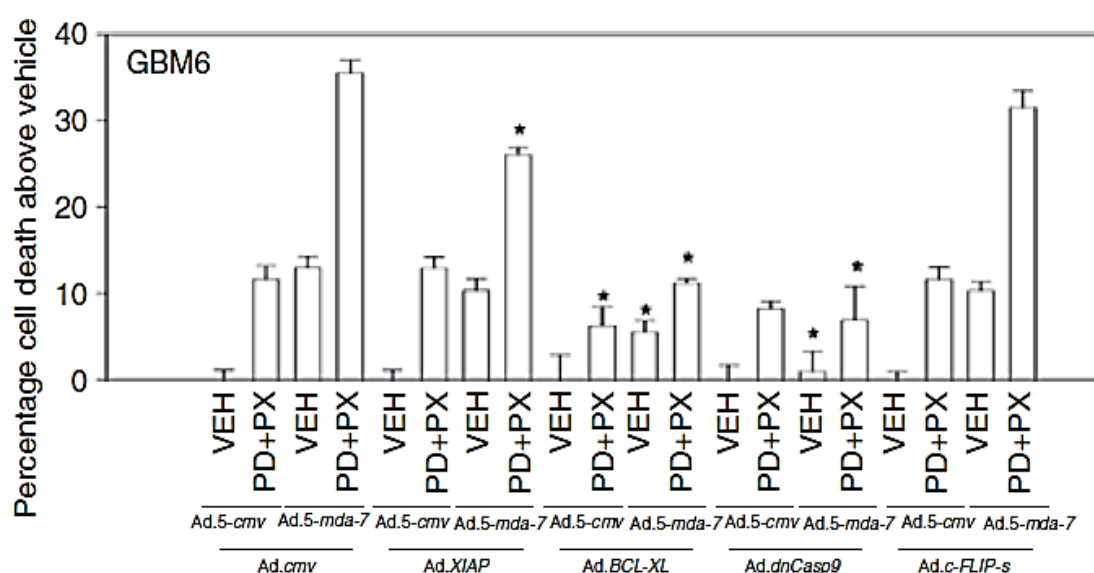


**Figure 7.8.1 Activation of the intrinsic pathway plays a key role in the facilitation of Ad.5-mda-7 toxicity by kinase inhibitors PD+PX.** GBM6 cells were infected with Ad.5-cmv or Ad.5-mda-7 in combination with viruses to express XIAP, BCL-XL, dominant negative (dn) caspase 9, or c-FLIP-s, and 12 hours after infection treated with vehicle [VEH; dimethyl sulfoxide (DMSO)], or PD184352 (PD, 1  $\mu$ mol/l) + PX866 (100 nmol/l) (PD+PX). At 48 hours after infection cells were isolated and cell viability was determined by Trypan blue exclusion assay (—SEM,  $n = 3$ ).



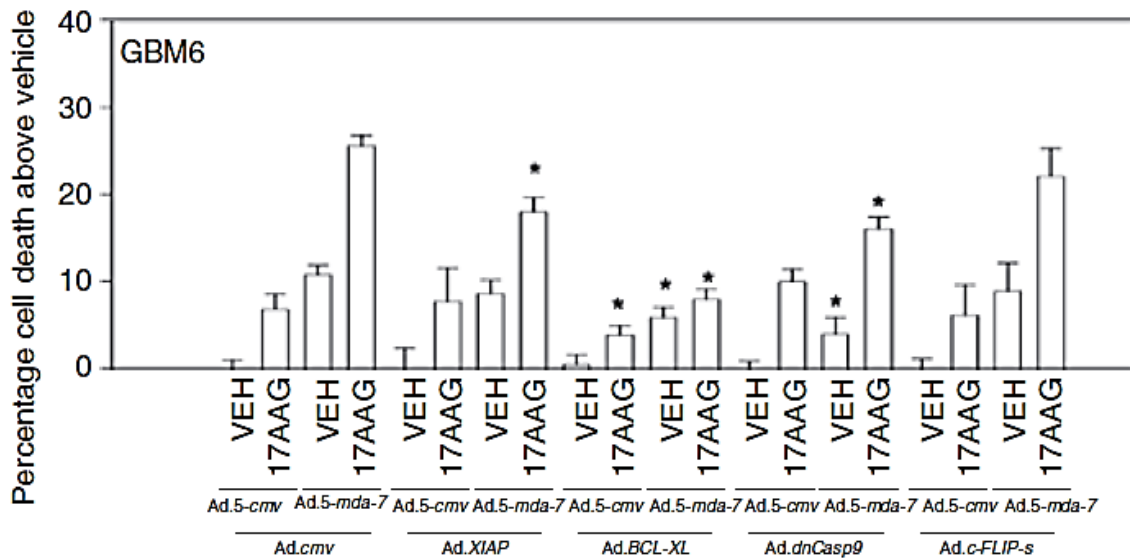


**Figure 7.8.2 Activation of the intrinsic pathway plays a key role in the facilitation of Ad.5-mda-7 toxicity by kinase inhibitor 17AAG.** GBM6 cells were infected with Ad.5-cmv or Ad.5-mda-7 in combination with viruses to express XIAP, BCL-XL, dn-caspase 9, or c-FLIP-s, and 12 hours after infection treated with VEH (DMSO), or 17AAG (100 nmol/l). At 48 hours after infection cells were isolated and cell viability was determined by Trypan blue exclusion assay (—SEM,  $n = 3$ ).

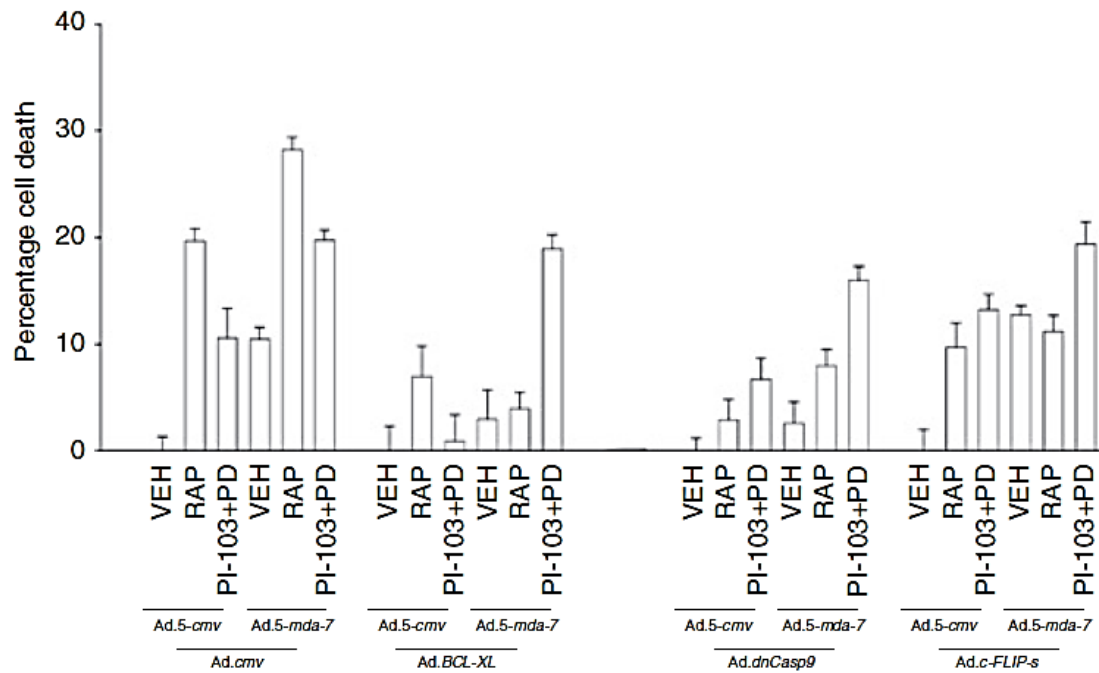


**Figure 7.8.3 Activation of the intrinsic pathway plays a key role in the facilitation of Ad5-*mda-7* toxicity by kinase inhibitors Rapamycin and PI-103+PD.** GBM6 cells were infected with Ad5-*cmv* or Ad5-*mda-7* in combination with viruses to express XIAP, BCL-XL, dn-caspase 9, or c-FLIP-s, and 12 hours after infection treated with VEH (DMSO), rapamycin (100 nmol/l), or PI-103 (200 nmol/l) + PD184352 (PD, 1  $\mu$ mol/l) (PI-103+PD). At 48 hours after infection cells were isolated and cell viability was determined by Trypan blue exclusion assay (—SEM,  $n = 3$ ).

**7.9 Infection of tumor cells with Ad.5-*mda-7* was shown to increase PERK phosphorylation and LC3-II processing, without further enhancement when Ad.5-*mda-7* was combined with the small molecule inhibitors, 17AAG or PD184352/PX866**

Previous studies have demonstrated that GST-MDA-7 is able to induce GBM cell death in a PERK-dependent fashion, attributed to increased levels of autophagy.<sup>35,36</sup> GBM6, 12 and 14 cells were infected (all virus infections at 10 m.o.i.) with empty vector control virus (Ad.*cmv*) or virus to express MDA-7/IL-24 (Ad.*mda-7*) and 12 hours after infection treated with vehicle (DMSO), PD (1  $\mu$ mol/l) + PX (100 nmol/l) (PD+PX), or 17AAG (100 nmol/l). Cells were isolated 24 and 48 hours after infection and SDS-PAGE and immunoblotting was performed upon cell lysates to assess the phosphorylation of PERK and the conversion of LC3 to LC3-II ( $n = 3$ ). These results indicated that as a single agent, 17AAG increased PERK phosphorylation and LC3-II processing, whereas PD+PX treatment reduced basal PERK phosphorylation and LC3-II processing (**Figure 7.9**). Infection of tumor cells with Ad.5-*mda-7* alone was shown to increase PERK phosphorylation and LC3-II processing.

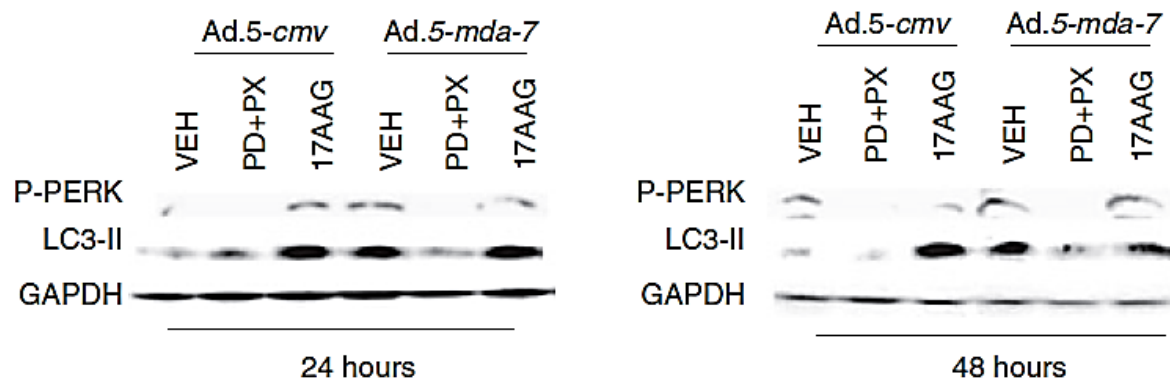


**Figure 7.9 Inhibition of signaling pathways enhances *Ad.5-mda-7*-induced autophagy, but does not promote additional activation of PERK.** GBM6 cells were infected with *Ad.5-cmv* or *Ad.5-mda-7* and 12 hours after infection treated with vehicle [VEH; dimethyl sulfoxide (DMSO)], PD184352 (PD, 1  $\mu\text{mol/l}$ ) + PX866 (100 nmol/l) (PD+PX), or 17AAG (100 nmol/l). Cells were isolated 24 and 48 hours after infection and sodium dodecyl sulfate–polyacrylamide gel electrophoresis and immunoblotting was performed to assess the phosphorylation of PERK and the conversion of LC3 to LC3-II ( $n = 3$ ).

### **7.10 17AAG or PD184352/PX866 treatments enhance Ad.5-*mda-7* induced autophagy by causing an increase in autophagic flux**

To further assess a role of these small molecular inhibitors in the induction of autophagy, the formation of LC3-GFP vesicles was assessed. GBM6 cells were plated in 4-well chamber slides, then infected with Ad.5-*cmv* or Ad.5-*mda-7* and in parallel transfected with a plasmid to express LC3-GFP and with either a siSCR or an siRNA to knock down Beclin1 (siBeclin1). Twelve hours after infection, cells were treated with vehicle (DMSO), 17AAG, or PD+PX. Twelve hours after drug treatment cells were examined using a fluorescent microscope ( $\times 40$  magnification) for the formation of intense GFP-staining vesicles ( $\pm$ SEM,  $n = 3$ ). These results indicated that infection of GBM6 cells with Ad.5-*mda-7* was shown to increase the number of autophagic vesicles in cells, judged using the transfected LC3-GFP construct (**Figure 7.10**). The signal transduction pathway inhibitory drugs 17AAG and PD+PX, were shown to increase Ad.5-*mda-7*-induced autophagy levels. Although the PD+PX treatment, which will inhibit MEK1 and PI3K respectively, was shown to suppress the detection of LC3-II via immunoblotting (**Figure 7.9**), the drug combination increased autophagy as judged by the formation of punctate LC3-GFP staining bodies. This result suggests that the combined inhibition of MEK1/2 and PI3K can lead to a large increase in autophagic flux.

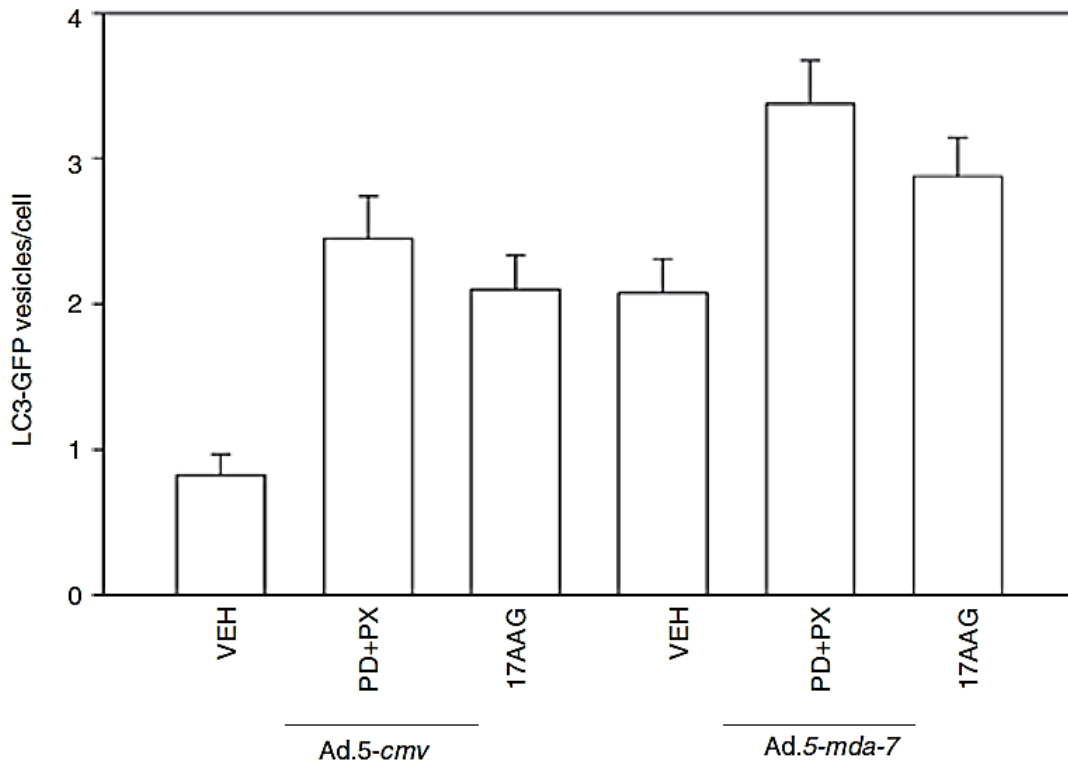


**Figure 7.10 Inhibition of signaling pathways enhances Ad.5-*mda-7*-induced autophagy, without promoting the additional activation of PERK.** GBM6 cells in 4-well chambered slides were infected with Ad.5-*cmv* or Ad.5-*mda-7* and in parallel transfected with a plasmid to express LC3-GFP and with either a scrambled siRNA (siSCR) or an siRNA to knockdown Beclin1 (siBeclin1). At 12 hours after infection cells were treated with vehicle (DMSO), 17AAG, or PD+PX. At 12 hours after drug treatment cells were examined using a fluorescent microscope ( $\times 40$  magnification) for the formation of intense GFP-staining vesicles (—SEM,  $n = 3$ ).

**7.11 Knockdown of Beclin1 or ATG5 abolished Ad.5-*mda-7* toxicity and significantly reduced the abilities of 17AAG and to a lesser extent PD184352/PX866 exposure to cause cell death**

Previous studies have demonstrated that GST-MDA-7 was able to induce autophagy and cell death in GBM cells that was blocked by knock down of Beclin1 or ATG5 expression.<sup>35</sup> The presence of a similar role for these proteins in GBM cells infected with *Ad.mda-7/IL-24* was assessed. GBM6 cells were infected with *Ad.5-cmv* or *Ad.5-mda-7* and, in parallel, transfected with either siSCR or siRNA molecules to knock down siATG5 or siBeclin1. Twelve hours after infection, the cells were treated with vehicle (DMSO), PD (1  $\mu$ mol/l) + PX (100 nmol/l) (PD+PX), or 17AAG (100 nmol/l). Forty eight hours after infection, cells were isolated and cell viability was determined by Trypan blue exclusion assay ( $\pm$ SEM,  $n = 3$ ). Results indicated that knock down of Beclin1 or ATG5 abolished *Ad.5-mda-7* toxicity and significantly reduced 17AAG mediated cell death. PD+PX induced cell death was also reduced. (**Figure 7.11**). Thus, the ability of GBM cells to respond to MDA-7/IL-24 expression with increased autophagy plays a key role in both *Ad.5-mda-7* toxicity as a single agent, and when combined with signal transduction modulating drugs (**Figures 7.9-7.11**).

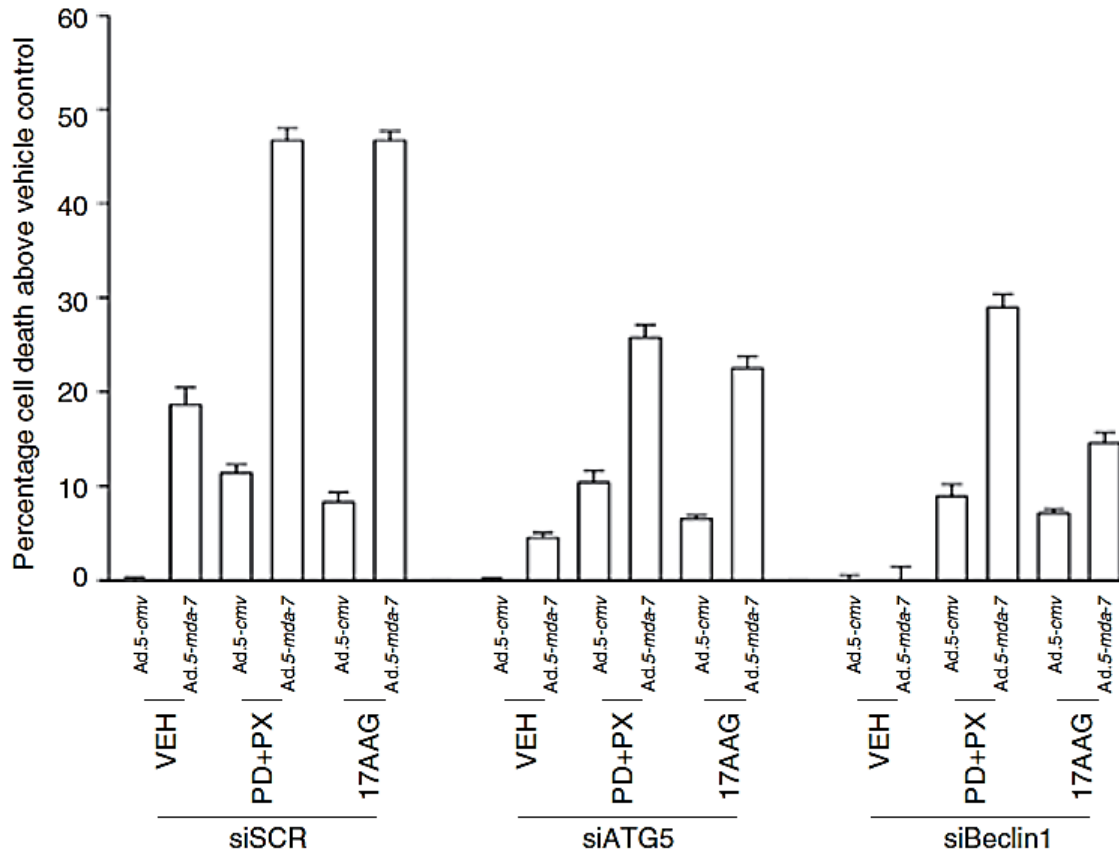


**Figure 7.11 Knockdown of Beclin1 or ATG5 abolished Ad.5-*mda-7* toxicity and significantly reduced the abilities of 17AAG and to a lesser extent PD184352/PX866 exposure to cause cell death.** GBM6 cells were infected with Ad.5-*cmv* or Ad.5-*mda-7* and in parallel transfected with either a scrambled siRNA (siSCR) or siRNA molecules to knockdown ATG5 (siATG5) or Beclin1 (siBeclin1). At 12 hours after infection cells were treated with vehicle (DMSO), PD184352 (PD, 1  $\mu$ mol/l) + PX866 (100 nmol/l) (PD+PX), or 17AAG (100 nmol/l). At 48 hours after infection cells were isolated and cell viability was determined by Trypan blue exclusion assay (—SEM,  $n = 3$ ).

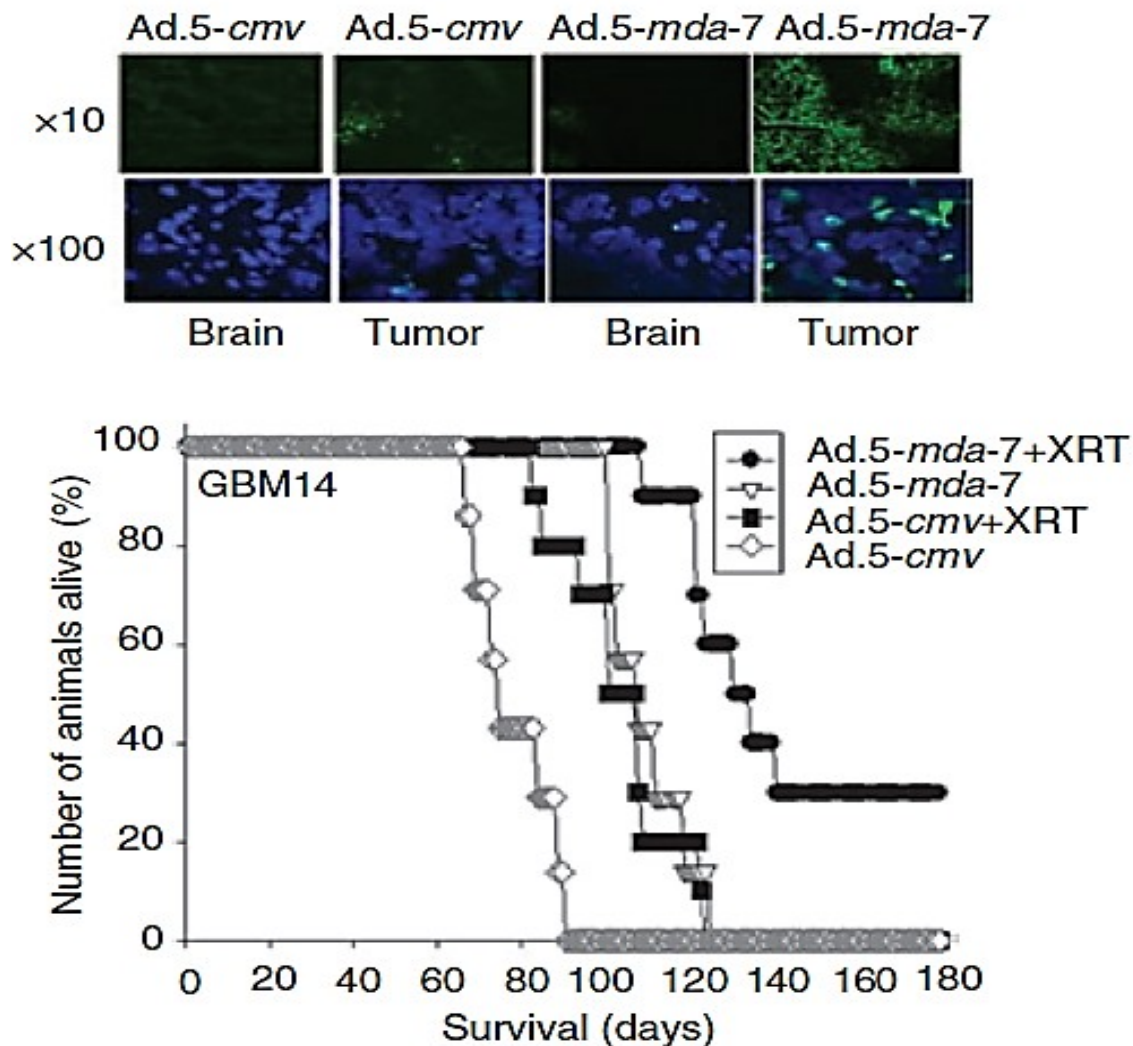


### 7.12 MDA-7/IL-24 sensitizes GBM cells to radiation therapy and enhances survival *in vivo*.

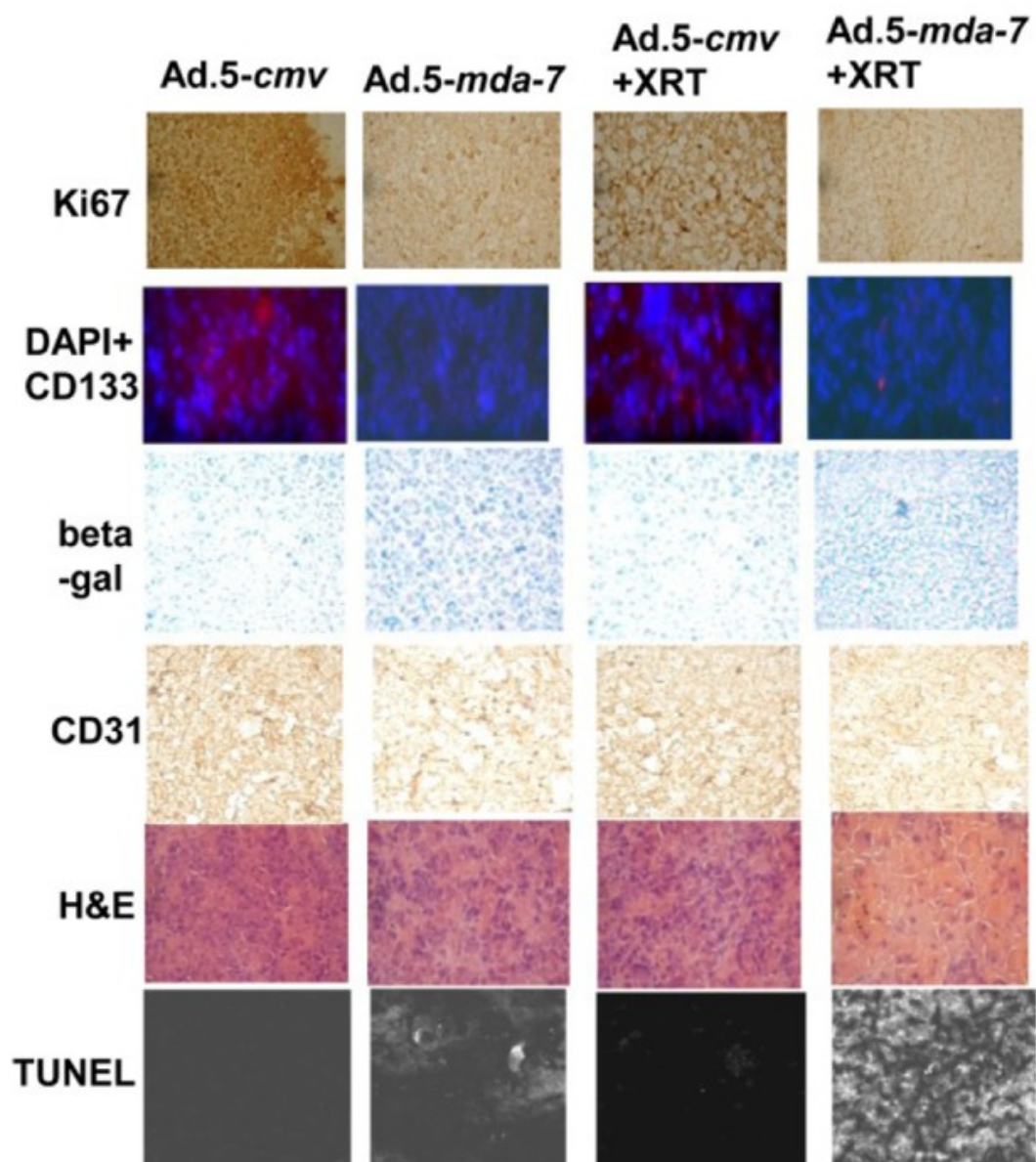
MDA-7/IL-24<sub>1</sub> has demonstrated tumor cell-specific killing and is also able to radiosensitize malignant glioma cells.<sup>33-36,133</sup> It has been demonstrated in our lab that specific signaling pathways may provide protection from *mda-7/IL-24*-induced cell death.<sub>1</sub> This current study aimed to assess the role of targeting these multiple-specific cytoprotective signaling pathways in combination with *mda-7/IL-24* treatment on human and rodent GBM both *in vitro* and *in vivo*. GBM14 cells<sub>1</sub>, lacking functional PTEN, were implanted into the brains of athymic nude mice. Fourteen days after implantation, the tumors were infused with Ad.5-*cmv* or Ad.5-*mda-7* and 48 hours after infection the head of each animal was irradiated twice with 4 Gy, irradiations were 24h apart. Animals were monitored daily and killed when approaching death. Survival of animals was plotted as a percentage of animals alive on any given day ( $\pm$ SEM,  $n = 2$ ). Inset panel: 2 days after infection, animal brains were isolated and TUNEL (terminal deoxynucleotidyl transferase dUTP nick-end labeling) stained for apoptotic cells.

Prior studies had shown that *in vivo* infection of an orthotopic tumor containing GBM6 or GBM12 cells with Ad.5-*mda-7* was able to prolong animal survival. Results presented here indicated that GBM14 cells which lack PTEN functionality allowed prolonged animal survival when infected with Ad.5-*mda-7* (**Figure 7.12.1**). In agreement with results seen in GBM6 and GBM12 tumors, GBM14 tumors infected with Ad.5-*mda-7* to express MDA-7/IL-24 in this study, exhibited elevated levels of apoptosis, as detected

by the TUNEL assay, enhanced  $\beta$ -galactosidase staining, and a reduced levels of Ki67 and CD133 staining (**Figure 7.12.2**).



**7.12.1 Ad.5-mda-7/IL-24 sensitizes GBM 14 cells to radiation therapy and enhances survival *in vivo*.** GBM14 cells were implanted into the brains of athymic nude mice and 14 days after implantation tumors were infused with Ad.5-cmv or Ad.5-mda-7 and 48 hours after infection the heads of each animal were irradiated ( $2 \times 4$  Gy, once every 24 hours). Animals were monitored daily and when approaching death were killed and survival of animals is plotted as a percentage of animals alive on any given day (—SEM,  $n = 2$ ). Upper panel: 2 days after infection, animal brains were isolated and TUNEL (terminal deoxynucleotidyl transferase dUTP nick-end labeling) stained for apoptotic cells.



**7.12.2 Ad.5-mda-7/IL-24 sensitizes GBM 14 cells to radiation therapy and enhances survival *in vivo*.**

### **7.13 MDA-7/IL-24 and temozolomide interact in at least an additive fashion to kill primary human GBM cells in short term viability assays.**

In an attempt to further enhance the apoptotic potential of MDA-7/IL-24, experiments were performed to assess whether Ad.5-*mda-7* lethality could be enhanced by temozolomide (TMZ), an established GBM therapeutic agent. GBM6, GBM12, and GBM14 cells were infected with Ad.5-*cmv* or Ad.5-*mda-7*. Twelve hours after infection cells were treated with vehicle (DMSO)] or increasing concentrations of TMZ. Forty eight hours after infection, cells were isolated and cell viability was determined by TUNEL assay ( $\pm$ SEM,  $n = 3$ ). These results indicated that TMZ was able to induce cell killing in a dose-dependent manner. In addition, this cell killing potential was increased by the expression of MDA-7/IL-24 in these cells (**Figure 7.13**).

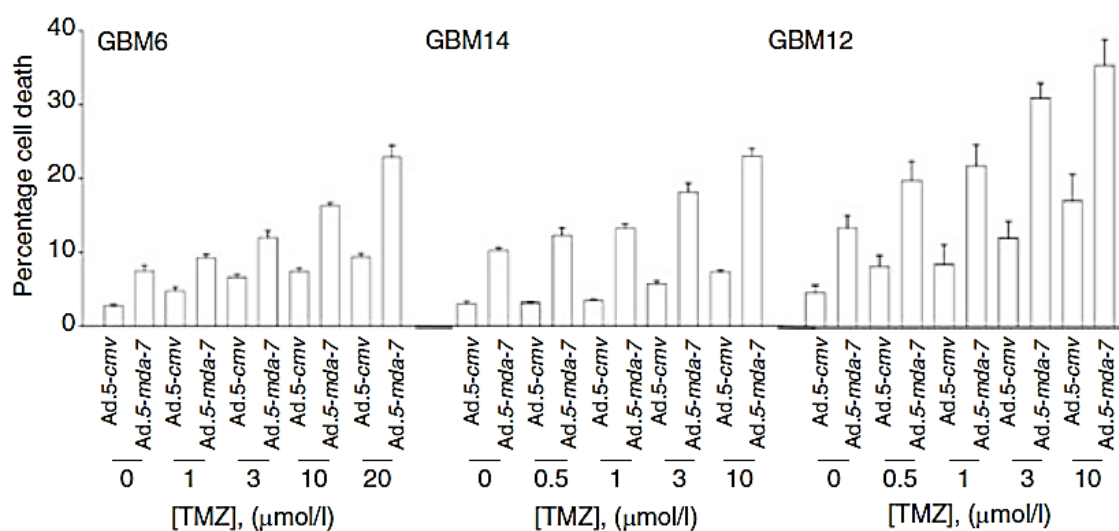


**Figure 7.13 Temozolomide (TMZ) potentiates Ad.5-*mda-7* lethality in GBM cells.** GBM6, GBM12, and GBM14 cells were infected with Ad.5-*cmv* or Ad.5-*mda-7*, and 12 hours after infection cells were treated with vehicle [dimethyl sulfoxide (DMSO)] or increasing concentrations of TMZ. At 48 hours after infection, cells were isolated and cell viability was determined by TUNEL assay (—SEM,  $n = 3$ ).

#### **7.14 Radiation, MDA-7/IL-24 and temozolomide interact in a greater than additive fashion to kill primary human GBM cells**

In order to examine the interaction(s) of TMZ and radiation and MDA-7/IL-24 in GBM cells, GBM6, GBM12, and GBM14 cells were infected with Ad.5-*cmv* or Ad.5-*mda-7*. Twelve hours after infection, the cells were treated with vehicle (DMSO) or increasing concentrations of TMZ. Twenty four hours after virus infection cells were irradiated (4 Gy). Forty eight hours after infection, cells were isolated and cell viability was determined by TUNEL assay ( $\pm$ SEM,  $n = 3$ ). These results indicated that a combination of radiation, MDA-7/IL-24, and TMZ were able to interact in at least an additive fashion to kill primary human GBM cells (**Figure 7.14**).

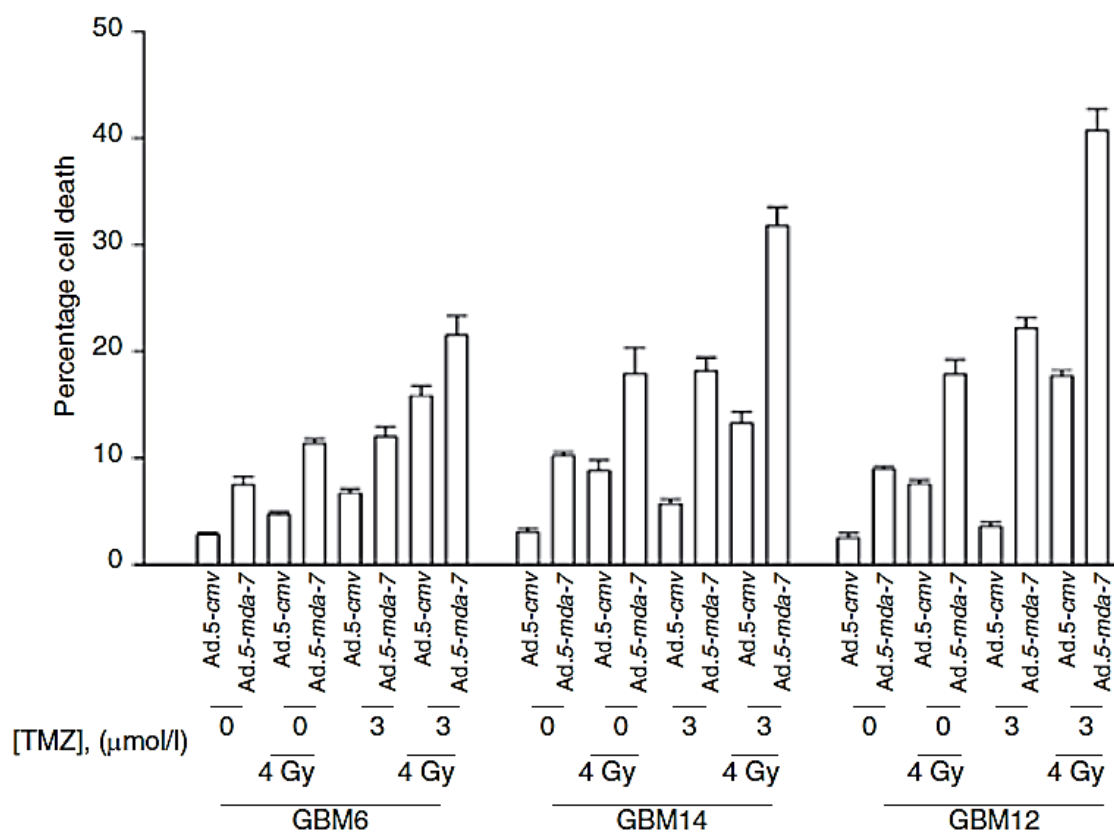


**Figure 7.14 Temozolomide (TMZ) potentiates Ad.5-mda-7 lethality and radiosensitivity.** GBM6, GBM12, and GBM14 cells were infected with Ad.5-cmv or Ad.5-mda-7, and 12 hours after infection cells were treated with vehicle (DMSO) or increasing concentrations of TMZ. At 24 hours after virus infection cells were irradiated (4 Gy). At 48 hours after infection, cells were isolated and cell viability was determined by TUNEL assay (—SEM,  $n = 3$ ).



**7.15 Radiation, MDA-7/IL-24 and temozolomide interact in a greater than additive fashion to kill primary human GBM cells in colony formation assays.**

In addition to short term assays of cell death, assessment of longer term colony formation was performed. GBM6, GBM12, and GBM14 cells were plated as single cells and were infected with Ad.5-*cmv* or Ad.5-*mda-7*, 12 hours after infection cells were treated with vehicle (DMSO) or increasing concentrations of TMZ. Twenty four hours after virus infection cells were irradiated (4 Gy). Forty eight hours after infection, media was replaced with fresh media lacking vehicle/drugs. Colonies of >50 cells were permitted to form over the following ~20 days, followed by fixing, staining, and counting of colonies ( $\pm$ SEM,  $n = 3$ ). Similar results as seen in previous short-term death assays were attained (**Figure 7.14**), indicating a greater than additive induction of cell killing by the combination of these agents (**Figure 7.15**).

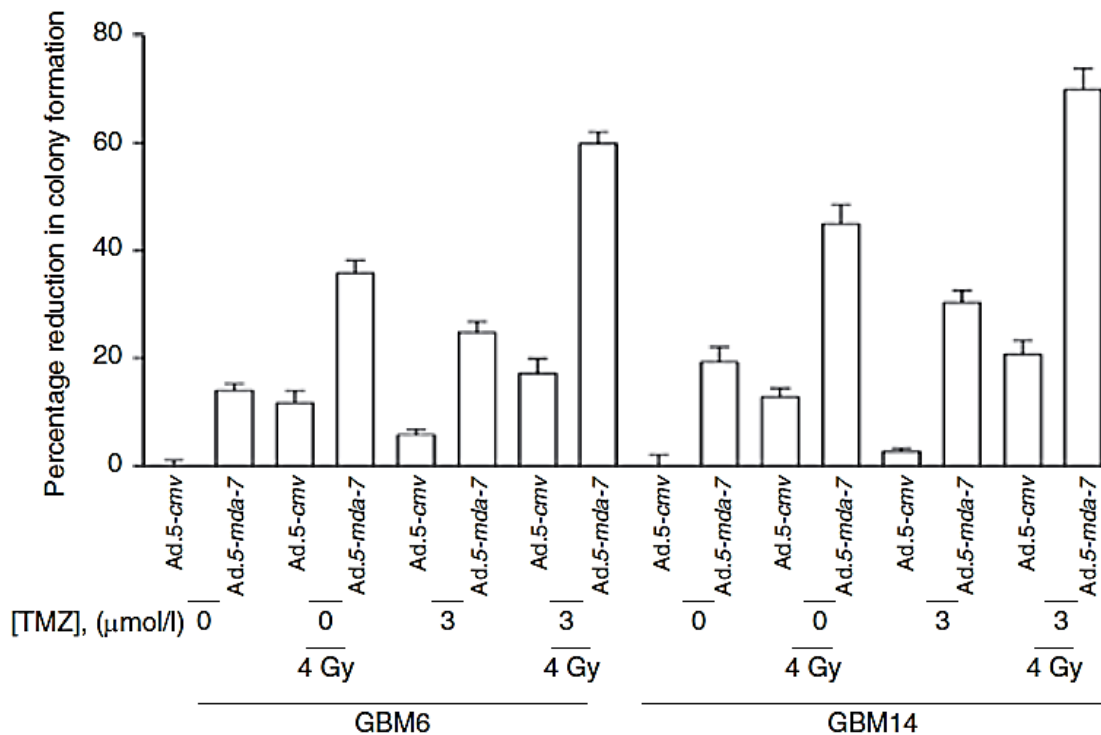


**Figure 7.15 Temozolomide (TMZ) potentiates Ad.5-*mda-7* lethality and radiosensitization.** GBM6 and GBM14 cells were plated as single cells and were infected with Ad.5-*cmv* or Ad.5-*mda-7*, and 12 hours after infection cells were treated with vehicle (DMSO) or increasing concentrations of TMZ. At 24 hours after virus infection cells were irradiated (4 Gy). At 48 hours after infection, the media was replaced with media lacking vehicle/drugs. Colonies of >50 cells were permitted to form over the following ~20 days, followed by fixing, staining, and counting (—SEM,  $n = 3$ ).

**7.16 A tropism-modified type 5/3 adenovirus infects GBM cells in a CAR independent fashion and to a greater extent than a serotype 5 virus *in vivo*.**

Biopsies from human GBM tumors *in situ* have been reported to express low levels of Coxsackievirus and adenovirus receptors (CARs), resulting in an inability of these cells to be infected with a serotype 5 adenovirus.<sup>30</sup> In an attempt to circumvent this problem, a new recombinant adenovirus to express MDA-7/IL-24 that comprises the tail and shaft domains of a serotype 5 virus and the knob domain of a serotype 3 virus was developed.<sup>147,148</sup> GBM6 (CAR+++) **(Figure 7.16.1)** and U87-MG (CAR+) **(Figure 7.16.2)** cells were infected with viruses expressing a luciferase gene, Ad.5-*luc* or with tropism-modified viruses Ad.5/3-*luc*, Ad.5-rgd-*luc*, Ad.5-D-rgd-*luc* and Ad.5-pK7-*luc* at, 10 **m.o.i**, as indicated (rgd motif binds to integrins; pK7 7 x lysine residues equating to electrostatic binding to cells). Cells were lysed 48 hours after infection and the luciferase activity was measured in triplicate ( $\pm$ SEM,  $n = 3$ ). Upper blot: GBM6/U87 cells were infected with Ad.5-*cmv*, Ad.5/3-*cmv*, Ad.5-*mda-7* or Ad.5/3-*mda-7* (10 MOI). Cells were isolated 24 hours after infection and MDA-7/IL-24 protein levels determined ( $n = 2$ ). Results indicated that the serotype 5/3 virus were able to infect GBM cells in a CAR-independent fashion and to a greater extent than a serotype 5 virus, these results were also evident in GBM6 cells that express significant levels of CAR **(Figure 7.16.1)**. This increased infectivity was also shown to correlate with elevated levels of MDA-7/IL-24 expression **(Figure 7.16.1, blotting panel)**. Of particular note, a recent study claimed that a serotype 5 virus with a “double RGD” knob modification to permit infection *via* binding to cell surface integrin

proteins, enhanced MDA-7/IL-24 delivery to GBM cells over a serotype 5 virus *in vitro* and *in vivo*.<sup>140</sup> The results presented here **Figure 7.16.1**, indicated that a serotype 5 virus with a “double RGD” knob modification was able to enhance gene delivery to GBM cells over a serotype 5 virus. However, the “double RGD” virus was shown to weakly infect GBM cells when compared to results seen for the serotype 5/3 virus.

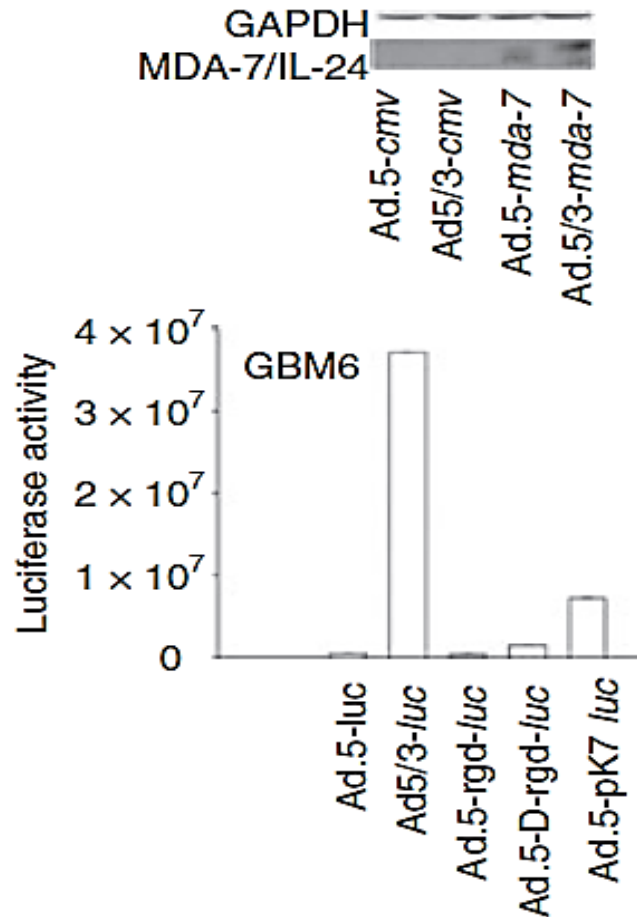


**Figure 7.16.1 A tropism-modified type 5/type 3 adenovirus infects GBM 6 cells more readily than a type 5 adenovirus.** GBM6 (CAR+++) cells were infected with Ad.5-*luc* or with tropism-modified viruses Ad.5/3-*luc*, Ad.5-rgd-*luc*, Ad.5-D-rgd-*luc*, Ad.5-pK7-*luc* at 10 MOI, as indicated. Cells were lysed 48 hours after infection and the luciferase activity was measured in triplicate (—SEM,  $n = 3$ ). Upper blot: GBM6 cells were infected with Ad.5-*cmv*, Ad.5/3-*cmv*, Ad.5-*mda-7* or Ad.5/3-*mda-7* (10 MOI). Cells were isolated 24 hours after infection and MDA-7/IL-24 protein levels determined ( $n = 2$ ).

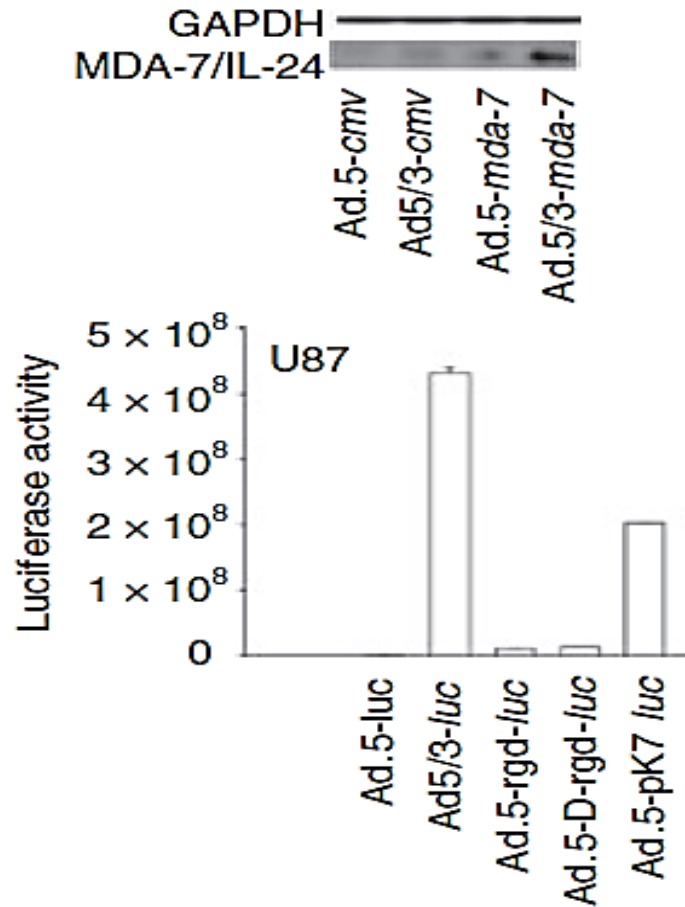


**Figure 7.16.2 A tropism-modified type 5/type 3 adenovirus infects U87 cells more readily than a type 5 adenovirus.** U87-MG (CAR+) cells were infected with Ad.5-luc or with tropism-modified viruses Ad.5/3-luc, Ad.5-rgd-luc, Ad.5-D-rgd-luc, Ad.5-pK7-luc at 10 MOI, as indicated. Cells were lysed 48 hours after infection and the luciferase activity was measured in triplicate (—SEM,  $n = 3$ ). Upper blot: U87-MG cells were infected with Ad.5-cmv, Ad.5/3-cmv, Ad.5-mda-7 or Ad.5/3-mda-7 (10 MOI). Cells were isolated 24 hours after infection and MDA-7/IL-24 protein levels determined ( $n = 2$ ).

**7.17 In a colony-formation assay, infection of GBM6, GBM12 and U87-MG cells with Ad.5/3-*mda-7* caused a greater reduction in cell survival than cells infected with Ad.5-*mda-7***

Given that Ad.5/3-*mda-7* was able to induce a greater virus infection and MDA-7/IL-24 expression in GBM6, GBM12 and U87-MG cells, in comparison with Ad.5-*mda-7*, the potential of Ad.5/3-*mda-7* in reducing colony formation to a greater extent than Ad.5-*mda-7* in these cells was assessed. GBM6, GBM12, and U87-MG cells were plated in sextuplicate as single cells and were infected with Ad.5-*cmv* or Ad.5-*mda-7* or with tropism-modified viruses Ad.5/3-*cmv* or Ad.5/3-*mda-7* at 0–50 m.o.i. Colonies of >50 cells were permitted to form over 14–20 days, followed by fixing, staining, and counting of colonies. Data in this section are presented as the real percentage reduction in colony formation, subtracting the effect of Ad.*cmv* (5 or 5/3) infection ( $\pm$ SEM,  $n = 3$ ). The results indicated that, in colony-formation assays, infection of GBM6, GBM12, and U87-MG cells with a serotype 5/3 adenovirus to express MDA-7/IL-24 (Ad.5/3-*mda-7*) caused a significant ( $*P < 0.05$ ) reduction when compared to cell survival per active virus particle, following infection using a serotype 5 adenovirus (Ad.5-*mda-7*) (**Figure 7.17**).

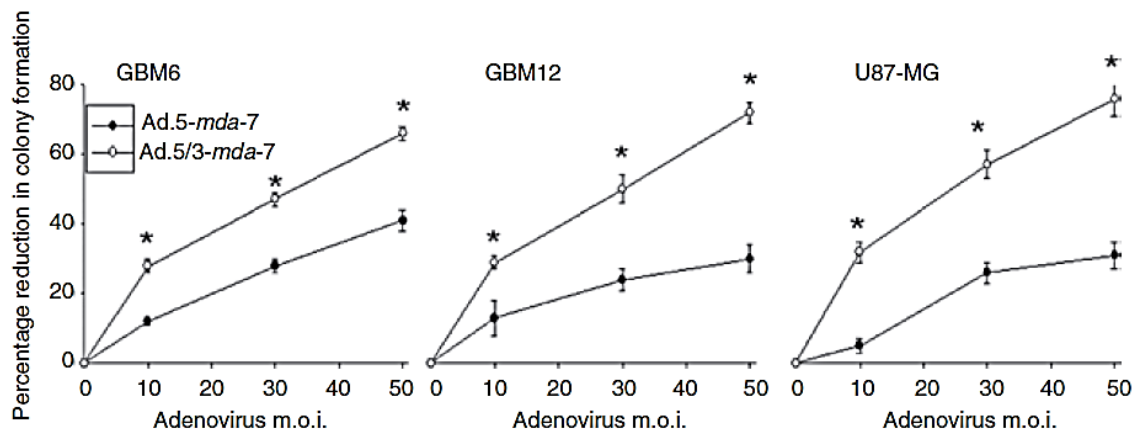


**Figure 7.17 A tropism-modified type 5/3 adenovirus infects GBM6, GBM12 and U87-MG cells more readily than a type 5 adenovirus, in a colony formation assay, to generate a greater cytotoxic effect.** GBM6, GBM12, and U87-MG cells were plated in sextuplicate as single cells and were infected with Ad.5-*cmv* or Ad.5-*mda-7* or with tropism-modified viruses Ad.5/3-*cmv* or Ad.5/3-*mda-7* at 0–50 multiplicity of infection (MOI). Colonies of >50 cells were permitted to form over 14–20 days, followed by fixing, staining, and counting. Data are presented as the real percentage reduction in colony formation subtracting the effect of Ad.*cmv* (5 or 5/3) infection (—SEM,  $n = 3$ ) \* $P < 0.05$  greater than Ad.5-*mda-7* infection.



**7.18 A tropism-modified type 5/3 adenovirus infects GBM cells more readily than a type 5 adenovirus, and enhances tumor killing *in vivo*.**

We next determined whether infection of pre-formed tumors with Ad.5/3-*mda-7* caused a greater reduction in tumor growth than infection with Ad.5-*mda-7*. GBM6 cells stably expressing luciferase were implanted into the brains of athymic nude mice. Fourteen days after implantation tumors were infused with Ad.5-*cmv* or Ad.5-*mda-7*, or Ad.5/3-*cmv* or Ad.5/3-*mda-7*. The tumors *in situ* were imaged using a Xenogen CCD system and the light intensity quantified before and for 18 days following adenovirus infusion ( $\pm$ SEM,  $n = 2$ ). These results indicated that infection of pre-formed GBM6 tumors with Ad.5-*mda-7* induced a significant reduction ( $*P < 0.05$ ), in tumor growth when compared to Ad.5-*cmv* treated cells. Further, infection of pre-formed GBM6 tumors with Ad.5/3-*mda-7* caused a significant reduction ( $\#P < 0.05$ ) in tumor growth when compared to infection with Ad.5-*mda-7* (**Figure 7.18.1**). In isolated tumor sections, taken at 2 and 7 days after infection, it was noted that Ad.5/3-*mda-7* caused a greater and more rapid induction in tumor apoptosis than Ad.5-*mda-7* (**Figure 7.18.2**). statistics \* and #

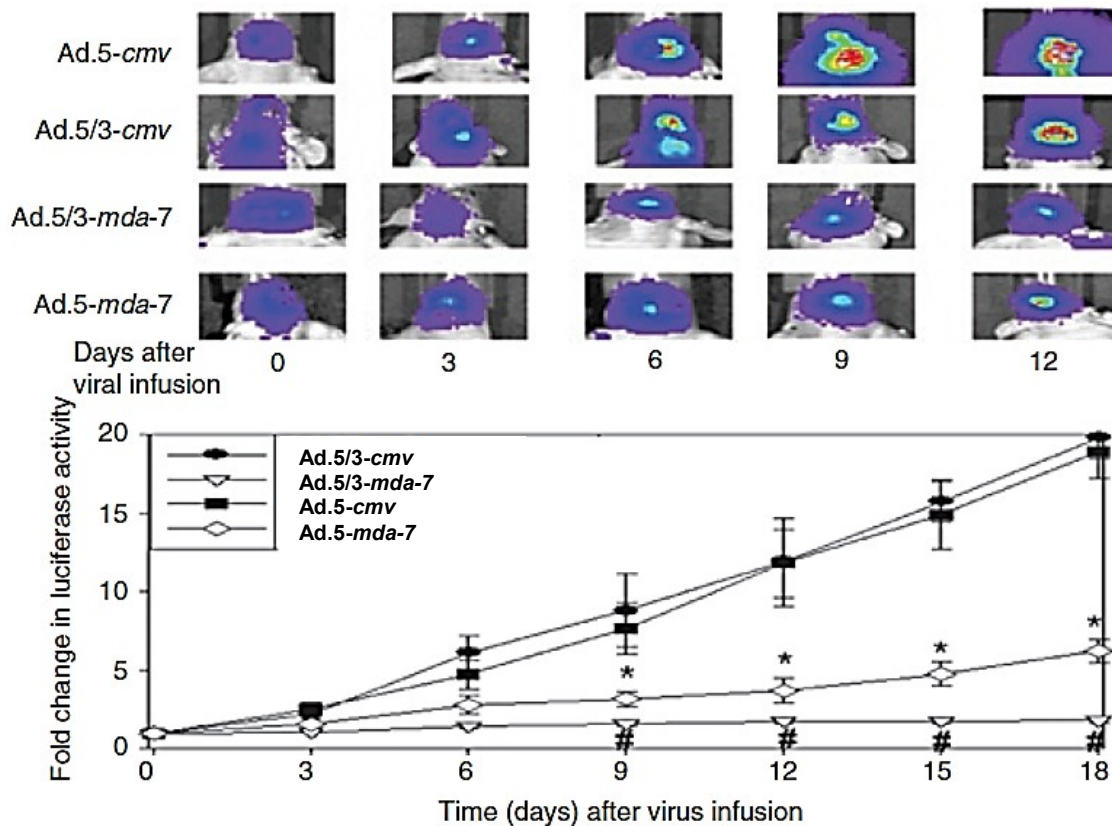


**Figure 7.18.1 A tropism-modified type 5/3 adenovirus infects GBM6 cells more readily than a type 5 adenovirus, and enhances tumor killing *in vivo*.** GBM6 cells that stably express luciferase were implanted into the brains of athymic nude mice and 14 days after implantation tumors were infused with Ad.5-cmv or Ad.5-mda-7, or Ad.5/3-cmv or Ad.5/3-mda-7. The tumors *in situ* were imaged using a Xenogen CCD system and the light intensity quantified before and for 18 days following adenovirus infusion (—SEM,  $n = 2$ ). \* $P < 0.05$  less than corresponding Ad.5-cmv treated cells; # $P < 0.05$  less than Ad.5-mda-7 value.

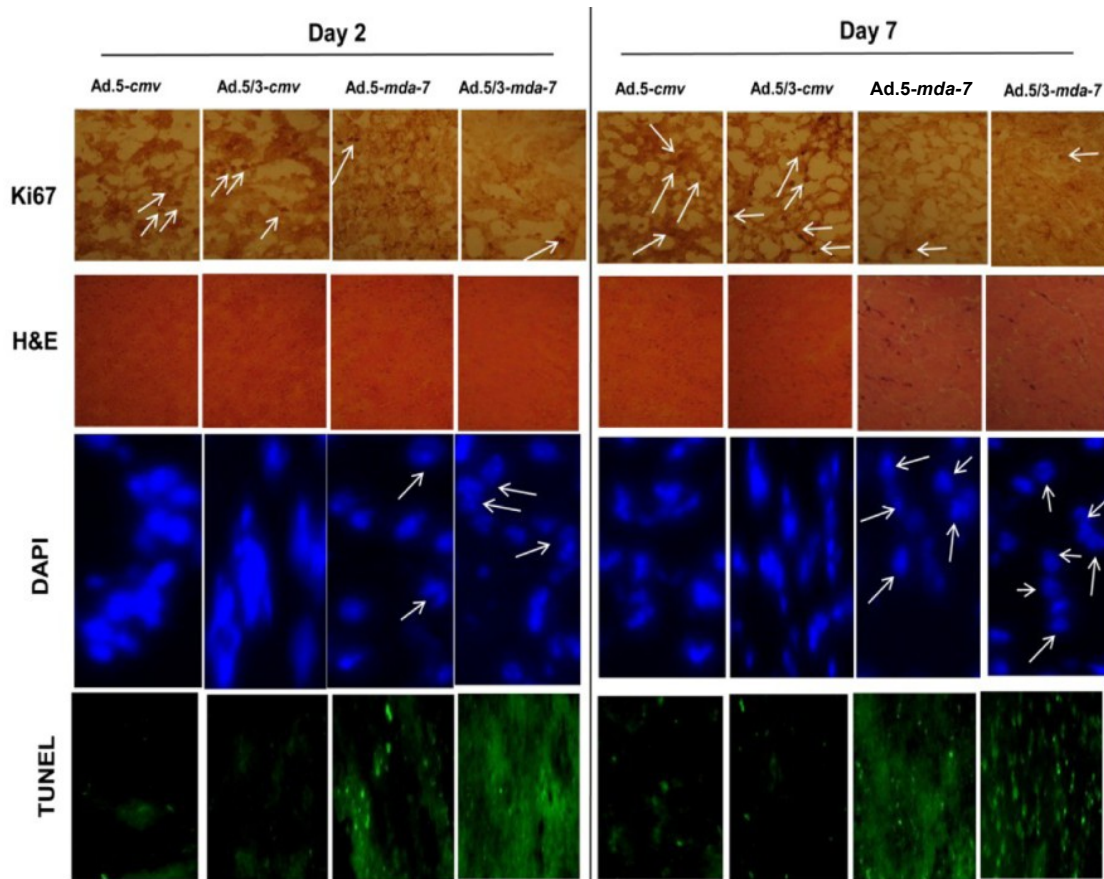


**Figure 7.18.2** In isolated GBM6 tumor sections, at 2 and 7 days after infection, *Ad.5/3-mda-7* caused a greater and more rapid induction of tumor apoptosis than *Ad.5-mda-7*

### **7.19 Ad.5/3-*mda-7* is more effective at killing and reducing rodent GL261 glioma viability *in vitro* and *in vivo*.**

We have also used GL261 mouse glioblastoma cells to confirm our *in vivo* studies using the serotype 5 and 5/3 forms of Ad.*mda-7/IL-24*, in immune competent mice, GL261 cells were infected with Ad.5-*cmv* or Ad.5-*mda-7* or with Ad.5/3-*cmv* or Ad.5/3-*mda-7* at 20 or 80 MOI. Forty eight hours after infection, cells were isolated and cell viability was determined by Trypan blue dye exclusion assay ( $\pm$ SEM,  $n = 3$ ). These results indicated that Ad.5/3-*mda-7* was able to induce significantly more cell death ( $*P < 0.05$ ), in GL261 cells than Ad.5-*mda-7* when cells were infected with virus at either 20 or 80 m.o.i. Indeed GL261 appeared resistant to serotype 5 virus infections (**Figure 7.19.1**). To assess whether these results would translate to an animal model, black C57 mice were implanted with GL261 cells stably expressing luciferase. Fourteen days post implantation; tumors were infused with Ad.5/3-*cmv* or Ad.5/3-*mda-7*. Tumors were imaged *in situ* using a Xenogen CCD system and the light intensity quantified before, and 6 days following, adenovirus infusion ( $n = 2$ ) showing a dramatic reduction of tumor growth (light intensity) (**Figure 7.19.2**). Six days after virus infusion, mouse brains were isolated and immunohistochemistry performed to detect the levels of Ki67, CD131 and TUNEL (terminal deoxynucleotidyl transferase dUTP nick-end labeling) staining ( $n = 2$ ). Following suit with our *in vitro* data, the levels of proliferation marker, Ki67, and progenitor cell marker, CD131 were significantly reduced. In addition, Ad.5/3-*mda-7/IL-24* increased the number of TUNEL positive cells as well as exhibiting negative effects on the morphology of these tumor cells (H/E staining) (**Figure 7.19.3**).

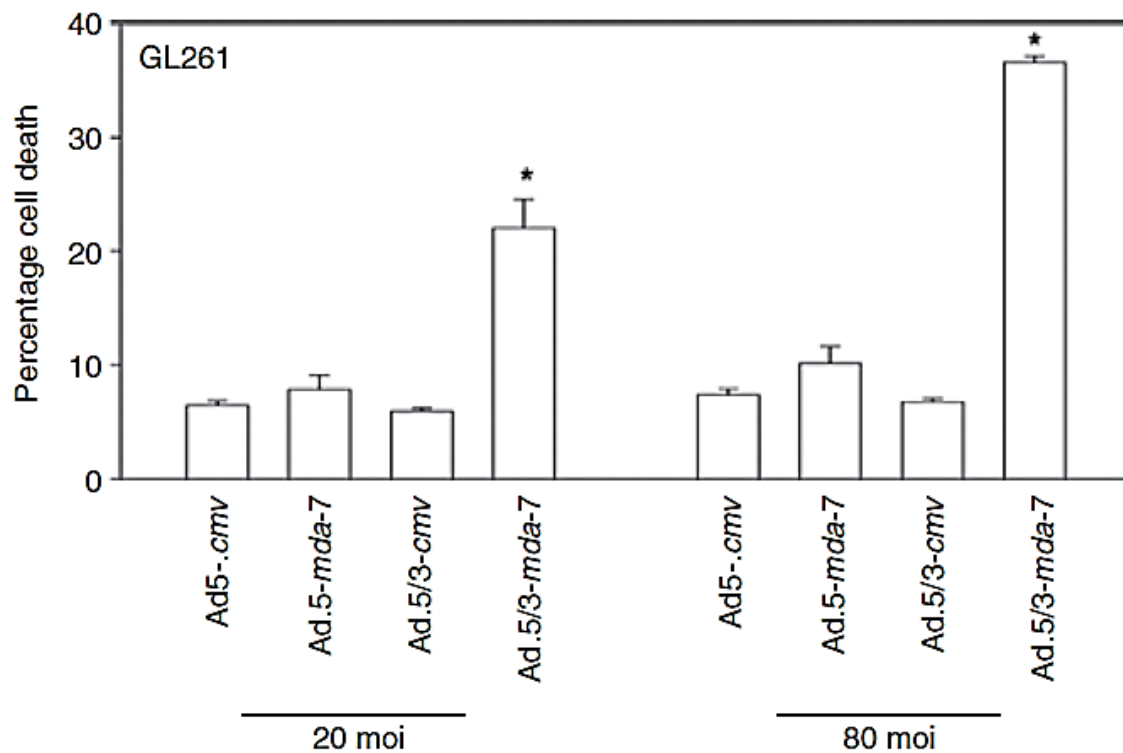


**Figure 7.19.1 Ad.5/3-*mda-7* is more effective at killing and reducing rodent GL261 glioma viability *in vitro*.** GL261 cells were infected with Ad.5-*cmv* or Ad.5-*mda-7* or with Ad.5/3-*cmv* or Ad.5/3-*mda-7* at 20 or 80 multiplicity of infection (MOI). At 48 hours after infection, cells were isolated and cell viability was determined by Trypan blue dye exclusion assay (—SEM,  $n = 3$ ). \* $P < 0.05$  greater than Ad.5-*mda-7* value.

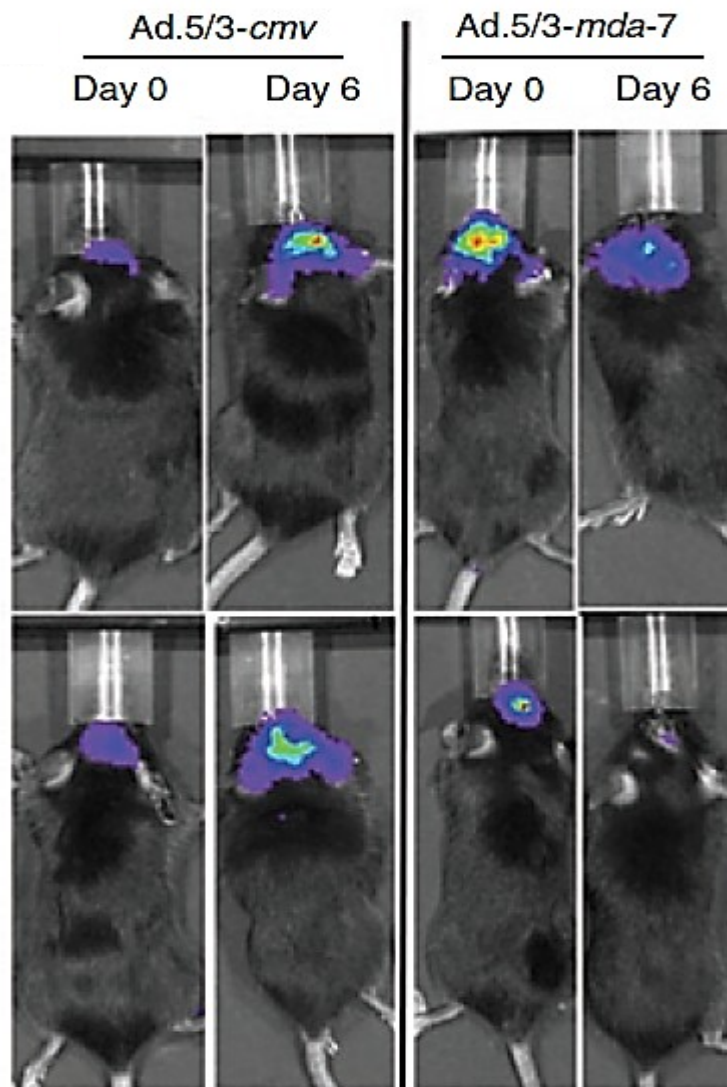


**Figure 7.19.2** *Ad.5/3-mda-7* is more effective at killing and reducing rodent GL261 glioma viability *in vivo*. C57 black mice were implanted with GL261 cells stably expressing luciferase. At 14 days after implantation tumors were infused with *Ad.5/3-cmv* or *Ad.5/3-mda-7*. The tumors *in situ* were imaged using a Xenogen CCD system and the light intensity quantified before and 6 days following adenovirus infusion ( $n = 2$ ).

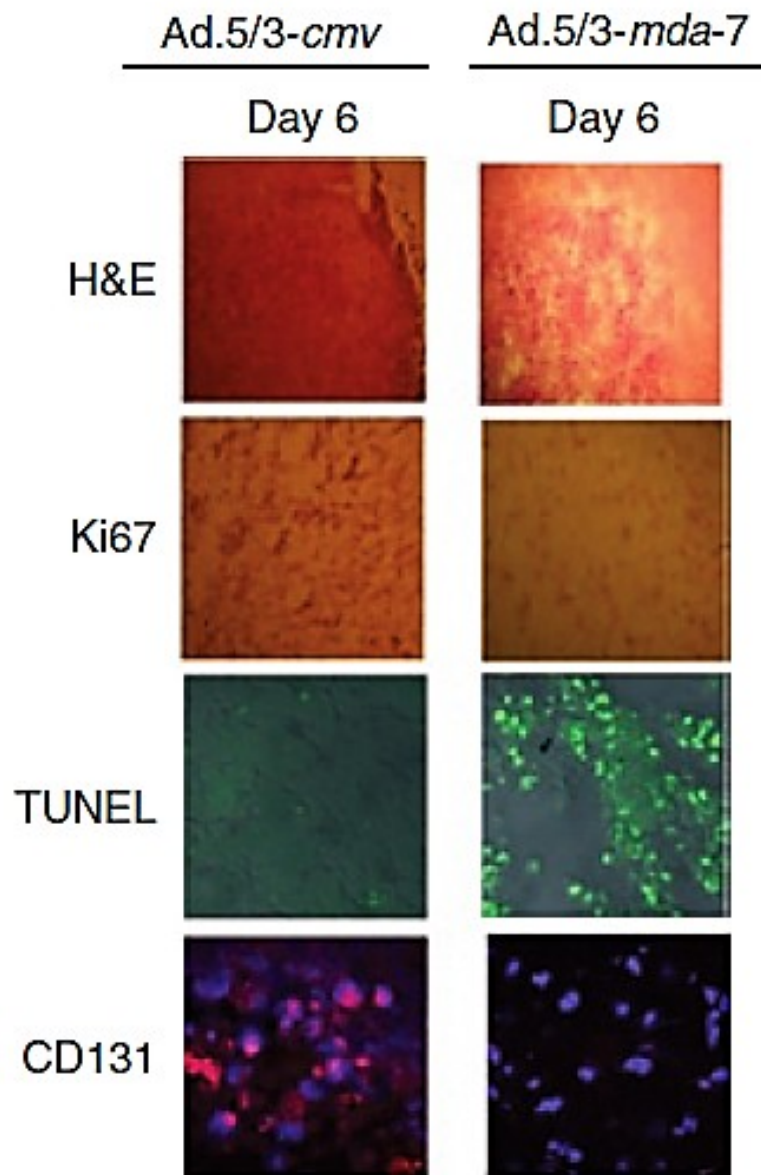


**Figure 7.19.3 Ad.5/3-*mda-7* is more effective at killing and reducing immune competent rodent GL261 glioma viability *in vivo*.** C57 black mice were implanted with GL261 cells stably expressing luciferase. At 14 days after implantation tumors were infused with Ad.5/3-*cmv* or Ad.5/3-*mda-7*. Six days after virus infusion mouse brains were isolated and immunohistochemistry performed to detect the levels of Ki67, CD131, and TUNEL (terminal deoxynucleotidyl transferase dUTP nick-end labeling) staining ( $n = 2$ )



## CHAPTER 8 DISCUSSION:

### INHIBITORS OF MULTIPLE PROTECTIVE SIGNALING PATHWAYS AND Ad.5/3 DELIVERY ENHANCES MDA-7/IL-24 KILLING

This study has focused on developing enhanced therapies for the treatment of GBM, a tumor that has been characterized with a rapid progression, with no treatment providing a long-term clinical benefit.<sup>1</sup> To achieve this objective, we utilized *mda-7/IL-24*, which has been shown by our group and others to have tumor cell-specific killing and radiosensitization abilities in malignant glioma cells.<sup>33-36,142</sup> Based upon previous observations that have illustrated specific signaling pathways which might provide protection from *mda-7/IL-24*-induced toxicity, the current study explored approaches aimed at targeting multiple-specific cytoprotective signaling pathways in combination with *mda-7/IL-24* on human and rodent GBM both *in vitro* and *in vivo*. The studies presented in this thesis highlight combinations of clinically relevant protein and lipid kinase inhibitors that increase MDA-7/IL-24 toxicity. In addition, a tropism-modified serotype Ad.5/3 was used as a means of enhancing the therapeutic delivery of MDA-7/IL-24 for GBM's.

Infection of GBM cells with a dose of Ad.5-*mda-7* virus particles able to cause modest levels of toxicity ~48 hours after exposure, correlated with the activation of the stress induced JNK1/2 and p38 MAPK pathways as well as the phosphorylation of PERK. In contrast, Ad.5-*mda-7* suppressed pro-survival ERK1/2, AKT, mTOR, and p70 S6K signaling. Multiple studies using a number of toxic stimuli have been documented,



showing that prolonged JNK1-3 and/or p38 MAPK activation in a wide variety of cell types can trigger cell death.<sup>143-145</sup> It is also well established that the balance between the readouts of ERK1/2 and JNK1-3 signaling can represent a general key homeostatic mechanism that regulates cell survival versus cell death processes.<sup>143-145</sup> Prior studies *in vitro* and *in vivo* treating primary human GBM cells with GST-MDA-7 and Ad.5-*mda-7* have demonstrated that JNK1-3 signaling represents a key pro-apoptotic signal generated by MDA-7/IL-24 exposure and the initial hypothesis in this study was that inhibition of ERK/AKT/mTOR signaling would promote the toxicity of Ad.5-*mda-7*, primarily through enhanced activation of JNK1-3.<sup>35,36</sup> Inhibition of MEK1/2 and PI3K enhanced MDA-7/IL-24-induced JNK1-3 activation that was causal in promoting cell killing. Whereas, combined inhibition of MEK1/2 and PI3K and mTOR did not lead to a further activation of the JNK pathway. Despite this finding, inhibition of the JNK pathway *in vitro* suppressed the toxicity of MEK1/2, PI3K and mTOR inhibition when combined with Ad.5-*mda-7*. Ad.5-*cmv* infected GBM cells lacking MEK1/2, PI3K, mTOR, and JNK signaling did not grow *in vitro* and did not form tumors *in vivo*. Thus, the relative role of JNK signaling *in vivo* with respect to Ad.5-*mda-7* effects could not be determined. It has been known for a number of years that JNK pathway signaling in GBM cells can promote cell killing as well as being essential for their proliferation.<sup>44</sup>

Although inhibition of mTOR function modestly enhanced Ad.5-*mda-7* lethality *in vitro*, this manipulation did not significantly alter tumor growth *in vivo*, in contrast to si-mTOR/dnMEK/dn-p85 expression. The lack of an *in vivo* effect after inhibition of mTOR upon MDA-7 toxicity likely reflects the fact that loss of only mTOR function *in vivo* may

not significantly impact on the long-term tumor-forming ability of GBM cells. It is also in general agreement with many observations over decades in which drug combination effect *in vitro* does not fully translate into an animal model system. Hence, inhibition of the primary Ad.5-*mda-7*-dependent “pro-death” JNK pathway signal could suppress all of the toxic responses emanating from expression of MDA-7/IL-24 in GBM cells.

Infection of cells with Ad.5-*mda-7* decreased the expression of BCL-XL and MCL-1, which we have previously demonstrated with GST-MDA-7 to be due to ER stress signaling *via* PERK-eIF2 $\alpha$ .<sup>35,36,134</sup> One pronounced effect of inhibiting the protective signaling pathways was to facilitate MDA-7/IL-24-induced reduction in the expression of multiple mitochondrial protective proteins, and over-expression of either BCL-XL or MCL-1 maintained tumor cell viability. In studies parallel to those in this thesis MDA-7/IL-24 induced JNK pathway signaling has been shown to mediate activation of the pro-apoptotic proteins BAX and BAK. Thus, the MDA-7/IL-24 induced ratio change of pro to anti-apoptotic proteins is exacerbated by inhibiting protective signaling pathways, leading to greater levels of tumor cell death.

Prior studies have demonstrated that GST-MDA-7 lethality in GBM cells required the induction of a toxic form of autophagy and that autophagy was dependent on PERK signaling.<sup>35,37</sup> Treatment of cells with inhibitors of PI3K/mTOR has been shown in many cell systems to enhance autophagy and we noted that inhibition of protective signaling pathways enhanced the numbers of autophagic vesicles per GBM cell and enhanced MDA-7/IL-24-induced autophagy.<sup>149</sup> However, this did not correlate with enhanced PERK phosphorylation, arguing that the signaling pathways are acting to modulate autophagy at a

downstream point, *e.g.*, ATG1/ATG13.<sup>150</sup> Knockdown of ATG5 or Beclin1 suppressed and reduced MDA-7/IL-24 toxicity, but did not abolish the death-inducing effects of the small molecule kinase inhibitors. Collectively, our data argue that inhibition of protective signaling pathways promotes MDA-7/IL-24 toxicity *via* increased JNK signaling, by decreased expression of BCL-XL and MCL-1 and by increasing levels of autophagy.

Temozolomide-based chemotherapy is a mainstay of GBM treatment.<sup>1</sup> MDA-7/IL-24 and temozolomide interacted in a greater than additive fashion to kill GBM cells and this effect was increased in at least an additive fashion by exposure to ionizing radiation. Temozolomide interacts with DNA inducing a wide spectrum of methyl adducts, *e.g.*, methyl-purines.<sup>151</sup> Temozolomide anti-tumor activity has been predominantly linked to the generation of *O*(6)-methyl-guanine, particularly as tumor cell sensitivity to the drug inversely correlates with the expression levels of *O*(6)-alkyl-guanine DNA alkyl-transferase and also requires intact mismatch DNA repair. We have recently shown that MDA-7/IL-24 toxicity is dependent on the generation of ceramide<sup>134,152</sup> and it has been shown that (i) DNA damage *via* ATM signaling increases ceramide levels and (ii) that temozolomide toxicity is enhanced by agents that block sphingosine kinase activity that will *de facto* increase ceramide levels.<sup>153</sup> Future studies beyond the scope of this thesis will be needed to define the molecular mechanisms by which temozolomide and MDA-7/IL-24 interact in promoting toxicity in GBM cells.

GBM was one of the earliest malignancies considered amenable to viral delivery of genetic-based therapeutics.<sup>139</sup> Serotype 5 human adenoviruses bind to and infect human cells through the CAR, a protein whose expression has been shown in several studies to be

significantly reduced in primary human GBM cells in culture and *in situ*.<sup>139</sup> Thus, delivery of therapeutic genes by this method to GBM cells was originally and unknowingly, hampered by the relative inefficiency of this gene delivery method. Multiple groups are attempting to solve the relative inefficiency of serotype 5 adenovirus infections in human GBM by modifying specific sequences within virus capsid proteins that directly associate with CAR, *i.e.*, they are applying targeting strategies to enhance viral infectivity *via* CAR independent pathways. Initial work from several groups involved modification of the infective viral capsid “knob” to bind instead to surface integrin proteins whose expression is enhanced upon transformation (RGD modification), or by insertion into the knob of multiple lysine residues (pK7), which will increase viral interaction with cells by electrostatic effects on the cell’s surface. Subsequently, more subtle modifications to the proteins expressed as part of the viral capsid knob have been made with the development of viruses expressing chimeric knobs containing components of different serotype viruses. For example, in some of these viruses the infective capsid knobs from serotype 3 adenoviruses were incorporated into the adenovirus type 5 knob. The studies in this thesis demonstrated that modified serotype 5/3 knob adenoviruses<sup>136,137</sup> are able to achieve enhanced gene transduction into low-CAR (and higher-CAR) containing human GBM tumor cells *in vitro* and *in vivo*. We also noted that a serotype 5/3 virus was more efficient at transducing genes into GBM cells than either an RGD/double RGD modification or a pK7 modification.<sup>140</sup> However, an additional problem of efficacy, exists for all gene therapy approaches and one that is exacerbated by the highly invasive and diffuse nature of GBM compared to other tumor cell types.<sup>1</sup> This problem highlights the need for

development of a toxic “bystander” effect in tumor cells that have not been infected by virus during the primary infection process. Using the rules of simple mass-action, *i.e.*, the total number of non-transformed cells within and around a GBM tumor compared to the total number of transformed cells in a tumor to the total number of virus particles being infused, it is not possible for all tumor cells in a highly invasive tumor cell type such as GBM to be infected by a nonreplicative, and in all likelihood even a conditionally replicative adenovirus. Furthermore, many prior studies in GBM using gene therapeutic tools have often expressed intracellular proteins that are not normally secreted, which will frequently result in only those cells that have been virally infected being subjected to the actions of the therapeutic gene.

The expression of MDA-7/IL-24 overcomes the problems associated with a lack of a “bystander” effect following gene therapeutic intervention.<sup>14-18,40,138,141</sup> MDA-7/IL-24 is secreted from infected GBM cells and as we have demonstrated in GBM,<sup>141</sup> media containing secreted MDA-7/IL-24 can induce apoptosis in uninfected GBM cells. The data in this thesis demonstrates that a type 5/3 recombinant adenovirus was more efficacious at delivering *mda-7/IL-24* to GBM cells than a type 5 virus, resulting in considerably higher expression of MDA-7/IL-24 protein. The greater expression of MDA-7/IL-24 using the serotype 5 / serotype 3 virus resulted in a greater amount of tumor cell killing. However, it is worthy of note, that although infection using Ad.5/3-*mda-7 in vitro* generated at least ~10-fold more MDA-7/IL-24 protein, it only reduced colony formation/survival approximately threefold more than Ad.5-*mda-7* infection. This argues that there may be a threshold at which expression of MDA-7/IL-24 becomes toxic to a

tumor cell and producing more MDA-7/IL-24 protein will not *per se* increase killing, at least in *in vitro* assays. The *in vivo* observations using Ad.5-*mda-7* and Ad.5/3-*mda-7* provide a more convincing demonstration of the enhanced effectiveness of using a serotype 5/3 virus over a serotype 5 virus. At 14 days after Ad.5-*mda-7* infection, tumors begin to exhibit a modest level of re-growth but Ad.5/3-*mda-7* tumors maintain a non-proliferative phenotype. These significant findings suggest that Ad.5/3-*mda-7* may provide enhanced clinical benefit in the context of GBM; validation of which will be attempted in future work.

## CHAPTER 9: CONCLUSIONS

In conclusion, the data in this work demonstrates that MDA-7/IL-24 interacts with OSU-03012 to enhance killing of primary human GBM cells in a greater than additive manner. The data also indicates that the use of two (or more) agents, that act to increase the autophagic response, will further facilitate GBM cell apoptosis. Furthermore, the inhibition of two or more survival signal transduction pathways is likely required to promote any additional MDA-7/IL-24 toxicity in GBM cells; an effect that is mediated by increased mitochondrial instability. Additionally, combining MDA-7/IL-24 with temozolomide and radiation increases MDA-7/IL-24 toxicity versus treatment with either agent alone. The data presented here also suggests that the serotype 5/3 viral delivery mechanism may provide a means of more effectively translating MDA-7/IL-24 therapy from the bench into the clinic for GBM. Based upon the results described in this thesis, future studies that target multiple protective signaling pathways in combination with enhanced delivery of MDA-7/IL-24 appear warranted.

## Literature Cited



### Literature Cited

1. Hanahan D, Weinberg RA. The hallmarks of cancer. *Cell* 2000; 100(1):57.
2. Globocan, IARC, 2008. World Health Organization – Cancer Fast Stats. Retrieved from: <http://globocan.iarc.fr/factsheets/populations/factsheet.asp?uno=900>.
3. Jemal A, Siegel R, Ward E, Hao Y, Xu J, Murray T, et al. Cancer statistics, 2008. *CA* 2008;58(2):71.
4. Tanaka K, Babic I, Nathanson D, Guo D, Gini B et al. Oncogenic EGFR signaling activates an mTORC2-NF-kB pathway that promotes chemotherapy resistance. *Cancer Discovery*, 2011; 1(6): 524-538.
5. Raizer JJ. HER1/EGFR tyrosine kinase inhibitors for the treatment of glioblastoma multiforme. *Journal of Neurooncology*, 2005 Aug; 74(1): 77-86.
6. Tentori L, Graziani G. Recent approaches to improve the antitumor efficacy of Temozolomide. *Curr. Med. Chem.*, 2009; 16: 245-257.
7. Ponnazhagan S, Curiel D, Shaw D, Alvarez R and Siegal G. Adeno-associated virus for cancer gene therapy. *Cancer Research* 2001; (61) 6316-6321.
8. Gomez-Navarro J and Curiel D. Conditionally replicative adenoviral vectors for cancer gene therapy. *Lancet Oncology* 2000; 1: 148-158.
9. Jiang H, Lin JJ, Su ZZ, Goldstein NI, Fisher PB. Subtraction hybridization identifies a novel melanoma differentiation associated gene, *mda-7*, modulated during human melanoma differentiation, growth and progression. *Oncogene* 1995; 11:2477-86.
10. Huang EY, Madireddi MT, Gopalkrishnan RV, Leszczyniecka M, Su Z, Lebedeva IV, et al. Genomic structure, chromosomal localization and expression profile of a novel melanoma differentiation associated (*mda-7*) gene with cancer specific growth suppressing and apoptosis inducing properties. *Oncogene* 2001; 20:7051-63.

11. Parrish-Novak J, Xu W, Brender T, Yao L, Jones C, West J, et al. Interleukins 19, 20 and 24 Signal through Two Distinct Receptor Complexes. Differences in receptor-ligand interactions mediate unique biological functions. *J Biol Chem* 2002; 277:47517-23.
12. Caudell EG, Mumm JB, Poindexter N, Ekmekcioglu S, Mhashilkar AM, Yang XH, et al. The protein product of the tumor suppressor gene, melanoma differentiation-associated gene 7, exhibits immunostimulatory activity and is designated IL-24. *J Immunol* 2002; 168:6041-6.
13. Pestka S, Krause CD, Sarkar D, Walter MR, Shi Y, Fisher PB. Interleukin-10 and related cytokines and receptors. *Annu Rev Immunol* 2004; 22:929-79.
14. Gupta P, Su ZZ, Lebedeva IV, Sarkar D, Sauane M, Emdad L, et al. *mda-7/IL-24*: multifunctional cancer-specific apoptosis-inducing cytokine. *Pharmacol Ther* 2006; 111:596-628.
15. Lebedeva IV, Sauane M, Gopalkrishnan RV, Sarkar D, Su ZZ, Gupta P, et al. *mda-7/IL-24*: exploiting cancer's Achilles' heel. *Mol Ther* 2005; 11:4-18.
16. Fisher PB, Gopalkrishnan RV, Chada S, Ramesh R, Grimm EA, Rosenfeld MR, et al. *mda-7/IL-24*, a novel cancer selective apoptosis inducing cytokine gene: from the laboratory into the clinic. *Cancer Biol Ther* 2003; 2:23-37.
17. Fisher PB. Is *mda-7/IL-24* a "magic bullet" for cancer? *Cancer Res* 2005; 65:10128-38.
18. Emdad L, Lebedeva IV, Su Z-z, Gupta P, Sauane M, Dash R, et al. Historical perspective and recent insights into our understanding of the molecular and biochemical basis of the antitumor properties of *mda-7/IL-24*. *Cancer Biol Ther* 2009; 8:391-400.
19. Jiang H, Lin JJ, Su ZZ, Goldstein NI, Fisher PB. Subtraction hybridization identifies a novel melanoma differentiation associated gene, *mda-7*, modulated during human melanoma differentiation, growth and progression. *Oncogene* 1995; 11:2477-86.
20. Ekmekcioglu S, Ellerhorst J, Mhashilkar AM, Sahin AA, Read CM, Prieto VG, et al. Downregulated melanoma differentiation associated gene (*mda-7*) expression in human melanomas. *Int J Cancer* 2001; 94:54-9.
21. Ellerhorst JA, Prieto VG, Ekmekcioglu S. Loss of MDA-7 expression with progression of melanoma. *J Clin Oncol* 2002; 20:1069-74.

22. Su ZZ, Lebedeva IV, Gopalkrishnan RV, Goldstein NI, Stein CA, Reed JC, et al. A combinatorial approach for selectively inducing programmed cell death in human pancreatic cancer cells. *Proc Natl Acad Sci USA* 2001; 98:10332-7.
23. Su ZZ, Madireddi MT, Lin JJ, Young CS, Kitada S, Reed JC, et al. The cancer growth suppressor gene *mda-7* selectively induces apoptosis in human breast cancer cells and inhibits tumor growth in nude mice. *Proc Natl Acad Sci USA* 1998; 95:14400-5.
24. Cunningham CC, Chada S, Merritt JA, Tong A, Senzer N, Zhang Y, et al. Clinical and local biological effects of an intratumoral injection of *mda-7* (IL24; INGN 241) in patients with advanced carcinoma: a phase I study. *Mol Ther* 2005; 11:149-59.
25. Tong AW, Nemunaitis J, Su D, Zhang Y, Cunningham C, Senzer N, et al. Intratumoral injection of INGN 241, a nonreplicating adenovector expressing the melanoma differentiation associated gene-7 (*mda-7*/IL-24): Biologic outcome in advanced cancer patients. *Mol Ther* 2005; 11:160-72.
26. Fisher PB, Sarkar D, Emdad L, Emdad L, Gupta P, Sauane M, et al. Melanoma differentiation associated gene-7/interleukin-24 (*mda-7*/IL-24): novel gene therapeutic for metastatic melanoma. *Toxicol & Appl Pharmacol* 2007; 224:300-7.
27. Lebedeva IV, Su ZZ, Chang Y, Kitada S, Reed JC, Fisher PB. The cancer growth suppressing gene *mda-7* induces apoptosis selectively in human melanoma cells. *Oncogene* 2002; 21:708-18.
28. Su ZZ, Lebedeva IV, Sarkar D, Emdad L, Gupta P, Kitada S, et al. Ionizing radiation enhances therapeutic activity of *mda-7*/IL-24: overcoming radiation- and *mda-7*/IL-24-resistance in prostate cancer cells overexpressing the antiapoptotic proteins bcl-x<sub>L</sub> or bcl-2. *Oncogene* 2006; 25:2339-48.
29. Gopalan B, Litvak A, Sharma S, Mhashilkar AM, Chada S, Ramesh R. Activation of the Fas-FasL signaling pathway by MDA-7/IL-24 kills human ovarian cancer cells. *Cancer Res* 2005; 65:3017-24.
30. Lebedeva IV, Su Z-z, Sarkar D, Kitada S, Dent P, Waxman S, et al. Melanoma differentiation associated gene-7, *mda-7*/IL-24, promotes apoptosis in prostate cancer cells by promoting mitochondrial dysfunction and inducing reactive oxygen species. *Cancer Res* 2003; 63:8138-44.

31. Gupta P, Walter MR, Su ZZ, Lebedeva IV, Emdad L, Randolph A, et al. BiP/GRP78 Is an intracellular target for MDA-7/IL-24 induction of cancer-specific apoptosis. *Cancer Res* 2006; 66:8182-91.
32. Sauane M, Gopalkrishnan RV, Choo HT, Gupta P, Lebedeva IV, Yacoub A, et al. Mechanistic aspects of *mda-7*/IL-24 cancer cell selectivity analysed via a bacterial fusion protein. *Oncogene* 2004; 23:7679-90.
33. Yacoub A, Mitchell C, Hong Y, Gopalkrishnan RV, Su ZZ, Gupta P, et al. MDA-7 regulates cell growth and radiosensitivity in vitro of primary (non-established) human glioma cells. *Cancer Biol Ther* 2004; 3:739-51.
34. Yacoub A, Hamed H, Emdad L, Dos Santos W, Gupta P, Broaddus WC, et al. MDA-7/IL-24 plus radiation enhance survival in animals with intracranial primary human GBM tumors. *Cancer Biol Ther* 2008; 7:917-33.
35. Yacoub A, Park MA, Gupta P, Rahmani M, Zhang G, Hamed H, et al. Caspase-, cathepsin- and PERK-dependent regulation of MDA-7/IL-24-induced cell killing in primary human glioma cells. *Mol Cancer Ther* 2008; 7:297-313.
36. Yacoub A, Gupta P, Park MA, Rhamani M, Hamed H, Hanna D, et al. Regulation of GST-MDA-7 toxicity in human glioblastoma cells by ERBB1, ERK1/2, PI3K and JNK1-3 pathway signaling. *Mol Cancer Ther* 2008; 7:314-29.
37. Yacoub A, Mitchell C, Brannon J, Rosenberg E, Qiao L, McKinstry R, et al. MDA-7 (interleukin-24) inhibits the proliferation of renal carcinoma cells and interacts with free radicals to promote cell death and loss of reproductive capacity. *Mol Cancer Ther* 2003; 2:623-32.
38. Sarkar D, Su ZZ, Lebedeva IV, Sauane M, Gopalkrishnan RV, Valerie K, et al. *mda-7* (IL-24) Mediates selective apoptosis in human melanoma cells by inducing the coordinated overexpression of the GADD family of genes by means of p38 MAPK. *Proc Natl Acad Sci USA* 2002; 99:10054-9.
39. Mhashilkar AM, Stewart AL, Sieger K, Yang HY, Khimani AH, Ito I, et al. MDA-7 negatively regulates the beta-catenin and PI3K signaling pathways in breast and lung tumor cells. *Mol Ther* 2003; 8:207-19.
40. Chada S, Bocangel D, Ramesh R, Grimm EA, Mumm JB, Mhashilkar AM, et al. *mda-7*/IL24 kills pancreatic cancer cells by inhibition of the Wnt/PI3K signaling pathways: identification of IL-20 receptor-mediated bystander activity against pancreatic cancer. *Mol Ther* 2005; 11:724-33.

41. Dent, P, Yacoub, A, Park, M, Sarkar, D, Shah, K, Curiel, DT *et al.* (2008). Searching for a cure: gene therapy for glioblastoma. *Cancer Biol Ther* 7: 1335–1340.
42. Kaliberova, LN, Krendelchtchikova, V, Harmon, DK, Stockard, CR, Petersen, AS, Markert, JM *et al.* (2009). CRAdRGDflt-IL24 virotherapy in combination with chemotherapy of experimental glioma. *Cancer Gene Ther* 16: 794–805.
43. Dent P, Yacoub A, Fisher PB, Hagan MP, Grant S. MAPK pathways in radiation responses. *Oncogene* 2003; 22(37):5885.
44. Grant S, Dent P. Kinase inhibitors and cytotoxic drug resistance. *Clinical cancer research* 2004;10(7):2205.
45. Dhillon AS. MAP kinase signalling pathways in cancer. *Oncogene* 2007;26(22):3279.
46. McCubrey JA, Steelman LS, Chappell WH, Abrams SL, Wong EW, Chang F, et al. Roles of the Raf/MEK/ERK pathway in cell growth, malignant transformation and drug resistance. *Biochim Biophys Acta* 2007 Aug; 1773(8):1263-84.
47. Allan LA, Morrice N, Brady S, Magee G, Pathak S, Clarke PR. Inhibition of caspase-9 through phosphorylation at Thr 125 by ERK MAPK. *Nature cell biology* 2003; 5(7):647.
48. Mori M, Uchida M, Watanabe T, Kirito K, Hatake K, Ozawa K, et al. Activation of extracellular signal-regulated kinases ERK1 and ERK2 induces Bcl-xL up-regulation via inhibition of caspase activities in erythropoietin signaling. *Journal of cellular physiology* 2003;195(2):290.
49. Ley R, Balmano K, Hadfield K, Weston C, Cook SJ. Activation of the ERK1/2 signaling pathway promotes phosphorylation and proteasome-dependent degradation of the BH3-only protein, Bim. *The Journal of biological chemistry* 2003;278(21):18811.
50. Wang YF, Jiang CC, Kiejda KA, Gillespie S, Zhang XD, Hersey P. Apoptosis induction in human melanoma cells by inhibition of MEK is caspase-independent and mediated by the Bcl-2 family members PUMA, Bim, and Mcl-1. *Clinical cancer research* 2007;13(16):4934.

51. Qiao L, Han SI, Fang Y, Park JS, Gupta S, Gilfor D, et al. Bile acid regulation of C/EBPbeta, CREB, and c-Jun function, via the extracellular signal-regulated kinase and c-Jun NH2-terminal kinase pathways, modulates the apoptotic response of hepatocytes. *Molecular and cellular biology* 2003;23(9):3052.
52. Kolch W. Meaningful relationships: the regulation of the Ras/Raf/MEK/ERK pathway by protein interactions. *Biochem J* 2000 Oct 15;351 Pt 2:289-305.
53. Kolch W. The role of Raf kinases in malignant transformation. *Expert reviews in molecular medicine* 2002;4(8):1.
54. Roberts PJ, Der CJ. Targeting the Raf-MEK-ERK mitogen-activated protein kinase cascade for the treatment of cancer. *Oncogene* 2007 May 14;26(22):3291-310.
55. Wan PTC, Garnett MJ, Roe SM, Lee S, Niculescu-Duvaz D, Good VM, et al. Mechanism of activation of the RAF-ERK signaling pathway by oncogenic mutations of B-RAF. *Cell* 2004;116(6):855.
56. Kyriakis JM, Avruch J. Mammalian mitogen-activated protein kinase signal transduction pathways activated by stress and inflammation. *Physiological reviews* 2001;81(2):807.
57. Lei K, Davis RJ. JNK phosphorylation of Bim-related members of the Bcl2 family induces Bax-dependent apoptosis. *Proceedings of the National Academy of Sciences of the United States of America* 2003;100(5):2432.
58. Roux PP, Blenis J. ERK and p38 MAPK-activated protein kinases: a family of protein kinases with diverse biological functions. *Microbiology and molecular biology reviews* 2004;68(2):320.
59. Han J, Sun P. The pathways to tumor suppression via route p38. *Trends in biochemical sciences* 2007;32(8):364.
60. Engelman JA, Luo J, Cantley LC. The evolution of phosphatidylinositol 3-kinases as regulators of growth and metabolism. *Nature reviews. Genetics* 2006;7(8):606.
61. Gaidarov I, Smith ME, Domin J, Keen JH. The class II phosphoinositide 3-kinase C2alpha is activated by clathrin and regulates clathrin-mediated membrane trafficking. *Molecular cell* 2001;7(2):443.

62. Nobukuni T, Joaquin M, Roccio M, Dann SG, Kim SY, Gulati P, et al. Amino acids mediate mTOR/raptor signaling through activation of class 3 phosphatidylinositol 3OH-kinase. *Proceedings of the National Academy of Sciences of the United States of America* 2005;102(40):14238.
63. Cully M, You H, Levine AJ, Mak TW. Beyond PTEN mutations: the PI3K pathway as an integrator of multiple inputs during tumorigenesis. *Nature reviews. Cancer* 2006;6(3):184.
64. Manning BD, Cantley LC. AKT/PKB signaling: navigating downstream. *Cell* 2007;129(7):1261.
65. Elmore S. Apoptosis: a review of programmed cell death. *Toxicologic pathology* 2007;35(4):495.
66. Martin AP, Miller A, Emad L, Rahmani M, Walker T, Mitchell C, Hagan MP, Park MA, Yacoub A, Fisher PB, Grant S, Dent P. (2008) Lapatinib Resistance in HCT116 cells Is Mediated by Elevated MCL-1 Expression and Decreased BAK Activation and Not by ERBB Receptor Kinase Mutation. *Mol Pharmacol* **74**:807-822.
67. Cameron DA, Stein S. (2008) Drug Insight: intracellular inhibitors of HER2-clinical development of Lapatinib in breast cancer. *Nature Clinical Practice-Oncology* **5**:512-520.
68. Zhang G, Park MA, Mitchell C, Hamed H, Rahmani M, Martin AP, Curiel DT, Yacoub A, Graf M, Lee R, Roberts JD, Fisher PB, Grant S, Dent P. (2008) Vorinostat and Sorafenib Synergistically Kill Tumor Cells via FLIP Suppression and CD95 Activation. *Clin Cancer Res* **14**:5385-5399.
69. Siegelin MD, Raskett CM, Gilbert CA, Ross AH, Altieri DC. (2010) Sorafenib exerts anti-glioma activity in vitro and in vivo. *Neuroscience Letters* **478**: 165-170.
70. Thiessen B, Stewart C, Tsao M, Kamel-Reid S, Schaiquevich P, Mason W, Easaw J, Belanger K, Forsyth P, McIntosh L, Eisenhauer E. (2010) A phase I/II trial of GW572016 (Lapatinib) in recurrent glioblastoma multiforme: clinical outcomes, pharmacokinetics and molecular correlation. *Cancer Chemother Pharmacol* **65**:353-361.

71. Schmidt-Ullrich RK, Contessa JN, Lammering G, Amorino G, and Lin PS (2003) ERBB receptor tyrosine kinases and cellular radiation responses. *Oncogene* 22:5855–5865.
72. Imai K and Takaoka A (2006) Comparing antibody and small-molecule therapies for cancer. *Nat Rev Cancer* 6:714–727.
73. Wang YF, Jiang CC, Kiejda KA, Gillespie S, Zhang XD, Hersey P. Apoptosis induction in human melanoma cells by inhibition of MEK is caspase-independent and mediated by the Bcl-2 family members PUMA, Bim, and Mcl-1. *Clinical cancer research* 2007;13(16):4934.
74. Elmore S. Apoptosis: a review of programmed cell death. *Toxicologic pathology* 2007;35(4):495.
75. Sharma K. Death the Fas way: regulation and pathophysiology of CD95 and its ligand. *Pharmacology therapeutics* 2000;88(3):333.
76. Schmitz I, Kirchhoff S, Krammer PH. Regulation of death receptor-mediated apoptosis pathways. *Int J Biochem Cell Biol* 2000 Nov-Dec;32(11-12):1123-36.
77. Adams JM, Cory S. The Bcl-2 apoptotic switch in cancer development and therapy. *Oncogene* 2007 Feb 26;26(9):1324-37.
78. Li H. Cleavage of BID by caspase 8 mediates the mitochondrial damage in the Fas pathway of apoptosis. *Cell* 1998;94(4):491.
79. Youle RJ. The BCL-2 protein family: opposing activities that mediate cell death. *Nature reviews. Molecular cell biology* 2008;9(1):47.
80. Dean EJ. Novel therapeutic targets in lung cancer: Inhibitor of apoptosis proteins from laboratory to clinic. *Cancer Treatment Reviews* 2007;33(2):203.
81. Levine B, Kroemer G. Autophagy in the Pathogenesis of Disease. *Cell* 2008 Jan 11;132(1):27-42.
82. Amaravadi RK, Thompson CB. The roles of therapy-induced autophagy and necrosis in cancer treatment. *Clin Cancer Res* 2007 Dec 15;13(24):7271-9.
83. Kundu M. Autophagy: basic principles and relevance to disease. *Annual review of pathology* 2008;3:427.



84. Mariño G. Autophagy: molecular mechanisms, physiological functions and relevance in human pathology. *Cellular and molecular life sciences* 2004;61(12):1439.
85. Mizushima N. Mouse Apg16L, a novel WD-repeat protein, targets to the autophagic isolation membrane with the Apg12-Apg5 conjugate. *Journal of cell science* 2003;116(9):1679.
86. Uchiyama Y. Autophagy-physiology and pathophysiology. *Histochemistry and Cell Biology* 2008;129(4):407.
87. Ding W, Yin X. Sorting, recognition and activation of the misfolded protein degradation pathways through macroautophagy and the proteasome. *Autophagy* 2008;4(2):141.
88. Mizushima N. Autophagy: process and function. *Genes development* 2007;21(22):2861.
89. Seglen PO. 3-Methyladenine: specific inhibitor of autophagic/lysosomal protein degradation in isolated rat hepatocytes. *Proceedings of the National Academy of Sciences of the United States of America* 1982;79(6):1889.
90. Petiot A. Distinct classes of phosphatidylinositol 3'-kinases are involved in signaling pathways that control macroautophagy in HT-29 cells. *The Journal of biological chemistry* 2000;275(2):992.
91. Mizushima N. Autophagy fights disease through cellular self-digestion. *Nature* 2008;451(7182):1069.
92. Saeki K. Bcl-2 down-regulation causes autophagy in a caspase-independent manner in human leukemic HL60 cells. *Cell death and differentiation* 2000;7(12):1263.
93. Hart FU. Molecular chaperones in cellular protein folding. *Nature* 1996 Jun 13;381(6583):571-9.
94. Morimoto RI. Regulation of the heat shock transcriptional response: cross talk between a family of heat shock factors, molecular chaperones, and negative regulators. *Genes Dev* 1998 Dec 15;12(24):3788-96.
95. Cullinan SB, Whitesell L. Heat shock protein 90: a unique chemotherapeutic target. *Semin Oncol* 2006 Aug;33(4):457-65.

96. Nakamoto H, Vigh L. The small heat shock proteins and their clients. *Cell Mol Life Sci* 2007 Feb;64(3):294-306.
97. Sun Y, MacRae TH. Small heat shock proteins: molecular structure and chaperone function. *Cell Mol Life Sci* 2005 Nov;62(21):2460-76.
98. Nollen EA, Morimoto RI. Chaperoning signaling pathways: molecular chaperones as stress-sensing 'heat shock' proteins. *J Cell Sci* 2002 Jul 15;115(Pt 14):2809-16.
99. Maurizi MR, Xia D. Protein binding and disruption by Clp/Hsp100 chaperones. *Structure* 2004 Feb;12(2):175-83.
100. Nathan DF, Vos MH, Lindquist S. In vivo functions of the *Saccharomyces cerevisiae* Hsp90 chaperone. *Proc Natl Acad Sci U S A* 1997 Nov 25;94(24):12949-56.
101. Wegele H, Muller L, Buchner J. Hsp70 and Hsp90--a relay team for protein folding. *Rev Physiol Biochem Pharmacol* 2004;151:1-44.
102. Picard D, Khursheed B, Garabedian MJ, Fortin MG, Lindquist S, Yamamoto KR. Reduced levels of hsp90 compromise steroid receptor action in vivo. *Nature* 1990 Nov 8;348(6297):166-8.
103. Xu Y, Lindquist S. Heat-shock protein hsp90 governs the activity of pp60v-src kinase. *Proc Natl Acad Sci U S A* 1993 Aug 1;90(15):7074-8.
104. Isaacs JS, Xu W, Neckers L. Heat shock protein 90 as a molecular target for cancer therapeutics. *Cancer cell* 2003;3(3):213.
105. Prodromou C, Roe SM, O'Brien R, Ladbury JE, Piper PW, Pearl LH. Identification and structural characterization of the ATP/ADP-binding site in the Hsp90 molecular chaperone. *Cell* 1997 Jul 11;90(1):65-75.
106. Minami Y, Kimura Y, Kawasaki H, Suzuki K, Yahara I. The carboxy-terminal region of mammalian HSP90 is required for its dimerization and function in vivo. *Mol Cell Biol* 1994 Feb;14(2):1459-64.
107. Compton SA, Elmore LW, Haydu K, Jackson-Cook CK, Holt SE. Induction of nitric oxide synthase-dependent telomere shortening after functional inhibition of Hsp90 in human tumor cells. *Mol Cell Biol* 2006 Feb;26(4):1452-62.

108. Ozawa K, Murakami Y, Eki T, Soeda E, Yokoyama K. Mapping of the gene family for human heat-shock protein 90 alpha to chromosomes 1, 4, 11, and 14. *Genomics* 1992 Feb;12(2):214-20.
109. Eustace BK, Sakurai T, Stewart JK, Yimlamai D, Unger C, Zehetmeier C, et al. Functional proteomic screens reveal an essential extracellular role for hsp90 alpha in cancer cell invasiveness. *Nat Cell Biol* 2004 Jun;6(6):507-14.
110. Moore SK, Kozak C, Robinson EA, Ullrich SJ, Appella E. Murine 86- and 84-kDa heat shock proteins, cDNA sequences, chromosome assignments, and evolutionary origins. *J Biol Chem* 1989 Apr 5;264(10):5343-51.
111. Voss AK, Thomas T, Gruss P. Mice lacking HSP90beta fail to develop a placental labyrinth. *Development* 2000 Jan;127(1):1-11.
112. Rabindran SK, Giorgi G, Clos J, Wu C. Molecular cloning and expression of a human heat shock factor, HSF1. *Proc Natl Acad Sci U S A* 1991 Aug 15;88(16):6906-10.
113. McMillan DR, Xiao X, Shao L, Graves K, Benjamin IJ. Targeted disruption of heat shock transcription factor 1 abolishes thermotolerance and protection against heat-inducible apoptosis. *J Biol Chem* 1998 Mar 27;273(13):7523-8.
114. Liu PC, Thiele DJ. Modulation of human heat shock factor trimerization by the linker domain. *J Biol Chem* 1999 Jun 11;274(24):17219-25.
115. Baler R, Dahl G, Voellmy R. Activation of human heat shock genes is accompanied by oligomerization, modification, and rapid translocation of heat shock transcription factor HSF1. *Mol Cell Biol* 1993 Apr;13(4):2486-96.
116. Shi Y, Mosser DD, Morimoto RI. Molecular chaperones as HSF1-specific transcriptional repressors. *Genes Dev* 1998 Mar 1;12(5):654-66.
117. Zou J, Guo Y, Guettouche T, Smith DF, Voellmy R. Repression of heat shock transcription factor HSF1 activation by HSP90 (HSP90 complex) that forms a stress-sensitive complex with HSF1. *Cell* 1998 Aug 21;94(4):471-80.
118. Whitesell L, Mimnaugh EG, De Costa B, Myers CE, Neckers LM. Inhibition of heat shock protein HSP90-pp60v-src heteroprotein complex formation by benzoquinone ansamycins: essential role for stress proteins in oncogenic transformation. *Proc Natl Acad Sci U S A* 1994 Aug 30;91(18):8324-8.

119. Schulte TW, Akinaga S, Soga S, Sullivan W, Stensgard B, Toft D, et al. Antibiotic radicicol binds to the N-terminal domain of Hsp90 and shares important biologic activities with geldanamycin. *Cell Stress Chaperones* 1998 Jun;3(2):100-8.
120. Roe SM, Prodromou C, O'Brien R, Ladbury JE, Piper PW, Pearl LH. Structural basis for inhibition of the Hsp90 molecular chaperone by the antitumor antibiotics radicicol and geldanamycin. *J Med Chem* 1999 Jan 28;42(2):260-6.
121. Kamal A, Thao L, Sensintaffar J, Zhang L, Boehm MF, Fritz LC, et al. A high-affinity conformation of Hsp90 confers tumour selectivity on Hsp90 inhibitors. *Nature* 2003 Sep 25;425(6956):407-10.
122. Supko JG, Hickman RL, Grever MR, Malspeis L. Preclinical pharmacologic evaluation of geldanamycin as an antitumor agent. *Cancer Chemother Pharmacol* 1995;36(4):305-15.
123. Egorin MJ, Rosen DM, Wolff JH, Callery PS, Musser SM, Eiseman JL. Metabolism of 17-(allylamino)-17-demethoxygeldanamycin (NSC 330507) by murine and human hepatic preparations. *Cancer Res* 1998 Jun 1;58(11):2385-96.
124. Schröder M. Endoplasmic reticulum stress responses. *Cellular and molecular life sciences* 2008;65(6):862.
125. Wek RC, Cavener DR. Translational Control and the Unfolded Protein Response. *Antioxid Redox Signal* 2007 Aug 30.
126. Hitomi J. Involvement of caspase-4 in endoplasmic reticulum stress-induced apoptosis and beta-induced cell death. *The Journal of cell biology* 2004;165(3):347.
127. Amaravadi RK, Thompson CB. The roles of therapy-induced autophagy and necrosis in cancer treatment. *Clinical Cancer Res* 2007 Dec 15;13(24):7271-9.
128. Patemot S and Roger P. Combined Inhibition of MEK and Mammalian Target of Rapamycin Abolishes Phosphorylation of Cyclin Dependent Kinase 4 in Glioblastoma Cell Lines and Prevents Their Proliferation. *Cancer Research* 2009 May19;69:4577-4581.
129. Westhoff MA, Kandenwein JA, Karl S, VellankiSH, et al. The pyridinylfuranopyrimidine inhibitor, PI-103, chemosensitizes glioblastoma cells for apoptosis by inhibiting DNA repair. *Oncogene* 2009 Oct. 8; 28(40):3586-96.
130. Kim Y, Liu T, Koul D, et al. Identification of novel synergistic targets for rational drug combinations with PI3 kinase inhibitors using siRNA synthetic lethality screening against GBM. *Neuro-Oncology* 2001; 13(4) 367-375.

131. Mendiburu M, Yin D, Hadaczek P, et al. Systemic rapamycin alone may not be a treatment option for malignant glioma: evidence from an in vivo study. *Journal of Neurooncology* 2012 May; 108(1):53-8.
132. Booth L, Cazanave S, Hamed H, et al. OSU-03012 suppresses GRP78/BiP expression that causes PERK-dependent increases in tumor cell killing. *Cancer Biol Ther*, 2012 Feb 15;13(4):224-36.
133. Hamed H, Yacoub A, Park M, et al. Inhibition of Multiple Protective Signaling Pathways and Ad.5/3 Delivery Enhances mda-7/IL-24 Therapy of Malignant Glioma. *Molecular Therapy* 2010 Feb 23;18(6):1130-1142.
134. Walker T, Mitchell C, Park MA, Yacoub A, Graf M, Rahmani M, et al. Sorafenib and vorinostat kill colon cancer cells by CD95-dependent and -independent mechanisms. *Mol Pharmacol* 2009; 76:342-55.
135. Lebedeva, IV, Emdad, L, Su, ZZ, Gupta, P, Sauane, M, Sarkar, D *et al.* (2007). mda-7/IL-24, novel anticancer cytokine: focus on bystander antitumor, radiosensitization and antiangiogenic properties and overview of the phase I clinical experience (Review). *Int J Oncol* **31**: 985–1007.
136. Yacoub A, Park MA, Hanna D, Hong Y, Mitchell C, Pandya AP, et al. OSU-03012 promotes caspase-independent but PERK-, cathepsin B-, BID- and AIF-dependent killing of transformed cells. *Mol Pharmacol* 2006; 70:589-603.
137. Park MA, Yacoub A, Rahmani M, Zhang G, Hart L, Hagan MP, et al. OSU-03012 stimulates PKR-like endoplasmic reticulum-dependent increases in 70-kDa heat shock protein expression, attenuating its lethal actions in transformed cells. *Mol Pharmacol* 2008; 73:1168-84.
138. Su Z-z, Emdad L, Sauane L, Lebedeva IV, Sarkar D, Gupta P, et al. Unique aspects of mda-7/IL-24 antitumor bystander activity: establishing a role for secretion of MDA-7/IL-24 by normal cells. *Oncogene* 2005; 24:7552-66.
139. Sauane M, Su Z-z, Gupta P, Lebedeva IV, Dent P, Sarkar D, et al. Autocrine regulation of mda-7/IL-24 mediates cancer-specific apoptosis. *Proc Natl Acad Sci USA* 2008; 105:9763-8.
140. Zhang G, Park MA, Mitchell C, Walker T, Hamed H, Studer E, et al. Multiple cyclin kinase inhibitors promote bile acid-induced apoptosis and autophagy in primary hepatocytes via p53-CD95-dependent signaling. *J Biol Chem* 2008; 283:24343-58.

141. Park MA, Zhang G, Martin AP, Hamed H, Mitchell C, et al. Vorinostat and sorafenib increase ER stress, autophagy and apoptosis via ceramide-dependent CD95 and PERK activation. *Cancer Biol Ther* 2008; 7:1648-62.
142. Park MA, Walker T, Martin AP, Allegood J, Vozhilla N, Emdad L, et al. MDA-7/IL-24-induced cell killing in malignant renal carcinoma cells occurs by a ceramide/CD95/PERK-dependent mechanism. *Mol Cancer Ther* 2009; 8:1-12.
143. Xia Z, Dickens M, Raingeaud J, Davis RJ, Greenberg ME. Opposing effects of ERK and JNK-p38 MAP kinases on apoptosis. *Science* 1995; 270:1326-31.
144. Martin AP, Park MA, Mitchell C, Walker T, Rahmani M, Thorburn A, et al. BCL-2 family inhibitors enhance histone deacetylase inhibitor and sorafenib lethality via autophagy and overcome blockade of the extrinsic pathway to facilitate killing. *Mol Pharmacol* 2009; 76:327-41.
145. Martin AP, Mitchell C, Rahmani M, Nephew K, Grant S, Dent P. Inhibition of MCL-1 enhances Lapatinib toxicity and overcomes Lapatinib resistance via BAK-dependent autophagy. *Cancer Biol Ther* 2009; 8:2084-96.
146. Levine B, Sinha S, Kroemer G. Bcl-2 family members: dual regulators of apoptosis and autophagy. *Autophagy* 2008; 4:600-6.
147. Dash R, Dmitriev IP, Su ZZ, Bhutia SK, Azab B, Vozhilla N *et al.* (2009). Enhanced delivery of mda-7/IL-2454 using a serotype chimeric adenovirus (Ad.5/3) improves therapeutic efficacy in low CAR prostate cancer cells. *Cancer Gene Ther* (epub ahead of print).
148. Murakami, M, Ugai, H, Belousova, N, Pereboev, A, Dent, P, Fisher, PB *et al.* (2010). Chimeric adenoviral vectors incorporating a fiber of human adenovirus 3 efficiently mediate gene transfer into prostate cancer cells. *Prostate* **70**: 362–376.
149. Lefranc, F, Rynkowski, M, DeWitte, O and Kiss, R (2009). Present and potential future adjuvant issues in high-grade astrocytic glioma treatment. *Adv Tech Stand Neurosurg* **34**: 3–35.
150. Jung, CH, Jun, CB, Ro, SH, Kim, YM, Otto, NM, Cao, J *et al.* (2009). ULK-Atg13-FIP200 complexes mediate mTOR signaling to the autophagy machinery. *Mol Biol Cell* **20**: 992–2003.

151. Tentori, L and Graziani, G (2009). Recent approaches to improve the antitumor efficacy of temozolomide. *Curr Med Chem* **16**: 245–257.
152. Sauane, M, Su, ZZ, Dash, R, Liu, X, Norris, JS, Sarkar, D *et al.* (2010). Ceramide plays a prominent role in MDA-7/IL-24-induced cancer-specific apoptosis. *J Cell Physiol* **222**: 546–555.
153. Bektas, M, Johnson, SP, Poe, WE, Bigner, DD and Friedman, HS (2009). A sphingosine kinase inhibitor induces cell death in temozolomide resistant glioblastoma cells. *Cancer Chemother Pharmacol* **64**: 1053–1058.
154. Dent P, Yacoub A, Hamed H, et al. NDA-7/IL-24 as a cancer therapeutic: from bench to bedside. *Anti-Cancer Drugs* 2010;21:725-731.

### VITA

Hossein Hamed, born September 5, 1979 in Oklahoma City, OK, earned a degree in Biological Sciences at The University of Mary Washington in 2003. During his undergraduate studies he served as captain of the university rugby team while actively pursuing a career in science. In his junior year, Hossein was awarded a stipend to continue his research on the Molecular Systematics of Phealenopsis Orchids for which he in turn was awarded the Virginia Academy of Sciences award consecutively for two years. After graduation, Hossein began working as a laboratory technician for Dr. William C. Gause at the Uniformed Services University in Bethesda, MD, where he studied the immune response to parasites and the elicitation of T-cell memory. Within one year Hossein was promoted to laboratory manager and continued working for Dr. Gause for another two years. During that time his contribution to research earned him seven publications. After meeting his future wife and relocating to Richmond, VA; Hossein began working for Dr. Paul Dent at the Massey Cancer Center. For the last six years, Hossein has not only served as the full-time laboratory manager, he has also completed his PhD research, over 40 credits of related course work, gain four first authorship manuscripts and contributed to over 25 other journal articles. This work is a product of over 10 years of experimentations and experience culminating into one thesis.